DEVELOPMENT AND EVALUATION OF MODIFIED NATURAL POLYMER BASED MATRIX TABLETS FOR SUSTAINED RELEASE OF A HIGHLY WATER SOLUBLE DRUG

Thesis Submitted by

KAUSHIK MUKHERJEE

Doctor of Philosophy (Pharmacy)

DEPARTMENT OF PHARMACEUTICAL TECHNOLOGY

FACULTY COUNCIL OF ENGINEERING & TECHNOLOGY

JADAVPUR UNIVERSITY

KOLKATA, INDIA

2024

Registration No. 1022213001 **Index No. 002/22/Ph**

1. Title of the Thesis:

Development and Evaluation of Modified Natural Polymer Based Matrix Tablets for Sustained Release of a Highly Water Soluble Drug

2. Name, Designation & Institution of the Supervisor/s:

A) Dr. Tapan Kumar Giri, Associate Professor, Department of Pharmaceutical Technology, Jadavpur University, Kolkata 700032, India.

3. List of Publication:

Published paper

[1] **Mukherjee K**, Dutta P, Giri TK. Al^{3+}/Ca^{2+} cross-linked hydrogel matrix tablet of etherified tara gum for sustained delivery of tramadol hydrochloride in gastrointestinal milieu. Int. J. Biol. Macromol. 2023;232:123448. Doi: https://doi.org/10.1016/j.ijbiomac.2023.123448.

[2] **Mukherjee K**, Roy S, Giri TK. Effect of intragranular/extragranular tara gum on sustained gastrointestinal drug delivery from semi-IPN hydrogel matrices. Int. J. Biol. Macromol. 2023;253:127176. Doi: https://doi.org/10.1016/j.ijbiomac.2023.127176.

[3] **Mukherjee K**, Dutta P, Badwaik HR, Saha A, Das A, Giri TK. Food industry applications of Tara gum and its modified forms. Food Hydrocolloids for Health. 2023;3:100107. Doi: https://doi.org/10.1016/j.fhfh.2022.100107.

4. List of Patents: NIL

5. List of Presentations in National/International/Conferences/Workshops:

[1] Mukherjee K, Giri TK. Effect of compressional force and drug load on tramadol hydrochloride release from Al^{3+}/Ca^{2+} cross-linked carboxymethyl tara gum hydrogel matrix tablets. APTICON 2023. Pranveer Singh Institute of Technology (Pharmacy), Kanpur, 2^{nd} – 3^{rd} September 2023.

STATEMENT OF ORIGINALITY

I, ***KAUSHIK MUKHERJEE*** registered on ***March 16, 2022***, do hereby declare that this thesis entitled "***Development and Evaluation of Modified Natural Polymer Based Matrix Tablets for Sustained Release of a Highly Water Soluble Drug***" contains literature survey and original research work done by the undersigned candidate as part of doctoral studies.

All information in this thesis have been obtained and presented in accordance with existing academic rules and ethical conduct. I declare that, as required by these rules and conduct, I have fully cited and referred all materials and results that are not original to this work.

I also declare that I have checked this thesis as per the "Policy on Anti Plagiarism, Jadavpur University, 2019", and the level of similarity as checked by iThenticate software is 4% (checked on 30.05.2024).

Kaushik Mukherjee 18/6/24.

(KAUSHIK MUKHERJEE)

Certified by Supervisor:

Tapan Kumar Giri 18/6/24

Dr. TAPAN KUMAR GIRI
Associate Professor
Department of Pharmaceutical Technology
Jadavpur University
Kolkata- 700032

Dr. Tapan Kumar Giri
Associate Professor
Dept. of Pharm. Tech.
Jadavpur University
Kolkata-700 032, India

CERTIFICATE FROM THE SUPERVISOR

This is to certify that the thesis entitled "***Development and Evaluation of Modified Natural Polymer Based Matrix Tablets for Sustained Release of a Highly Water Soluble Drug***" submitted by **KAUSHIK MUKHERJEE (Registration No. 1022213001; Index No. 002/22/Ph)**, who got his name registered on **16.03.2022** for the award of **Ph.D. (Pharmacy)** degree of Jadavpur University is absolutely based upon his own work under the supervision of **Dr. Tapan Kr. Giri** and that neither his thesis nor any part of the thesis has been submitted for any degree/diploma or any other academic award anywhere before.

Tapan Kumar Giri 18/6/24

Dr. Tapan Kr. Giri
Department of Pharmaceutical Technology
Jadavpur University
Kolkata- 700032

Dr. Tapan Kumar Giri
Associate Professor
Dept. of Pharm. Tech.
Jadavpur University
Kolkata-700 032, India

ACKNOWLEDGEMENT

This thesis is the result of a long, difficult journey during which many individuals helped and supported me. Everything I've accomplished is a direct result of their ongoing support and encouragement. It is a pleasure to have this opportunity to thank them.

At the beginning, I wish to express my sincere thanks, deep gratitude and profoundness to my mentor **Dr. Tapan Kumar Giri**, *Department of Pharmaceutical Technology, Jadavpur University for guiding me well throughout the research work from title selection to finding the results. I am deeply grateful to him for his unremitting advice, excellent guidance, encouragement and affection throughout the entire tenure of my research work..*

I would also express my heartfelt gratitude and sincere thanks to my other mentor **Prof. Biswanath Sa,** *ex-Professor, Department of Pharmaceutical Technology, Jadavpur University who taught me the basics and fundamentals of formulation development.*

I owe my deep respect to **Prof. Amalesh Samanta**, *Head, Department of Pharmaceutical Technology, Jadavpur University and former Head of the Department* **Prof. Sanmoy Karmakar & Prof. Kunal Roy** *for their continuous help and encouragement.*

I am thankful to all of my respected **Teachers, colleagues, and other non-teaching staffs of the department** *for their support and help. I am grateful to the authorities of* **Jadavpur University,** *Kolkata for providing all the necessary facilities to pursue my research work.*

I would not forget to specially mention **Dr. Chandan Ghosh,** *Assistant Professor, School of Material Science and Nanotechnology, Jadavpur University,* **Dr. Debabrata Bera,** *Associate Professor, Department of Food Technology and Bio-Chemical engineering, Jadavpur University, and* **Prof. Partha Pratim Ray**, *Department of Physics, Jadavpur University for giving me access to instrumental facilities related to my research work..*

I am thankful to my scholars **Ms. Pallabita Rakshit, Ms. Riya Hazra, Ms. Angita Malakar** and **Mr. MD Sahil** for their help and support. I would also like to thank the scholars of my mentor's laboratory, especially **Mrs. Pallobi Dutta**, for their cooperation and support.

My sincere thanks to numerous other individuals and organizations who have, directly or indirectly, contributed during the entire period of research work..

I am grateful to **my parents and my parents-in-law** who remembered me in their prayers for the ultimate success. I would like to thank my beloved wife **Mom**, for being always with me for extending her continuous support and sharing many moments of joy, sorrow and my dreams.

Last but not the least, I would like to thank my little daughter **Satavisha**, for sacrificing her wishes without which it would not have been possible to carry out the doctoral research work..

Date: 18/6/24

Place: Jadavpur, Kolkata

Kaushik Mukherjee

(KAUSHIK MUKHERJEE)

Dedicated to my beloved Parents

and respected Supervisor.

PREFACE

The uses of natural polymers in pharmaceutical and allied industries have increased over the years. Natural polysaccharides have been extensively used to develop sustained release matrix tablets owing to their biocompatibility, easy availability, non-toxicity and wide regulatory acceptance. **Chapter 1** provides a detailed description about the versatility of the natural polysaccharides in development of sustained release matrices. We have discussed how natural polymers can be tailored to produce the specific drug dissolution. In the next chapter **(chapter 2)** we have discussed about different natural polysaccharides which have been used to develop hydrogel matrices for sustained drug delivery applications. The next two chapters (Chapter 3 and 4) deals with the polymer and drug of choice in this research work. **Chapter 3** outlines the source, properties, and literatures based of tara gum. **Chapter 4** details the various aspects of tramadol hydrochloride, like its chemical composition, class, pharmacokinetics, pharmacodynamics, and uses. We have also given some insights on why tramadol hydrochloride can be used as a model drug. We have also discussed the various sustained release formulations based on tramadol hydrochloride. The aims and objectives of the research work have been deliberated in **chapter 5.** The analytical profiling of tramadol hydrochloride has been presented in **chapter 6.** Next, we have discussed about the synthesis and optimization of carboxymethyl tara gum **(chapter 7).** The characterisation of the synthesised gum is also elaborated. The sub-chronic oral toxicity profile of the synthesised gum has also been detailed. The synthesised gum was then used for the development of single and dual cross-linked matrices. We have elaborated the development and evaluation of the single and dual cross-linked matrices in the **chapter 8.** The optimized dual cross-linked matrices were used for the development of extragranular and intragranular tara gum based semi-IPN hydrogel matrices **(chapter 9).** The optimized semi-IPN hydrogel matrices was evaluated for *in-vivo* pharmacokinetic profile and accelerated stability studies. Finally, we have given a summary and conclusion of the research work in **chapter 10.** We hope that the thesis will encourage researchers to undertake research work on formulation of hydrogel matrices using modified natural polymers for sustained drug delivery applications.

CONTENTS

Chapter 1:

Introduction

1. Drug Delivery through conventional tablet dosage form

There are different routes by which a drug can be delivered like oral, transdermal, parenteral, rectal etc. Oral delivery is by far the most acceptable and favorable mode of drug delivery. The reason for such popularity is its non-invasiveness, self-administration, and low cost. This leads to high patient acceptability. Approximately 90% of all medications provided for a systemic effect are taken orally [1]. The dosage forms for oral delivery of drugs primarily includes tablets, capsules and various liquid formulations. The tablets dosage form is one of the most preferred dosage form both by physicians and patients. Tablets are unit dosage forms where one unit of the dose is accurately loaded, which minimizes any error of administering the right dose of the drug. The tablet dosage form thus offers the minimum content variability and highest dose accuracy. Additionally, the cost of tablets is the lowest of all solid dosage form, and they are the compact and lightest of all oral dosage forms. Lastly, tablets are the most suited for large scale production with minimum tableting infrastructure among all unit oral forms [1].

The tablet dosage form when taken orally, first disintegrates to release the granules. The drug from the granules then solubilizes in the gastrointestinal medium, which is then absorbed and the drug reaches the blood circulation. Since the total amount of drug is exposed in the gastrointestinal medium and is available for absorption, the rate and amount of drug absorption increases exponentially and the blood drug concentration steadily increases with time. As the blood drug concentration attains a certain concentration, known as the minimum effective concentration, the therapeutic onset of drug action takes place. The time at which the therapeutic onset of drug action occurs is called the time of onset of action. Gradually with time the plasma drug concentration increases to attain the maximum plasma drug concentration. When the plasma drug concentration exceeds a certain concentration, known as the maximum safe concentration, side effects of the drug starts to appear. After the maximum plasma concentration, the blood drug concentration starts to decline and is known as the elimination phase. So far the drug concentration is above the minimum effective concentration, the therapeutic effect of the drug persists, after which the drug therapeutic effect terminates. The time at which the drug therapeutic effect terminates is known as the termination of action, and at this point the second dose of the drug is to be given to maintain a steady therapeutic action of the drug. Thus the plasma drug concentration fluctuates and is known as the “see-saw” or “peak-valley” pattern of plasma concentration. The typical plasma drug concentration v/s time curve after oral administration of drug is given in Fig. 1.1.

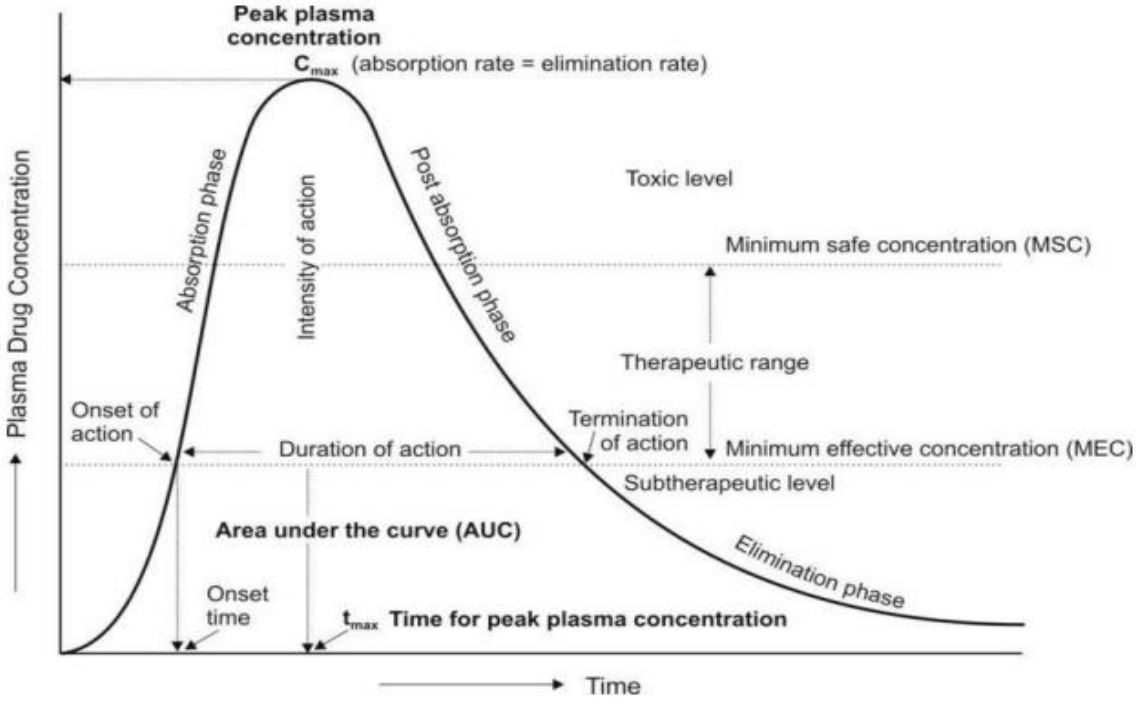

Fig. 1.1. The Plasma drug concentration v/s time curve.

If it is necessary to keep a sustained therapeutic plasma level of drug between the medication intervals, then a greater drug dose has to be dispensed. This higher drug dose may produce inordinately high and often toxic drug levels for significant periods. For attenuating toxic manifestations due to high drug levels, the dose of the drug has to be reduced. This may, on the other hand, produce plasma levels of the drug which for much of the period of treatment will remain below the threshold efficacy. In either case, the fraction of administered dose utilized by the patient is depressingly small amount. Maximum availability of the drug from drug delivery systems utilizing minimum amounts of the drugs can be achieved by repeated administration of small increments of the total dose. However, uninterrupted dispensing of the drugs by conventional delivery systems is both impractical and impossible. Repeated administration of the drug may also be associated with chronic side effects of the drug. The cost of therapy also escalates and all these factors contribute towards poor patient compliance and acceptability.

Thus, the conventional tablet dosage form has the following limitations:

1. The blood drug concentration (i.e. the site of drug action) varies over subsequent dosing intervals even at the "steady state" situation. It is difficult to sustain a fixed therapeutic drug concentration at plasma for the duration of treatment. At best, the average of the minimum and maximum plasma concentrations of each subsequent dose remains constant for the period of drug treatment.

2. The variations in the plasma drug concentrations may result in an under or over medicated patient for periods of time if the values of steady state maximum and minimum plasma concentrations fluctuates beyond the therapeutic limits of the drug.
3. Frequent dosing for the drugs having shorter biological half-lives are necessary to maintain steady state plasma concentration within the therapeutic limits. For such drugs, maintaining therapeutic plasma concentration is dependent to the consequences of the overnight no dose period and missed doses.
4. The regimens requiring frequent administration of conventional dosage form leads to patient non-compliance. This is an important reason behind therapeutic failure or inefficiency.

2. The modified release drug delivery system (MRDDS)

The rate and amount of drug release from the modified release drug delivery system is different from the conventional delivery system. The MRDDS is a broad concept and covers a variety of different approaches, shown in Fig. 1.2. They are:

2.1. Delayed release dosage forms: They release the drug after some time of drug administrations. There is a lag time between the drug administrations and the appearance of the drug in the blood. The delayed release formulations target the drug release at a distinct region of the gastrointestinal tract. Examples include colon specific drug release [2].

2.2. Gastro-resistant dosage forms: They are formulated not to release the drug in the acidic environment of the stomach. The drug is released at a higher pH of the small intestine. Enteric coated formulations fall in this category [3].

2.3. Extended release dosage forms: They minimize the frequency of drug administration compared to the conventional dosage forms. The plasma drug concentrations are sustained for longer time periods [3].

2.4. Repeat action dosage forms: They contain dual doses of a single drug, where one dose of the drug is in the form of immediate release and the other for delayed released. Bi-layered tablets are designed in this fashion [2].

2.5. Controlled release dosage forms: They are formulated to release the drug at a predetermined and predictable manner to maintain an optimal plasma concentration of the drug for extended time periods. The controlled release dosage forms show zero order

pharmacokinetics and sustains a steady drug level within the therapeutic window of the drug [4].

2.6. Sustained release dosage forms: They achieve the slow release of the medication over a prolonged duration after administration a single drug dose [4]. The sustained release dosage forms immediately release a dose of the drug to achieve the minimum plasma therapeutic concentration and then maintain the same for an extended duration.

Fig. 1.2. The various types of modified release drug delivery system.

3. The rationale behind the sustained release dosage forms

The sustained release dosage forms provide the following advantages over the conventional delivery systems (Fig. 1.3.) [2].

1) **Reduced variations of plasma drug levels**: Controlled release of the drug form the delivery system reduces the “peak-valley” or “see-saw” pattern of drug levels in the blood.

2) **Reduced frequency of drug administration**: Maintenance of constant therapeutic blood level for extended duration of time reduces the dosing interval.
3) **Enhanced patient conformity and convenience**: This is because of reduction in the frequency and number of doses required to sustain the intended therapeutic response. Even the therapeutic effect of the drug is maintained during overnight no-dose periods.
4) **Reduction in adverse effects**: Maintenance of constant plasma levels within the therapeutic range of the drug, reduces/eliminates any adverse effects of the drug.
5) **Reduction in overall therapy cost**: Because sustained-release dosage forms have better bioavailability, less dosage requirements, and more therapeutic efficacy, their initial costs may be higher than those of conventional forms, but eventual treatment costs is lower.

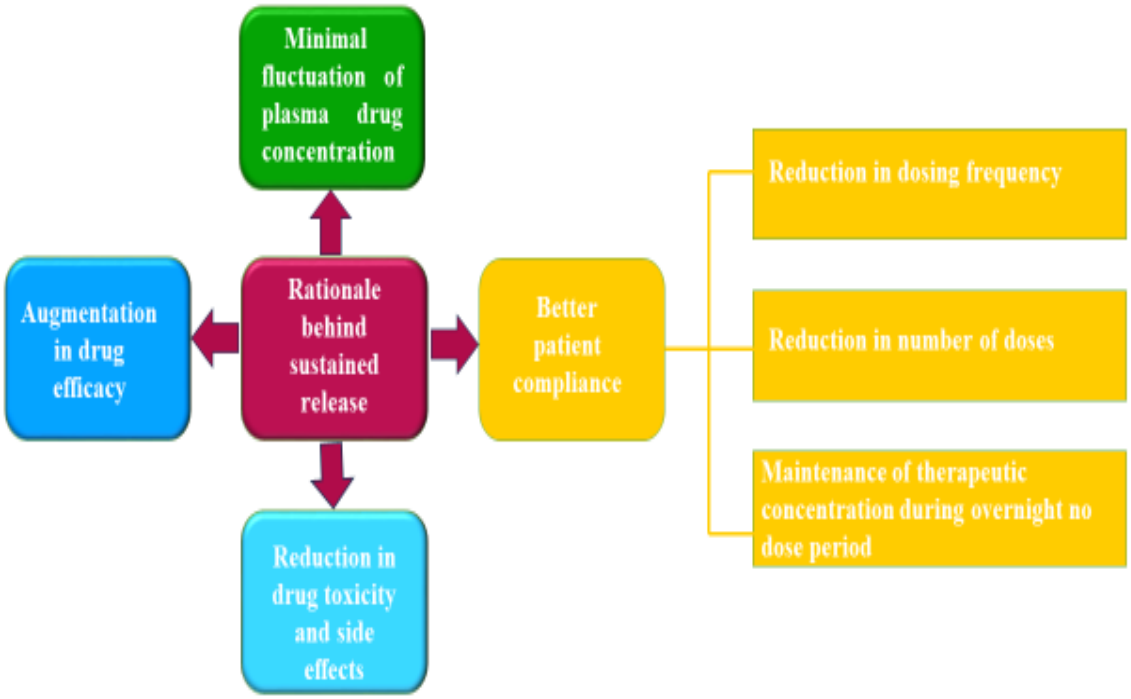

Fig. 1.3. The rationale behind sustained release drug delivery systems.

4. Drug candidates for sustained release dosage forms

All drugs are not suitable to be developed for sustained release dosage forms. Drug candidates suitable to be incorporated into a sustained release delivery system should have the following prerequisites [2]:

a) **The drug should not exhibit very slow or very fast rate of absorption or excretion**: Drugs having slower absorption and excretion rates are conventionally long acting and do not require to be incorporated into a sustained release delivery system. Drugs with extremely short half-lives (2 hours or less) are also not good candidates for sustained release systems.

b) **The drug should be evenly absorbed from the gastrointestinal system**: Drugs for sustained release should have optimum solubility and sufficient residence time in the gastrointestinal tract. Drugs which are not absorbed uniformly throughout the gastrointestinal tract are not suitable to be formulated into sustained release dosage forms.

c) **The dose of the drug should be small**: Large doses of the drug would be difficult to incorporate into the sustained release tablet or capsule as the patient may not be able to swallow the dosage form easily.

d) **The drug should possess a large therapeutic index**: Because of the technological constraints of accurate control over release rates, drugs with low therapeutic indices are not good candidates for development into sustained-release formulations.

e) **Drugs that are required for treatment of chronic conditions** are better suited for sustained release dosage forms as they require long term therapy.

5. Classification of sustained release drug delivery systems

The sustained release drug delivery systems can be broadly classified into two categories: the reservoir based system and the matrix based system [4].

a) **Reservoir based system**: Here, the drug is encapsulated within a polymeric coating layer. The solubilization of the encapsulated drug is dependent on the properties of the polymer (viscosity, molecular weight), coating layer thickness, and physicochemical properties of the drug like its particle size, solubility, and molecular weight.

b) **Matrix based system**: Here the drug is suspended/embedded within the polymeric matrix. Drug release from the matrix systems is either by dissolution or by erosion of the polymeric matrix.

6. Matrix tablets as sustained release drug delivery systems

Matrix technologies are prominent oral sustained release drug delivery systems because of their high level of reproducibility, simplicity, stability of the dosage forms and ease of scale-up, manufacturing, and process validation. Scientific progress in the field of matrix formulations have made sustained release product development easier, simpler, and improved. Matrix technologies are able to deliver a wide range of drugs with divergent biopharmaceutical and physicochemical properties. The basic components of a sustained release matrix tablet include:

-The drug,
-Matrix formers (release controlling agents),
-Matrix modifiers like wicking agents, channeling agents, solubilizers, etc.
-Lubricants and flow aiding agents.

Based on the nature of matrix forming materials, the matrix tablets can be differentiated into 3 types:

i) Lipid matrices
ii) Insoluble polymer matrices
iii) Hydrophilic colloidal matrices.

I) Lipid matrices:

A lipid matrix system consists of the drug, wax matrix formers, channelling agents, solubilizers, pH modifiers, antiadherents and lubricants. The powdered components are blended and compressed into tablets. Although these matrices can be easily manufactured using roller compaction, direct compression, or hot melt granulation, these are not commonly used now-a-days.

II) Insoluble polymer matrices:

In these systems, a drug is inserted into an inert polymer which is insoluble in gastrointestinal fluids. The major concerns of using insoluble polymer as matrix material is that the initiators and residual catalysts used in the preparation of polymers could be leached out of the drugs. Moreover, as the matrices remain intact during gastrointestinal transit, impaction may take place in large intestine and “ghost” matrix may be seen in the stool. Drug dissolution from an inert matrix is similar to leaching from a sponge. The release rate depends on drug solutions diffusing through capillary network formed between the compacted polymer particles. Modifications in tortuosity and porosity of the matrix alters the drug release rates.

III) Hydrophilic colloidal matrices:

This system consists of a blend of a drug, water swellable hydrophilic polymer, and glidant or lubricant. On contact with water the hydrophilic polymer swells, forms gel, undergoes erosion or dissolves in aqueous medium. The diffusion of water into the core matrix is controlled by the hydrated matrix layer which in turn controls the diffusion of drug through the matrix. The outer hydrated layer erodes with dilutions. The rate of erosion, however, depends on colloidal nature of the polymer.

The hydrophilic colloid matrix systems do not form true hydrogels. Instead they form viscous solution. In presence of water, the polymer forms a matrix the viscosity of which increases by the simple entanglement of the adjacent polymeric chains without cross linking. The chains are capable of moving relative to one another and this results in drug diffusion through the channels and pores, although the pathway is not fixed.

7. Natural polysaccharides based sustained release matrix tablets

Polysaccharides are the most widely available polymers and can be obtained from algal, plant and animal sources [5]. Polysaccharides consists of monosaccharide units linked together by glycosidic bonds. They are carbohydrates having great number of sugar molecules covalently interconnected by glycosidic bonds. D-glucose is the widespread basic component of the carbohydrates, though D-fructose, D-xylose, D-galactose, D-mannose, and L-arabinose are also seen. Amino sugars (D-galactosamine and D-glucosamine) and their derivatives (N-acetylmuramic acid) are also the monosaccharides units found in the polysaccharide chains. The polysaccharides can be of many categories. They can be non-ionic (like tara gum, xanthan gum), cationic (like chitosan) and can also be anionic (like sodium alginate, pectin). The polysaccharide can also be of plant origin (tara gum), animal origin (chitosan), and algal origin (carrageenan) [6].

Natural polysaccharides have been extensively used to develop sustained release matrix tablets owing to their biocompatibility, easy availability, non-toxicity and wide regulatory acceptance [7]. Different hydrophilic polysaccharides like xanthan gum, guar gum, sodium alginate, and gellan gum have been successfully used as matrix materials for sustained delivery of drugs. These hydrophilic polysaccharides can hydrate and swell in water and form a concrete, viscous layer over the surface of the matrix tablets by simple mix-up of the polymer chains [7]. The drug diffusion through the swollen viscous layer is controlled by the viscosity of that layer. The relationship between drug release and polymer viscosity has been cited in the literature [8]. The viscosity of the polymeric layer is dependent on the concentration and molecular

weight of the polymer. Higher the molecular weight and the concentration of the polymer, slower will be the drug diffusion from the viscous matrix layer. Drug release from HPMC matrices containing different concentrations of HPMC decreased with the increase in the polymer concentration in the matrices [9]. Similarly, drug release from chitosan (molecular weight 55 kDa) matrices was faster compared to drug release from chitosan (molecular weight 550 kDa) matrices. In addition to the viscosity of the swollen layer, the hydrating property of the polymer, and the mechanical and physical characteristics of the swollen layer also dictates the rate of drug release from the swollen matrix [8]. The release of drug from the hydrophilic matrix is also dependent on the extent of erosion of the polymeric matrix. Thus, the swelling, viscosity, and erosion of the polymeric matrix controls the rate of drug release from the polymeric matrix tablets.

Though natural polysaccharides find wide use in the development of sustained release matrix tablets, they also have some limitations. Natural polysaccharides like gum cordia and delonix regia exhibit exceptionally high and uncontrolled viscosity, which have profound effect on the drug release rate from the matrix [10, 11]. The high erosion of the alginate matrix at low pH values results in burst release of the drug [12]. The non-ionic nature of certain natural polysaccharides like delonix regia, xanthan gum results in low water dispersion capabilities at room temperature. Low water dispersion will retard the wetting and consequently the swelling of the matrix. All this will affect the drug release from the matrix. Quite often, a matrix based on a single polysaccharide cannot give the desired drug release pattern, which necessitates the addition of a release modifying agent to the matrix to get the tailored drug release.

8. Ionically cross-linked sustained release hydrogel matrix tablets using natural polysaccharides

Drug dissolution from a natural hydrophilic polysaccharide matrix is generally dictated by the erosion, swelling, and viscous nature of the concerned polysaccharide [7]. Drug release from such matrices can be tailored by controlling the viscosity, erosion and swelling of the polysaccharide. Crosslinking of the polysaccharide chains is a simple procedure to control the viscosity, erosion and swelling of the polysaccharide and thus to monitor the drug release from the hydrophilic polysaccharide matrix. Cross-linking can ionic or chemical. Chemical cross-linking of the polysaccharide polymer chains involves the use of harmful chemical reagents like glutaraldehyde, tripolyphosphate, and is thus not recommended. Ionic crosslink can be done under mild aqueous conditions by use of metal cations like Ca^{2+}, Ba^{2+}, Al^{3+}, Fe^{3+}. Ionic crosslink of natural polysaccharide chains is thus advocated.

The natural polysaccharides are available in different molecular weights and diverse chemical structure. The chemical structure of the polysaccharides contains numerous reactive groups which can take part in different chemical reactions. The various reactive groups that are present in the polysaccharide structure are the hydroxyl, amine, carboxyl, carbonyl groups etc.

The carboxylic acid group present in certain natural polysaccharides (like alginate, pectin and gellan) can selectively react with different metal cations (Ca^{2+}, Ba^{2+}, Al^{3+}, and Fe^{3+}) to form water insoluble hydrogels. Hydrogels are 3-D cross-linked polymeric structures capable of absorbing huge amounts of water. They are biodegradable and mimics biological tissue. Additionally, its soft and rubbery nature diminishes inflammatory reactions of neighbouring tissue. Hydrogels have wide applications in drug delivery, diagnostics, dietary supplements, cell encapsulation, and biological sensors [13]. Hydrogels are also employed in the development of contact lenses, prosthetic muscles, and wound care products [14].

In mild environments, sodium alginate can combine with divalent metal cations to produce hydrogels with an "egg-box" framework due to the huge number of carboxyl groups present in the structure [6]. Ca^{2+} ions are the most commonly used crosslinking agent among all other types of cations because it is inexpensive and non-hazardous. Diltiazem loaded Ca^{2+} - alginate hydrogel matrix has been prepared for sustained delivery of the drug [12]. The concentration of the cation was crucial for getting the optimum drug release characteristics. At low concentrations of the calcium ions diltiazem release was faster. Diltiazem release slowed down with the increase in the concentration of the Ca^{2+} ions. However, beyond a certain concentrations of the Ca^{2+} ions, the drug release again became faster. The Ca^{2+} ions reacts with the free carboxylic acid groups of alginate and forms the egg-box hydrogel structure. Increase in the concentration of the Ca^{2+} ions increases the crosslink density of the hydrogel, which decreases the drug release from the alginate matrices. However, after a certain concentrations of the Ca^{2+} ions when all the free carboxylic acid groups of alginate have been cross-linked, further increase in the concentrations of the Ca^{2+} makes them to be present in an excess uncross linked quantity within the matrix. The excess Ca^{2+} ions then acts as channelling agent within the matrix, increasing the diltiazem release from the matrix. Similar reports are available with calcium cross-linked pectin matrices [15]. Reduction in drug release was observed by increasing the amount of calcium acetate (as a source of calcium ions) from 6 mg/tablet to 12 mg/tablet. However, when the amount of calcium acetate in the tablet was 24 mg, drug release was faster. The reason was the formation of a non-homogeneous gel layer due to excessive crosslink at a high concentration of the calcium ions.

Ionic crosslink between chitosan and different anions like citrate, sulfate is also reported in literature [16]. Cross-linking with citrates and sulfates were immediate. The electrostatic interactions between the anions and chitosan significantly impacted the drug dissolution from the cross-linked matrix. In the simulated stomach fluid, the cross-linked matrices expanded, evenly disintegrated, and released the medication fully in five hours. On the other hand, the medication release was prolonged beyond 24 hours due to controlled swelling in the intestinal fluid.

9. Ionically cross-linked sustained release hydrogel matrix tablets using modified natural polymers

Natural polysaccharides as matrix materials for sustained delivery of drugs have been extensively exploited. But they suffer from some drawbacks. Natural polysaccharides are prone to microbial contaminations, varying physicochemical properties, batch-to-batch variations and possibility of heavy metal contaminations. More importantly, the aqueous solubility, uncontrolled rate of hydration and swelling, and rapid matrix erosion and degradations inhibit the natural polymers from becoming an effective matrix material [6]. Sodium alginate forms the water soluble alginic acid in an acidic environment, resulting in burst release of the loaded drug in the acidic pH [12]. Psyllium husk matrix is also associated with burst effects at low to intermediate polymeric concentrations. Grewia polysaccharide exhibits fast matrix erosion and drug release in phosphate buffer and greater swelling in acidic buffer pH 1.2 [17]. The rapid dissolution in aqueous media and low mechanical strength of gelatin limits its application as a sustained drug delivery carrier [18].

The polysaccharide polymeric chains have diverse chemical compositions and functional groups which lend themselves for various chemical derivatization. The derivatization of the polysaccharide polymeric chains can bypass the inherent problems of the polysaccharide and opens up for newer avenues of applications. Chemical derivatization of polysaccharides includes phosphorylation, sulfation, thiolation, carboxymethylation etc. Tailor made derivatives of the natural polysaccharides can be synthesised under simple and mild conditions. These tailored derivatives have been utilized in drug delivery and allied fields.

The derivatization of the natural polysaccharides are done to modify the physicochemical, rheological, and biological properties of the polysaccharides to make them potential candidates as drug delivery carriers. The solubility and viscosity profiles, swelling and erosion characteristics of the polysaccharides are fine-tuned according to the requirements of the drug delivery carriers by the chemical derivatization process.

Carboxymethylation is one of the most versatile and popular derivatization process. Carboxymethylation is done under mild alkaline aqueous environments and involves the incorporation of o-carboxymethyl groups in the polysaccharide polymeric chains. The hydroxyl groups of the polymers are substituted by the o-carboxymethyl groups during the reaction. Carboxymethylation imparts an anionic nature to the polysaccharide making it amenable to crosslink with divalent and trivalent metal ions and form water insoluble hydrogels, by a process known as ionotropic gelation. Ionotropic cross-linking of the polysaccharide polymeric chains is a suitable procedure for controlling the erosion, swelling, and drug delivery from the polysaccharide hydrogel matrix.

Ca^{2+}-cross-linked carboxymethyl xanthan hydrogel mini-matrix have been developed and the erosion, swelling, and prednisolone dissolution from the hydrogel mini-matrix have been investigated [7]. Burst swelling of the carboxymethyl xanthan mini-matirx was observed in the first hour, then declined in the next hour, and finally steadily declined with time in both buffer solution of pH 1.2 and 7.4. Calcium cross-linking of the carboxymethyl xanthan hydrogel mini-matrix attenuated the swelling of the mini-matrices substantially compared to carboxymethyl xanthan mini-matrix. Prednisolone delivery from uncross-linked carboxymethyl xanthan mini-matrix was slow, releasing 15% prednisolone in acid buffer pH 1.2 after 2 h, and 50% in alkaline buffer pH 6.8 in the next 8 h. The development of a viscous, thick gel layer surrounding the matrix surface was the cause of the delayed release of prednisolone. Calcium cross-linking of the carboxymethyl xanthan mini-matrix significantly impacted the prednisolone release behaviour from the mini-matrix. Up to 40% w/w concentration of $CaCl_2$ in the mini-matrix attenuated the prednisolone dissolution from the hydrogel mini-matrix. Further increment in $CaCl_2$ concentration to 50% w/w accentuated the prednisolone dissolution from the mini-matrix. At an optimum concentration, Ca^{2+} ions cross-link with the free carboxylic acid groups of the carboxymethyl xanthan chains and restricts the migration of the polymeric chains. This results in the evolution of a thick and rigid hydrogel layer on the mini matrix surface, which retards the release of prednisolone. However, at an increased concentration of the Ca^{2+} ions, they remain uncross-linked within the matrix. The unreacted Ca^{2+} ions within the matrix creates channels within the matrix resulting in rapid drug release.

Similarly, carboxymethylation of guar gum and development of sustained release hydrogel matrix have been reported [19]. The erosion, swelling, and metronidazole solubilization from the hydrogel matrix have been evaluated. The swelling profiles of the uncross-linked carboxymethyl guar gum tablet was more compared to the Ca^{2+} cross-linked carboxymethyl

guar gum hydrogel matrix. Percentage swelling of the uncross-linked carboxymethyl guar gum tablet was 172% in acid solution pH 1.2 at 2 h and 300% in buffer solution pH 7.4 after 5 h. Percentage swelling of the Ca^{2+} cross-linked carboxymethyl guar gum hydrogel matrix was 120% in acid solution pH 1.2 at 2 h and 240% in buffer solution pH 7.4 after 5 h. Percentage erosion profiles of the uncross-linked and cross-linked carboxymethyl guar gum matrix tablets also followed the same pattern. The erosion profiles of the uncross-linked carboxymethyl guar gum tablet was more compared to the Ca^{2+} cross-linked carboxymethyl guar gum hydrogel matrix. Percentage erosion profiles of the uncross-linked and cross-linked carboxymethyl guar gum matrix tablets after 10 h was 63.43% and 52.25% respectively. Metronidazole release from the uncross-linked and cross-linked carboxymethyl guar gum matrix tablets correlated well with the erosion and swelling profiles. Decrease in the percentage erosion and swelling of the matrix resulted in decrease in the drug release. Metronidazole release from uncross-linked carboxymethyl guar gum tablet was 25.56%, 40.53%, and 85.75% after 2 h, 5 h, and 12 h respectively. Metronidazole release from Ca^{2+} cross-linked carboxymethyl guar gum hydrogel matrix was 11.69%, 25.86% and 58.39% at 2 h, 5 h and 12 h respectively. The results indicated that cross-linked carboxymethyl polymeric hydrogel matrices is able to produce sustained release of the loaded drug.

References

1. Lachman L, Lieberman HA, Kanig JA. The Theory and Practice of Industrial Pharmacy. 3rd ed., Varghese Publishing House, Mumbai, 1987.

2. Loyd VA, Howard CA. Ansel's Pharmaceutical Dosage Forms and Drug Delivery Systems. 10th ed, Wolters Kluwer, Philadelphia, 2011.

3. Michael EA, Kevin MGT, Aulton's Pharmaceutics: The Design and Manufacture of Medicines. 4th ed., Elsevier 2013.

4. Adepu S, Ramakrishna S. Controlled Drug Delivery Systems: Current Status and Future Directions. Molecules. 2021;26:5905.

5. Mukherjee K, Dutta P, Badwaik HR, Saha A, Das A, Giri TK. Food industry applications of Tara gum and its modified forms. Food Hydrocolloids for Health. 2023;3:100107

6. Mukherjee K, Dutta P, Saha A, Dey S, Sahu V, Badwaik H, Giri TK. Alginate based semi-IPN and IPN hydrogel for drug delivery and regenerative medicine. J. Drug Deliv. Technol. 2024;92:105402.

7. Maity S, Sa B. Ca-carboxymethyl xanthan gum mini-matrices: Swelling, erosion and their impact on drug release mechanism. Int. J. Biol. Macromol. 2014;68:78–85.

8. Chakravorty A, Barman G, Mukherjee S, Sa B. Effect of carboxymethylation on rheological and drug release characteristics of locust bean gum matrix tablets. Carbohydr. Polym. 2016;144:50-58
9. Penkov D, Lukova P, Manev H, Dimitrova S, Kassarova M. Polymer Tablet Matrix Systems for the Controlled Release of Dry Betula pendula Leaf Extract. Polymers. 2023;15:3558.
10. Ali R, Masood HS. The Rheological Modeling and Effect of Temperature on Steady Shear Flow Behavior of Cordia abyssinica Gum. J. Food Process Technol. 2014;5(3):1000309
11. Pacheco-Aguirre J, Rosado-Rubio G, Betancur-Ancona D, Chel-Guerrero L. Physicochemical properties of carboxymethylated flamboyant (Delonix regia) seed gum. CyTA-Journal of Food. 2010;8(3):169–176.
12. Mandal S, Basu SK, Sa B. Sustained Release of a Water-Soluble Drug from Alginate Matrix Tablets Prepared by Wet Granulation Method. AAPS Pharm Sci. Tech. 2009;10(4):1348-1356.
13. Laftah WA, Hashim S, Ibrahim AN. Polymer hydrogels: a review. Polym. Plast. Technol. Eng. 2011;50:1475–1486.
14. Varaprasad K, Raghavendra GM, Jayaramudu T, Yallapu MM. Sadiku R. A mini review on hydrogels classification and recent developments in miscellaneous applications. Mater.Sci.Eng C. 2017;79:958–971.
15. Sungthongjeen S, Sriamornsak P, Pitaksuteepong T, Somsiri A, Puttipipatkhachorn S. Effect of degree of esterification of pectin and calcium amount on drug release from pectin-based matrix tablets. AAPS Pharm Sci. Tech. 2004;5(1):9.
16. Shu XZ, Zhu KJ. Controlled drug release properties of ionically cross-linked chitosan beads: the influence of anion structure. Int. J. Pharm. 2002;233:217–225.
17. Nep EI, Mahdi MH, Adebisi AO, Dawson C, Walton K, Bills P, Conway BR, Smith AM, Asare-Addo K, The influence of hydroalcoholic media on the performance of Grewia polysaccharide in sustained release tablets. Int. J. Pharm. 2017;532(1): 352-364.
18. Migliaresi C, Chen J, Mangilio D, Bonani W, Qian Q. Modulating the release of drugs from alginate matrices with the addition of gelatin microbeads. J. Bioact. Compat. Pol. 2014;29(3): 193-207.
19. Singh R, Maity S, Sa B, Effect of ionic crosslink on the release of metronidazole from partially carboxymethylated guar gum tablet. Carbohydr. Polym. 2014;106:414-421.

Chapter 2: Literature Survey

Maity et al. developed carboxymethyl xanthan gum hydrogel tablets using calcium chloride as cross-linking agent and investigated the influence of the calcium ions on prednisolone release behavior from the hydrogel matrix tablets [1]. The hydrogel matrices were within the pharmacopoeial limits of weight variation, friability and content uniformity. The in-vitro prednisolone dissolution from the hydrogel matrix was greatly influenced by the concentration of the calcium ions in the matrices. Matrix tablets prepared with only carboxymethyl xanthan gum released prednisolone slowly and no burst release effect was observed in pH 1.2, pH 7.4 and pH 6.8. The carboxymethyl xanthan gum matrices released 13%, 25% and 51% prednisolone after 2 h, 5 h, and 10 h respectively in pH 1.2, pH 7.4 and pH 6.8. The slow release of prednisolone was because of the poor solubility of prednisolone in the respective buffer media and the formation of a viscous, swollen polymer layer over the tablet surface which hindered drug dissolution. The introduction of calcium ions into the hydrogel matrices produced concentration-dependent variations in prednisolone release. Calcium ions concentration up to 40% w/w of the matrices produced slower prednisolone release, beyond which prednisolone release became faster. Prednisolone release from matrices containing 40%w/w calcium ions was 5%, 12%, and 20% after 2 h, 5 h, and 10 h respectively in pH 1.2, pH 7.4 and pH 6.8. Prednisolone release accentuated when the concentration of calcium ions was 50% w/w of the matrices. Prednisolone release from matrices containing 50% w/w calcium ions was 12%, 32%, and 85% after 2 h, 5 h, and 10 h respectively in pH 1.2, pH 7.4 and pH 6.8. The carboxyl groups of the carboxymethyl xanthan gum crosslinks *in situ* with the calcium ions to form hydrogels. This crosslink restricts the migration of the polymeric chains resulting in the evolution of true gel layer which retards the prednisolone dissolution from the hydrogel matrices. The concentrations of the carboxyl groups are critical in the formation of the true hydrogel layer. At an optimum concentration of the calcium ions effective crosslink takes place with the carboxyl groups. When the concentration of the ions is more, excessive crosslink takes place which weakens the gel strength due to formation of a non-homogenous gel layer. This resulted in faster prednisolone release. Additionally, the excess (than that required for optimum crosslink) crosslinking ions acts as channeling agents which promotes faster prednisolone delivery. The authors concluded that the concentration of the crosslinking ions are crucial to get the tailored drug release from the matrices.

Calcium gluconate-sodium alginate hydrogel matrix tablets was developed to investigate the release of diltiazem, a water soluble drug, from the hydrogel matrix [2]. The hydrogel tablets were prepared by the wet granulation technique. The influence of calcium gluconate on the

hardness of the tablets and diltiazem release at different pH was evaluated. Additionally, the impact of different formulation parameters like ratio between sodium alginate and calcium gluconate, hardness of the tablets, and drug load on diltiazem dissolution from the matrices have also been evaluated. Calcium gluconate induced significant effects on the hardness of the tablets. At a constant compressional force, increase in the amount of calcium gluconate in the hydrogel tablets made the tablets harder, although the tablet thickness was almost constant. When the ratio between sodium alginate and calcium gluconate was high at 3:1, diltiazem release was fastest, and diltiazem release decreased as the ratio between sodium alginate and calcium gluconate was gradually decreased to 1:2. Further decrease in the ratio between sodium alginate and calcium gluconate to 1:3, made diltiazem release faster. The diltiazem release pattern from the hydrogel tablets were the same in both the acidic and alkaline buffer media of pH 1.2 and pH 6.8. Diltiazem release in acidic pH 1.2 after 2 h was rapid, ranging from 50% to 68% according to the ratio between sodium alginate and calcium gluconate. Following dissolution in acidic pH 1.2 for 2 h, the hydrogel tablets were transferred to alkaline media pH 6.8. Diltiazem release in pH 6.8 was extended from 4 h to 13 h depending on the ratio between sodium alginate and calcium gluconate. Solubilization of calcium gluconate during wet massing and dissolution study resulted in the formation of Ca^{2+} ions. The Ca^{2+} ions reacted with the carboxyl groups of sodium alginate to form the calcium alginate gel. In acidic pH, sodium alginate is converted to alginic acid. Though alginic acid is water-insoluble, it can swell appreciably. Matrices made with the highest ratio between sodium alginate and calcium gluconate (3:1), contained the highest and lowest amount of sodium alginate and calcium gluconate respectively. An increase in the amount of sodium alginate in the hydrogel tablets increased the formation of alginic acid, that in turn increased the overall swelling of the tablets and resulted in rapid diltiazem release from the hydrogel tablets in the acid media. As the ratio between sodium alginate and calcium gluconate is decreased, the formation of alginic acid is decreased and that of calcium alginate gel is increased. An increase in the calcium alginate gel reduced the swelling of the matrices and formed a true highly viscous gel layer. This resulted in a decrease in diltiazem release with a decrease in the ratio between sodium alginate and calcium gluconate. However, when the ratio between sodium alginate and calcium gluconate is decreased to 1:3, the diltiazem release increases. Probably at such a low ratio between sodium alginate and calcium gluconate, all sodium alginate has been converted to calcium alginate and some excess unreacted calcium gluconate remained inside the matrices, which acted as a channeling agent to increase diltiazem release. An increase in the hardness of the tablets decreased the matrix porosity, which delayed the drug release. An increase in drug loading in

the matrices increased the concentration gradient of the drug within the matrix resulting in faster drug diffusion and drug release. The authors concluded that optimization of the concentration of the crosslinking agent and the polymer is crucial to get the desired drug pattern from the matrices.

Mandal et al. reported the synthesis of polyacrylamide grafted sodium alginate copolymers and their partially hydrolyzed forms [3]. Three copolymers and their partially hydrolyzed forms were synthesized having percentage of grafting 110%, 256%, and 418%. The copolymers and their partially hydrolyzed forms were then used for the development of the Ca^{2+} cross-linked sustained-release diltiazem hydrogel tablets. The weight variation, content uniformity, and friability of the hydrogel tablets complied with the requirements of the official compendia. The release of diltiazem from the hydrogel tablets prepared with different percentages of grafting in acid media pH 1.2 was almost the same and was between 34.5%-34.9%. However, in the intestinal pH buffer, the release of diltiazem got faster with the increase in the percentage grafting of the copolymer. Diltiazem release was 79% after 12 h from the hydrogel matrices prepared with a copolymer having a percentage grafting of 110%, while complete diltiazem release was obtained after 5.5 h from hydrogel matrices prepared with a copolymer having a percentage grafting 418%. The diltiazem release from the hydrogel matrices prepared with the partially hydrolyzed forms of the copolymers was the same as that from the grafted copolymers in acidic buffer media. However, in the intestinal fluid, the diltiazem release decreased with the increase in the percentage grafted of the partially hydrolyzed forms of the copolymers. The authors opined that drug release from a co-polymeric matrix is dependent upon several interlinked parameters of which swelling and viscosity of the co-polymeric matrix play an important role. In aqueous media, the co-polymeric matrix will absorb water and form a gel layer around it. The increase in viscosity of the gel layer will retard the diffusion of the drug, while the increase in the swelling of the gel layer will promote the drug release. An increase in the percentage grafting of the copolymers increased the hydrophilic amide groups in the copolymers, which facilitated swelling of the co-polymeric matrix. An increase in swelling of the co-polymeric hydrogel matrix increased the diltiazem release from the matrices. The viscosity of the gel layer of the matrices prepared with the partially hydrolyzed forms of the copolymers increased substantially with the increase in the percentage grafting. The viscosity of the co-polymeric partially hydrolyzed gel layer having a percentage grafting of 110% was 757 cP, and that of the gel layer having a percentage grafting of 418% was 2577 cP. The increase in the viscosity of the gel layer of the hydrogel matrices prepared with the partially

hydrolyzed forms of the copolymers resulted in a decrease in diltiazem release from the matrices. An increase in the Ca^{2+} ion concentration in the matrices increased the diltiazem release from the matrices prepared irrespective of the grafted copolymers or their partially hydrolyzed forms. Ca^{2+} was incorporated into the matrix tablets so that it can react with the guluronic acid residues of sodium alginate and form a water-insoluble calcium alginate matrix which can prolong the diltiazem release. However, the Ca^{2+} ions increased the diltiazem release. Grafting reduced the guluronic acid residues of the grafted polymer. Ca^{2+} ions were thus unable to form the water-insoluble calcium alginate matrix and acted as a channeling agent to fasten diltiazem release.

Saha et al. reported the development of grafted tamarind kernel polysaccharide based hydrogel matrices for sustained delivery of drug [4]. Tamarind kernel polysaccharide as a sole matrix material was not suitable for the development of the matrix tablets because the matrices disintegrated within 5 min of dissolution. Grafting of tamarind kernel polysaccharide was done to bypass the problem of the native tamarind kernel polysaccharide. Grafting of tamarind kernel polysaccharide was done by the free radical polymerization method using ammonium persulfate as the initiator. Optimization of the grafting reaction was done and the grafted copolymer was characterized. However, the tablet matrices based on the grafted copolymer also disintegrated within 5 min of the dissolution study. Aluminium hydroxide [$Al(OH)_3$] was then introduced into the formulation to serve two purposes. The dissociation of aluminium hydroxide during the dissolution study of tablets would furnish Al^{3+} ions. The Al^{3+} ions would crosslink with the carboxylic groups of the grafted polymer to form a cohesive mass which would prevent the tablet to disintegrate and at the same time the cross-linked grafted copolymer would form a water-insoluble viscous hydrogel layer over the tablet surface which would produce sustained delivery of the loaded drug. The thickness and weight variation of the tablets were within ±5% of the respective mean values. The content uniformity of the tablets was as per the USP limits. $Al(OH)_3$ produced significant changes in the hydrogel tablets. The disintegration time of the tablets containing 30% w/w $Al(OH)_3$ was 2 h and that containing 40% w/w of $Al(OH)_3$ was extended up to 7 h. Hydrogel tablets containing more than 40% w/w of $Al(OH)_3$ didn't disintegrated. The swelling and erosion profiles of the tablets were greatly influenced by the concentration of $Al(OH)_3$ in the tablets. $Al(OH)_3$ concentration of up to 50% w/w in the matrices reduced the erosion and swelling profiles of the tablets. Drug release from the hydrogel tablets also followed the same pattern and was extended up to 10 h. The drug release mechanism from the hydrogel tablets was by the Fickian diffusion model. The authors

concluded that Al^{3+} cross-linked grafted tamarind kernel polysaccharide may serve as an excellent matrix for the sustained delivery of drugs.

Bayomi et al. prepared theophylline loaded sustained-release hydrogel tablets by moisture activated dry granulation method [5]. Definite amounts of theophylline, sodium alginate, and calcium gluconate were blended and triturated with 3% demineralized water, passed through #10 mesh and then oven dried for 4 h at 40ºC. The dried granules were then mixed with different concentrations (2.5% to 10% w/w) of carbopol 934 and magnesium stearate and compressed in 9 mm flat punches. The moisture activated dry granulation method provided an efficient cross-linking reaction between sodium alginate and calcium gluconate. The granules were irregularly shaped and had a rough surface texture, but displayed acceptable flow properties, with angle of repose values between 35º-37º. An increase in calcium gluconate content in the tablet composition made the granules hard and increased the granules size. The friability of the granules also decreased with the increase in calcium gluconate content in the tablet. All these observations indicated the optimum cross-linking reaction between calcium gluconate and sodium alginate. The addition of carbopol 934 to the granules further improved the flow properties of the granules as indicated by the decrease in the angle of repose of the granules to 29º-31º. Theophylline release from hydrogel tablets was evaluated. The release of theophylline was dependent on the ratio between calcium gluconate and sodium alginate. At low ratios of calcium gluconate and sodium alginate (3:4), theophylline release was faster. When the ratio was increased to 1:1 and 5:4, theophylline release decreased. The results pointed out that calcium alginate formed by the interaction between calcium gluconate and sodium alginate acted as a reservoir for sustaining theophylline release. Calcium alginate is a hydrogel matrix that is insoluble and hydrophobic. The poor hydration and slow diffusion of theophylline from the calcium alginate hydrogel matrix resulted in sustained dissolution of theophylline from the matrix. In-vitro theophylline release profiles from the hydrogel matrices were compared with commercial formulations. The commercial tablets released the total theophylline in 3 h, while the formulated hydrogel tablets released the total theophylline after 6 h.

Carboxymethylation of guar gum and the development of sustained-release hydrogel matrix have been reported [6]. The erosion, swelling, and metronidazole solubilization from the hydrogel matrix have been evaluated. The swelling profiles of the uncross-linked carboxymethyl guar gum tablet were more compared to the Ca^{2+} cross-linked carboxymethyl guar gum hydrogel matrix. The percentage swelling of the uncross-linked carboxymethyl guar

gum tablet was 172% in acid solution pH 1.2 at 2 h and 300% in buffer solution pH 7.4 after 5 h. The percentage swelling of the Ca^{2+} cross-linked carboxymethyl guar gum hydrogel matrix was 120% in an acid solution of pH 1.2 at 2 h and 240% in a buffer solution of pH 7.4 after 5 h. Percentage erosion profiles of the uncross-linked and cross-linked carboxymethyl guar gum matrix tablets also followed the same pattern. The erosion profiles of the uncross-linked carboxymethyl guar gum tablet were more compared to the Ca^{2+} cross-linked carboxymethyl guar gum hydrogel matrix. Percentage erosion profiles of the uncross-linked and cross-linked carboxymethyl guar gum matrix tablets after 10 h were 63.43% and 52.25% respectively. Metronidazole release from the uncross-linked and cross-linked carboxymethyl guar gum matrix tablets correlated well with the erosion and swelling profiles. A decrease in the percentage erosion and swelling of the matrix results in a decrease in the drug release. Metronidazole release from uncross-linked carboxymethyl guar gum tablet was 25.56%, 40.53%, and 85.75% after 2 h, 5 h, and 12 h respectively. Metronidazole release from Ca^{2+} cross-linked carboxymethyl guar gum hydrogel matrix was 11.69%, 25.86% and 58.39% at 2 h, 5 h and 12 h respectively. The mechanism of metronidazole release from uncross-linked and cross-linked carboxymethyl guar gum matrix tablets followed anomalous or non-Fickian release kinetics. The results indicated that cross-linked carboxymethyl polymeric hydrogel matrices are able to produce sustained release of the loaded drug.

In-situ Al^{3+} or Ca^{2+} cross-linked sodium alginate polymeric hydrogel matrices have been prepared for sustained theophylline release [7]. The effect of Al^{3+} or Ca^{2+} ions on theophylline release from the matrices has been evaluated. An increase in the concentration of Al^{3+} ions from 0.0001 to 0.00068 moles resulted in a decrease in theophylline release from the matrices. Matrices containing 0.0001 moles of Al^{3+} ions released 96% of theophylline after 8 h of dissolution, and matrices containing 0.00034 and 0.00068 moles of Al^{3+} ions released 40% and 30% of theophylline respectively in the same time frame. An increase in the concentration of Ca^{2+} ions from 0 to 0.00034 moles expedited theophylline release from the matrices, but a further increase in the concentration of Ca^{2+} ions decreased the theophylline release from the matrices. The release pattern of theophylline from the Ca^{2+} ions cross-linked alginate matrices indicates that at low concentrations of the Ca^{2+} ions in the matrices theophylline release is faster, while at high concentrations the theophylline release is slower. At low concentrations of the Ca^{2+} ions, the water-insoluble hydrogel that is formed by the crosslink between the Ca^{2+} ions and carboxylic acid groups of alginate polymeric chains is not strong enough to control and retard the diffusion and release of theophylline from the matrices. When the concentrations

of the Ca^{2+} ions are increased, an effective crosslink reaction takes place and a better, stronger hydrogel layer is formed that is capable of decreasing the diffusion of theophylline from the hydrogel matrix. Since Al^{3+} ions have an extra positive charge, it is able to crosslink effectively and efficiently even at low concentrations to form a strong, and stiff hydrogel layer which is capable of reducing the penetration of the dissolution fluid into the matrix and diffusion of theophylline from the matrices. The authors also observed different theophylline release profiles from the matrices containing the same molar concentrations of the Al^{3+} ions and Ca^{2+} ions. At the same molar concentrations of the Al^{3+} ions and Ca^{2+} ions, aluminium ions are more effective in retarding theophylline release from the matrices compared to the Ca^{2+} ions. Low concentrations of Al^{3+} ions (0.00034 moles) and high concentrations of Ca^{2+} ions (0.00068 moles) produced almost the same theophylline release profiles. The difference in theophylline release from the matrices can be attributed to the difference in crosslink capacities/strength of the respective metal cations. The additional positive charge of the Al^{3+} ions makes it possible to crosslink efficiently at low concentrations and produce a strong and rigid hydrogel layer capable of retarding theophylline release. This was the reason behind Al^{3+} ions retarding theophylline release at low concentrations and also producing more sustained theophylline release at equal concentrations with Ca^{2+} ions. The authors concluded that the concentrations of the metal cations are crucial to get the desired drug release from the matrices.

References

1. Maity S, Sa B. Ca-carboxymethyl xanthan gum mini-matrices: Swelling, erosion and their impact on drug release mechanism. Int. J. Biol. Macromol. 2014;68:78–85.

2. Mandal S, Basu SK, Sa B. Sustained Release of a Water-Soluble Drug from Alginate Matrix Tablets Prepared by Wet Granulation Method. AAPS Pharm Sci. Tech. 2009;10(4):1348-1356.

3. Mandal S, Ray R, Basu SK, Sa B. Evaluation of a Matrix Tablet Prepared with Polyacrylamide-g- Sodium Alginate Co-polymers and Their Partially Hydrolyzed Copolymers for Sustained Release of Diltiazem Hydrochloride. J. Biomater. Sci. Polym. Ed. 2010; 21(13):1799-1814.

4. Saha A, Mukherjee K, Ghosh B, Giri TK. Grafted tamarind kernel polysaccharide based Al^{3+} cross-linked hydrogel matrices for sustained release of drug in the gastrointestinal milieu. Pharmaceutical Science Advances. 2024;2:100022.

5. Bayomi MA, Al-Suwayeh SA, El-Helw ARM. Excipient-Excipient Interaction in the Design of Sustained-Release Theophylline Tablets: In Vitro and In Vivo Evaluation. Drug Dev. Ind. Phar. 2001;27(6):499-506.

6. Singh R, Maity S, Sa B, Effect of ionic crosslink on the release of metronidazole from partially carboxymethylated guar gum tablet. Carbohydr. Polym. 2014;106:414-421.

7. Nokhodchi A, Tailor A. In situ cross-linking of sodium alginate with calcium and aluminum ions to sustain the release of theophylline from polymeric matrices. IL FARMACO. 2004;59: 999–1004.

Chapter 3: Tara Gum

1. Source

Tara gum (TG) is a seed endosperm galactomannan non-ionic polysaccharide obtained from *caesalpinia spinose* tree. It is generally known as tara and belongs to the family Fabaceae or Leguminosae [1]. The origin of the plant is in Peru and it is also seen in northern and southern America. The gum is identified by different names in different countries like peruvian carob, guaranga, and huarango [2]. TG is extensively grown and its pods are a good source of pyrogallol tannin. Some specifications related to TG is given in Table 3.1.

Table 3.1. Some basic information about TG [3].

Description	Properties
Plant Source	*Caesalpinia spinosa*
Seed Endosperm (%)	20–22
Seed size	10 mm
Seed Coat (%)	Around 40%
Seed Cotyledon (%)	38–40
M/G ratio	2.5–3
Acid insoluble matter	< 2
E Number	E4 17
Loss on drying	< 15
Protein	< 3.5
Total Ash	< 1.5

2. Structure

Galactomannan TG has related functional and structural characteristics like other galactomannans fenugreek gum and locust bean gum. TG backbone is primarily comprised of a linear main chain of (1–4)- β- d -mannopyranose units joined by (1–6) linkage with α- d - galactopyranose units (Fig. 3.1.) [4-5]. The Mannose:Galactose (M:G) ratio of TG is 3:1. Several attributes of galactomannans (like solubility) are significantly predisposed by the M:G ratio. The solubility increases with an increase in galactose content. Solutions of TG achieves increased viscosity rapidly when dispersed in water and also have synergistic interaction with xanthan gum [6].

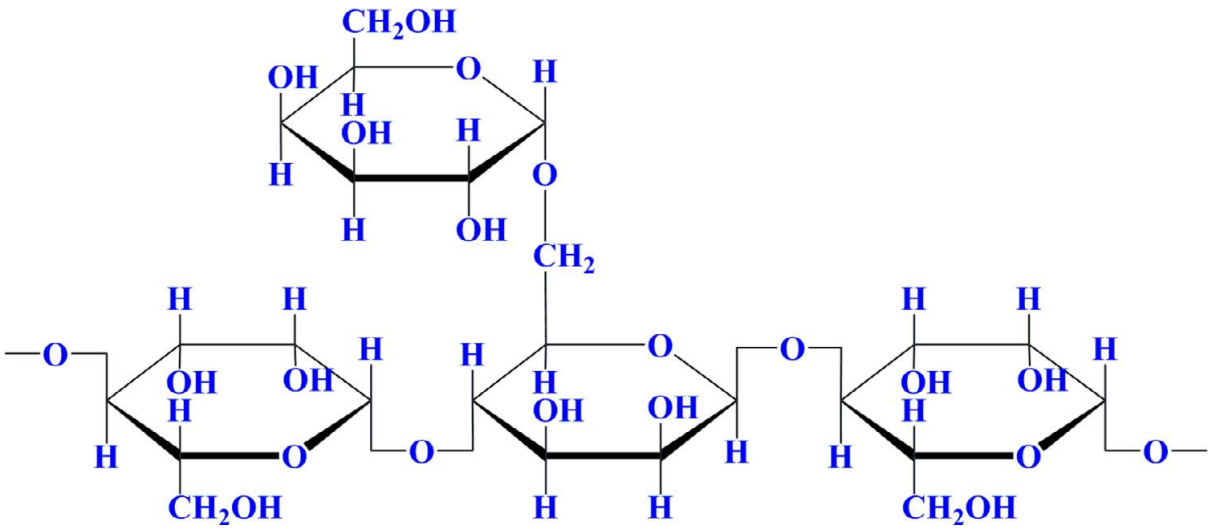

Fig. 3.1. Structure of Tara gum. Adapted from reference [4].

3. Physicochemical characteristics

At room temperature, TG dissolves in water and achieves 3/4th of its total viscosity capacity [7]. When TG is heated to 95ºC and then temperature is brought down to 25ºC, the gum becomes opaque with tan-colored sols. Viscosities of 1% w/v TG solutions attains viscosities of 300 to 400 cps, which is influenced by the extraction quality of the gum. At any fixed shear rate, viscosities of TG solutions remain stable over different pH conditions. TG solutions represent pseudoplastic rheology.

Polymeric chains of TG can be cross-linked by certain metal ions. Borax is a recognized cross-linker for galactomannans, and can crosslink with TG. Borax binds with cis-hydroxyl groups of D-mannosyl or D-galactosyl moieties when solution pH is more than 9. Chromium (III) and antimony (III) also cross-links with TG solutions [8]. TG solutions are also gelled by intermolecular associations. This is accomplished by adding excess sucrose or ethylene glycol or freeze-thaw process. All these processes decrease or eliminate the free water available from the solutions, thereby making the gum solution more concentrated and prompting interaction [6].

4. Rheological properties of TG

The rheological profiles of TG dispersions and how it is affected by temperature, pH and salts were analysed in detail by Wu et. al. [2]. TG solutions at concentration range 0.2-1% w/v are shear thinning in nature when the shear rate is between 0-100/s. The TG solutions viscosity decreases with the elevation in the shear rate, pointing out the shear thinning non-Newtonian characteristics of the gum (Fig. 3.2A.). The viscosity of TG sols is also influenced by the concentrations of the solutions. The viscosity of the TG solutions bears a direct relationship with the concentration of the gum solution. The 1% w/v TG solution viscosity is higher as

compared to TG solutions of lower concentrations (Fig. 3.2A.). The viscosity of TG solutions is due to the development of hydrogen bonds between the hydroxyl groups of the gum. This bond formation results in entanglement of the TG chains. Increase in gum solution provides more hydroxyl groups, strengthening the hydrogen bond formations and increasing the entanglement of the polymeric chains. This attributes to increase in viscosity of TG solutions with the increase in gum concentrations. If any external force is applied to the TG solutions the hydrogen bonds are broken and this results in an open chain structure of the gum, reducing the viscosity of TG solutions. This explains the shear thinning nature of TG solutions. TG solutions also exhibit non-thixotropic characteristics. The shear rate of 0.5% w/v TG solution was slowly increased to 300/sec and then kept there for some time and then again slowly decreased. The down-curve and up-curve nearly superimposed and hysteresis loop was absent (Fig. 3.2B.). This indicated that the broken microarchitecture is quickly rebuilt and the solution immediately attains its original viscosity upon decreasing the shear rate.

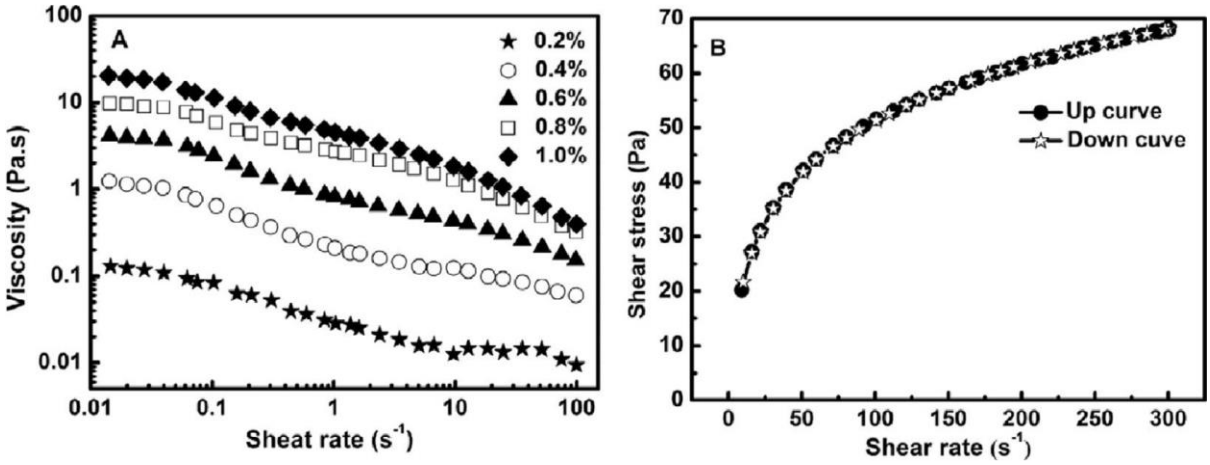

Fig. 3.2. A) The effect of TG concentration on TG solutions viscosity. B) The non-thixotrophic nature of TG solutions. Adapted from reference [2].

The TG solution viscosities are greatly affected by the presence of salts. The surge in the $CaCl_2$ concentration decreased the viscosities of TG solutions [9]. Divalent salts have a greater viscosity reducing affect than monovalent salts [10]. Sucrose also affects the TG solutions viscosity. The viscosity of 0.5% w/v TG solutions at low concentrations (less than 20mg/ml) of sucrose solutions was low. However, at high concentrations of sucrose (30 mg/ml) the viscosity of TG solutions increased. Atomic force microscopy images can be used to explain such behaviour (Fig. 3.3.). TG molecules in solution state are in stretched and expanded form due to intermolecular electrostatic repulsive forces, and thus structure resembles branched-like patterns. Addition of sucrose in small amounts decreased the water accessible for hydration of gum and the complete stretching and branch like orientation of the TG molecules are hindered.

Accordingly, at high concentrations, the viscosity would have further diminished. However, at high concentration of sucrose, the density of the TG solutions increases significantly, which contributes for high viscosity of the TG solutions at high concentrations of sucrose.

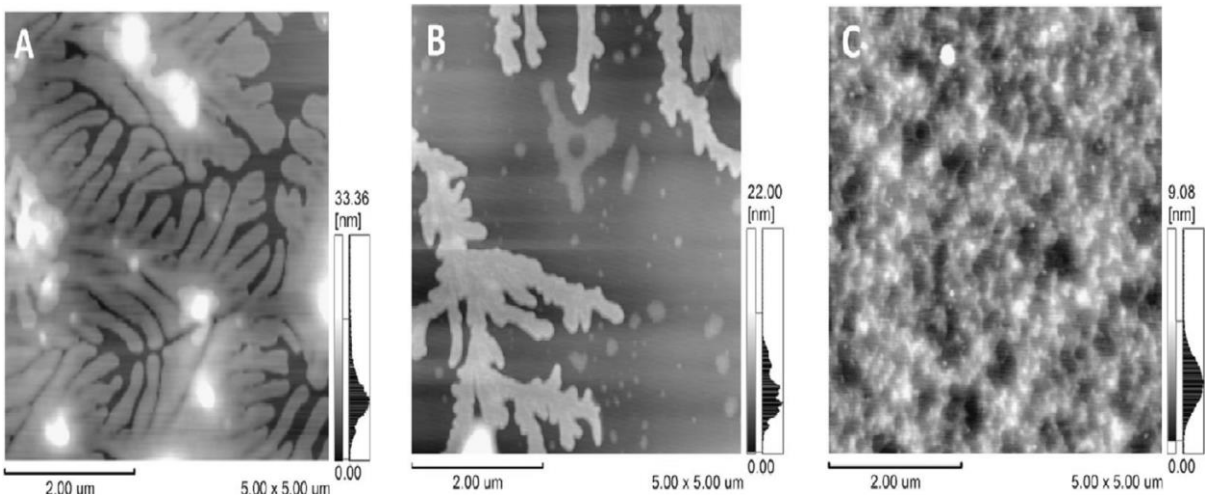

Fig. 3.3. Atomic force microscopy images of 0.5% TG solutions. Concentration of sucrose 0 mg/ml (A). 5 mg/ml (B), and 30 mg/ml (C). Adapted from reference [2].

5. Toxicological profile of TG

Toxicity of TG has been studied in detail [11-12]. The study revealed that there is no sign of acute or chronic toxicity or any carcinogenic effect of TG in mice and rats at doses of 25000 and 50000 ppm for 103 weeks. Genotoxicity of TG was examined in strains of *Salmonella Typhimurium.* Negative results were obtained in all the strains in the presence or absence of metabolomic stimulation. In another *in vivo* study, the number of micronuclei in mice treated with TG didn't show any statistically significant difference to the equivalent control groups. A three-generation reproduction study was conducted on Sprague Dawley (CD) strain rats. The rats received 5% TG while the control group received 5% α-cellulose. Treated rats gave birth to normal offspring's in each generations and the mean percentage viable progeny between the treated and control didn't deviate much. All reproductive indices like fecundity, mating, fertility index, were almost comparable between the treated and the control group. Foetal development and embryogenic studies were conducted on 25 pregnant wistar rats. The rats were fed with different concentrations of TG ranging from 0.1% to 5% TG. The study revealed no TG-induced abnormalities in any dose groups nor any dose-related anomalies in any reproductive data in the treated and control group. Foetuses were examined and no teratogenic and embryogenic effects related to TG consumption was reported. A reverse mutation study on TG was reported using 05 strains of *Salmonella Typhimurium.* No TG induced genotoxicity was reported.

6. Derivatizations of TG

TG contains numerous hydroxyl groups in its structure. This hydroxyl groups can be substituted with other functional groups to produce the TG derivative having personalised physicochemical and biological properties. TG has been widely derivatized to meet specific requirements.

Carboxymethylation of TG has been reported [13]. Carboxymethylation was done by base catalysed reaction with sodium hydroxide and monochloroacetic acid. The reaction conditions were optimized. Molar mass of the carboxymethyl TG was determined by static light scattering method. Molar mass of carboxymethyl TG was 6.28×10^5. Zeta potential of carboxymethyl TG was found out to be −2.3 at pH 2.0 to −37.9 at pH 7.0. TGA analysis revealed that carboxymethyl TG lost around 10% of molar mass between 100ºC to 200ºC, indicative of loss of adsorbed water. The second mass loss of 45% occurred at 285ºC representing the thermal degradation of carboxymethyl TG. DSC thermograms revealed two peaks at 154ºC and 249ºC indicating water loss and thermal decomposition of carboxymethyl TG. SEM studies revealed irregular and elongated particles of carboxymethyl TG. Rheological analysis of the carboxymethyl TG revealed pseudoplastic behaviour of the gum and the viscosities of carboxymethyl TG was less as compared to TG at the same concentrations.

Grafting of TG with polyacrylic acid is reported [14]. Grafting was done at 60ºC under nitrogen atmosphere. Ammonium persulfate was used as the initiator. The grafted polymer had super absorbent properties and swelled to a great extent in distilled water. Morphological analysis revealed 3D network with numerous interlinked pores. This 3D network with numerous interlinked pores was responsible for its super absorbent qualities. The grafted polymer also had antibacterial properties.

Microwave grafting of TG is also reported in literature [15]. Monomers acrylonitrile and poly methyl methacrylate, cobalt complex and ammonium persulfate were used as the cross-linker and initiator respectively. The water absorption properties of the grafted polymer were enhanced. The grafted polymer had improved tensile strength and stability as compared to the native polymer. The grafted polymer was biodegradable and was able to form interpenetrating polymer networks with antibacterial and superabsorbent effects.

Sulfated derivatives produces significant effects on the physiological role of polymers [16]. Sulfated galactomannans exerts greater cytotoxic effects to tumour cells in comparison to native galactomannans [17]. Research also claims that anticoagulant and antithrombotic effects of sulfated guar gum and other sulfated galactomannans have increased with the increase in the degree of substitution and depolymerisation of the galactomannan polysaccharide. The sulfated

derivative of TG was prepared using chlorosulfonic acid and pyridine [18]. The sulfation reaction decreased the molecular weight of TG. The decrease in molecular weight of TG was due to the extensive hydrolysis in acidic conditions by the different substrates of the sulfation reaction. The sulfation reaction also changed the solution conformation of TG. Sulfated TG demonstrated a more stretched solution orientation as compared to native TG.

Gamma radiation induced cross-linking of TG with acrylic acid was reported [19]. The cross-linked TG hydrogels had semi-interpenetrating polymer network structures where TG was physically incorporated within the acrylic acid networks. Swelling and gel content determination of the TG hydrogels was done in sodium chloride and urea solution and also in water. Increase in temperature increased the swelling of the hydrogels. The swelling of the hydrogels decreased with the increase in the degree of cross-linking. The elastic properties and mechanical strength of the TG hydrogels were also increased. The author opined that the optimum swelling and mechanical properties of the hydrogels could be beneficial when used as absorbents for body fluids.

7. Literatures on TG

Buccoadhesive tablets using TG was prepared for controlled delivery of chlorpheniramine maleate [20]. The main objective of the study was to increase buccal retention and decrease pre-systemic metabolism of the drug. The mucoadhesive strength of TG buccoadhesive tablets were evaluated against the force of detachment from goat buccal mucosa. The mucoadhesive potential of TG was analogous with others polymers carbopol 974P and methocel K4M. Dissolution of chlorpheniramine maleate from the buccoadhesive tablets were studied. After 1 h, 35% of drug was released and complete drug release took place after 8 h. *In vivo* pharmacokinetic study of the buccoadhesive tablet was done and matched with oral drug solution. The buccoadhesive tablet showed better pharmacokinetic profile as compared to the oral drug solution. Peak plasma levels of buccoadhesive tablets was higher (20.33 ± 2.49 ng/ ml) when equated to that of oral drug solution (17.66 ± 1.24 ng/ ml). The AUC was also more for the buccoadhesive tablets (4691.003 ng/ml min) compared to oral solution (3163.18 ng/ml min). The pharmacokinetic parameters revealed that the TG buccoadhesive tablets displayed higher drug absorption and absolute bioavailability compared to oral solution.

Carboxymethyl TG was used for microencapsulation of vitamin D_3 [21]. The objective of the research was to reduce the degradation of the vitamin D_3 in the acidic atmosphere inside the GIT, thereby refining its stability and bioavailability. In vitro vitamin D_3 release experiments revealed that in simulated gastric medium, approximately 5% of the bioactive was released within the first half hour and 50% by the end of the two hours. In contrast, 60% of vitamin D_3

was released in the first 30 minutes and the remaining was released in the next two hours in simulated intestinal medium. The bioactive was protected from degrading in the stomach by this release pattern, which increased its bioaccessibility. The potential of carboxymethyl TG in the administration of bioactives that are susceptible to environmental and gastric medium degradation was demonstrated by the release pattern.

Similarly, brazilian cherry juice was encapsulated in microparticles developed with TG, xanthan, and xanthan-TG hydrogels. The objective was to enhance the antioxidant activity, stability, and release properties of the phenolic and carotenoids bioactive [22]. The microparticles were assessed for their encapsulation efficacy and release features. While TG and xanthan showed comparable encapsulation efficiency, the encapsulation effectiveness of xanthan gum was higher with the phenolic compounds. The release of brazilian cherry juice in simulated intestinal and gastric media depended on the type and concentration of gum. After 3 h in gastric fluid, xanthan microparticles released its total load, TG-coated microparticles liberated 22% of brazilian cherry juice, while the hydrogels liberated 19% of the bioactive. The release of the bioactive in intestinal fluids was similar pattern to that in gastric fluids, with TG microparticles releasing the least amount, hydrogels releasing a relatively higher amount, and xanthan microparticles releasing most quickly. Xanthan-tara hydrogels offered the best protection against temperature and light followed by TG microparticles and then xanthan microparticles.

TG is also used to prepare edible films for food packaging. TG films reinforced with cellulose nanocrystals were prepared [5]. TG films was smooth and uniform, incorporation of cellulose nanocrystals made the film coarse and rough. However, cellulose nanocrystals improved the mechanical and tensile strength of the TG film. The TG films showed desirable water vapour, oxygen and carbon dioxide barrier properties and could be used for packaging of food. Similarly, TG films incorporated with oleic acid was prepared [4]. The effect of oleic acid on the optical properties, moisture content, mechanical properties, water vapour permeability and surface morphologies was studied. Oleic acid reduced the micro pores of the TG films and made the films look opaque and yellowish. Oleic acid didn’t have any effect on the film thickness, but imparted hydrophobicity to the films, decreasing the moisture content and water vapour permeability. TG and Oleic acid were very compatible and enriched the hydrophobicity and mechanical strength.

References

1. Yadav H, Maiti S. Research progress in galactomannan-based nanomaterials: Synthesis and application. Int. J. Biol. Macromol. 2020;163:2113–2126.

2. Wu Y, Ding W, Jia L, He Q. The rheological properties of TG (Caesalpinia spinosa). Food Chem. 2015;168:366–371.

3. Mukherjee K, Dutta P, Badwaik HR, Saha A, Das A, Giri TK. Food industry applications of Tara gum and its modified forms. Food Hydrocolloids for Health. 2023;3:100107.

4. Ma Q, Hu D, Wang H, Wang L. TG edible film incorporated with oleic acid. Food Hydrocoll. 2016;56:127–133.

5. Ma Q, Hu D, Wang L. Preparation and physical properties of TG film reinforced with cellulose nanocrystals. Int. J. Biol. Macromol. 2016;86:606–612.

6. Dea ICM, Morrison AA. Chemistry and interactions of seed galactomannans. Adv. Carbohydr. Chem. Biochem. 1975;31:241–312.

7. Maier H, Anderson M, Karl C, Magnuson K, Whistler RL. Guar, locust bean, tara, and fenugreek gums. In Industrial gums, California, Academic Press Inc, 1993;215–218.

8. Conway MW, Almond SW, Briscoe JE, Harris LE. Chemical model for the rheological behavior of cross-linked fluid systems. J. Pet. Technol. 1983;35:315–320.

9. Huamaní-Melendez VJ, Mauro MA, Darros-Barbosa R. Physicochemical and rheological properties of aqueous TG solutions. Food Hydrocoll. 2021;111:106195.

10. Medina-Torres L, Brito-De La Fuente E, Torrestiana-Sanchez B, Katthain R. Rheological properties of the mucilage gum (Opuntia ficusindica). Food Hydrocoll. 2000;14:417–424.

11. Raj V, Chun KS, Lee S. State-of-the-art advancement in tara gum polysaccharide (Caesalpinia spinosa) modifications and their potential applications for drug delivery and the food industry. Carbohydr. Polym. 2023;323(1):121440.

12. Borzelleca JF, Ladu BN, Senti FR, Egle JL Jr. Evaluation of the Safety of Tara Gum as a Food Ingredient: A Review of the Literature. Int. J.Toxicol. 1993;12: 81

13. Santos MB, dos Santos CHC, de Carvalho MG, de Carvalho CWP, Garcia Rojas EE. Physicochemical, thermal and rheological properties of synthesized carboxymethyl tara gum (Caesalpinia spinosa). Int. J. Biol. Macromol. 2019;134: 595-603.

14. Li B, Shen J, Wang L. Development of an antibacterial superabsorbent hydrogel based on TG grafted with polyacrylic acid. Int. J. Environ. Res.Public Health. 2017;4 (2):30–35.

15. Priyadarsini M, Biswal T. Green synthesis, swelling behaviour and orthopaedic application of polysaccharide based hydrogel. Indian J. Chem. Technol. 2020;27:515–520.

16. Francielli C, Sierakowski MR, de Andrade Uchoa DE, Nozawa C, Sassaki GL, Gorin P A J, Ono L. In vitro antiherpetic and antirotaviral activities of a sulfate prepared from Mimosascabrella galactomannan. Int. J. Biol. Macromol. 2009;45:453–457.
17. Wang C, Meng M, Liu S, Wang L, Hou L, Cao X. A chemically sulfated polysaccharide from Grifola frondos induces HepG2 cell apoptosis by notch1–NF κB pathway. Carbohydr. Polym. 2013;95(1):282–287.
18. Qin X, Li R, Zhu S, Hu J, Zeng X, Zhang X, Xu H, Kong W, Liang J, Zhang H. A comparative study of sulfated tara gum: RSM optimization and structural characterization. Int. J. Biol. Macromol. 2020;150:189–199.
19. Abd Alla SG, Sen M, El-Naggar AWM. Swelling and mechanical properties of superabsorbent hydrogels based on Tara gum/acrylic acid synthesized by gamma radiation. Carbohydr. Polym. 2012;89(2):478–485.
20. Sabale V, Paranjape A, Patel V, Sabale P. Characterization of natural polymers from jackfruit pulp, calendula flowers and tara seeds as mucoadhesive and controlled release components in buccal tablets. Int. J. Biol. Macromol. 2017;95:321–330.
21. Santos MB, de Carvalho MG, Garcia-Rojas EE. Carboxymethyl tara gum-lactoferrin complex coacervates as carriers for vitamin D_3: Encapsulation and controlled release. Food Hydrocoll. 2021;112:106347.
22. Rutz JK, Zambiazi RC, Borges CD, Krumreich FD, da Luz SR, Hartwig N, da Rosa CG. Microencapsulation of purple Brazilian cherry juice in xanthan,TG and xanthan-tara hydrogel matrixes. Carbohydr. Polym. 2013;98(2):1256–1265.

Chapter 4:

Tramadol Hydrochloride

1. Introduction

Tramadol hydrochloride (TH), is a synthesized analgesic having non-opioid and also opioid characteristics [1-3]. TH mainly works on the central nervous system. TH was sanctioned by the USFDA (United States Food and Drug Administration) for controlling, treating and mitigating modest to extreme pain in 1955 [4-6]. TH has structural similarities to morphine and codeine, but 10-times and 6000-times less potent than codeine and morphine respectively. The anti-nociceptive attributes of TH arise due to the dual (opioid and non-opioid) mode of action. TH works on μ-opioid and k-opioid receptors with poor affinity, exercising a mild agonistic effect, and it upsets monoamine receptor organizations by obstructing serotonin (5-HT) and norepinephrine (NE) reuptake, accountable for the prohibition of pain transmission in the spinal cord [7,8]. TH is much preferred over other opioid analgesic due to its exceptional pharmacological profile, exhibiting lower abuse potential and side effects and [8-9]. Table 4.1 lists the various details about TH. The structure of TH is shown in Fig. 4.1.

Table 4.1 Technical specifications of TH.

IUPAC name	(1RS,2RS)-2-[(dimethylamino)methyl]-1-(3-methoxyphenyl)cyclohexanol hydrochloride (1:1)
Chemical formula and class	$C_{16}H_{26}ClNO_2$; Phenylpropylamine
Pharmacological category of drug	Narcotics; Opioid agonist; Analgesic (moderate to severe pain).
Average molecular weight	299.84g/mol
Solubility in distilled water at 27ºC	813.40 mg/ml
Solubility in pH 1.2 at 27ºC	870.33 mg/ml
Solubility in pH 7.4 at 27ºC	687.58 mg/ml.
pKa	9.41
Melting point	180ºC
Decomposition/Degradation temperature	200ºC-260ºC
UV-Vis λ_{max}	270 nm
Plasma Half-life	5.5 h
Toxicity profile	LD_{50} (350 mg/kg;orally; mice)
CAS number	22204-88-2

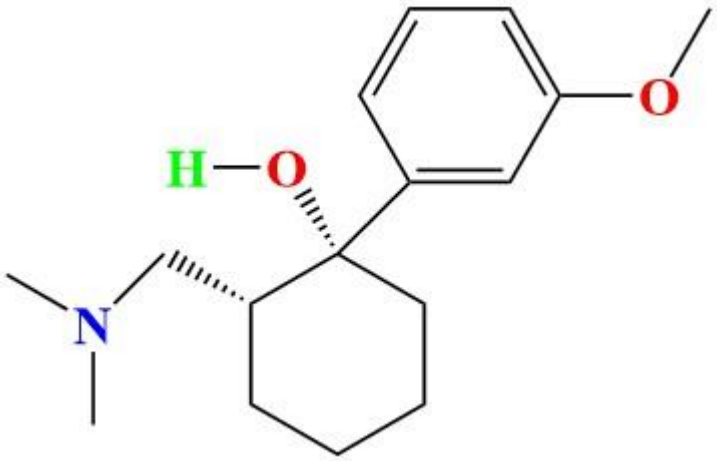

Fig. 4.1. Structure of TH.

2. Pharmacokinetics

TH is formulated in diverse pharmaceutical formulations (tablets, capsules, injections etc.) and delivered via different routes like oral, sub-cutaneous, intravenous, intramuscular and sublingual. TH is readily and almost totally absorbed following oral intake. The average peak blood concentration of TH is reached after 2 h of intake and following first pass effect, the bioavailability is around 70%. 20% of TH is plasma protein bound and TH exhibits a plasma half-life of 5.5 h. TH is largely metabolized by the liver by cytochrome P450 isoenzymes (3A4, 2D6 and 2B6) to N-desmethyltramadol (M2) and O-desmethyltramadol (M1) respectively. They are the prime phase-I metabolites. The phase-I metabolites are again metabolized to three secondary metabolites, viz. N,O-desmethyltramadol, N,N-didesmethyltramadol, and N,N,O-tridesmethyltramadol. All metabolites are ultimately conjugated with sulfate and glucuronic acid before being excreted in urine [1,5,10]. TH is primarily eliminated through the kidneys. Almost 1/3rd of the intake dose is excreted unmodifed in the urine, and 60% is excreted as metabolites. The remaining TH is excreted through faeces [1,4,5].

3. Pharmacodynamics

TH occurs as a racemic mix with significant variances in activity, bonding, and targets connected with the two enantiomers [3,11]. The (+) enantiomer has greater attraction to opioid receptors and favourably impedes 5-HT uptake and augments 5-HT liberation, while the (-) enantiomer prevents reuptake of NE. The synergistic effect of the two enantiomers is accountable for the pain-relieving activity of TH [12,13]. Precisely, the M1 metabolite is regarded as the most pharmacologically effective, being 6 times more effective and powerful than native TH in relieving pain, and 200 times more competent and powerful in μ-opioid binding [2,7,14].

TH displays anti-nociception in laboratory pain simulations, and the association of opioid, serotonergic and noradrenergic systems has been established. Additionally, to systemic actions, research reports anti-nociception after local peripheral and spinal intake. TH has been testified to collaborate with other cellular targets (e.g. N-methyl-D-aspartate (NMDA) receptors, Na^+ channels, and transient potential vanilloid-1 receptors), promoting anti-nociceptive effects particularly at high blood concentrations after local administration.

Due to the monoaminergic attributes of TH, anxiolytic-like and antidepressant actions have also been accredited to TH. TH prohibits via α_2-adrenoceptors, which controls anxiety and pain, where the neuronal action is adjusted by antidepressant, anxiolytics, and opiate analgesics. The antidepressant action is also moderated by 5-HT ($5\text{-}HT_{1A}$) receptors [15].

TH minimizes the binding of α_2-adrenoceptors, $5\text{-}HT_{2A}$ receptors, and frontocortical β-adrenoceptors, and increases the binding of dopamine receptors and α_1-adrenoceptors, inducing alterations in the CNS. TH has been used for some anxiety-like and psychiatric ailments [15,16]. The anti-depressant activity of TH is due to the dopaminergic (D1/D2 receptors), noradrenergic (α_2-adrenoceptors), and imidazoline (I1/I2) receptors [16]. Additionally, analgesic and anti-shivering properties were also ascribed to TH, without experiencing alarming sedation in post-operative conditions [6,17].

TH is also clinically useful for controlling premature ejaculation. The hindrance of neuronal reuptake of NE and 5-HT, anti-nociceptive effects, augmentation of 5-HT efflux, and prohibition of spinal somatosensory aroused potentials are responsible for this activity [4].

4. Adverse effects

The most common adverse actions after therapeutic administration of TH comprise dizziness, followed by nausea, vomiting, constipation, and lethargy. However, TH is deliberated as a better option for pain release with respect to NSAIDs because their chronic intake results in worsening of renal activity and gastrointestinal damages, and compared to other opioids for its agreeable safety profile and low dependence rate [18]. Nevertheless, TH has been used along with NSAIDs in osteoarthritic patients [2].

The prohibition of NE and 5-HT reuptake may trigger two noteworthy unwanted events: serotonin syndrome and seizures, specifically if TH is overdosed, or co-delivered with antidepressants or intake by epileptic patients [17,19-20]. These effects are probably due to the GABA pathways inhibition, precisely by inhibiting GABA receptors [14].

Nausea and the associated emesis are the unwanted effects usually witnessed with opioid analgesic. At clinical blood concentrations, TH effectively inhibits the human NET, and exerts a mild effect on $5\text{-}HT_{3A}$ receptor. $5\text{-}HT_3$ receptors are elaborated during emesis. Serotonin

transporters (SERT) are membrane proteins accountable for the swift reuptake of the liberated 5-HT into presynaptic nerve terminals. SERT is abundant in 5-HT nerve junctions, also in enterochromaffin cells and platelets. Thus, SERT is essential for both the control of 5-HT plasma concentration and the variation of the concentration of 5-HT in the synaptic gaps. APIs that inhibit SERT, like selective 5-HT reuptake inhibitors (antidepressants), may result in excessive synaptic and plasma 5-HT concentrations, arousing 5-HT_3 receptors. Additionally, TH use is associated with dependence. Dopamine liberations in various areas of CNS is accounts for this phenomenon [14].

A case of deep hyponatremia following a TH overdose has been reported [21]. Opioids alter renal excretion of sodium and water by several mechanisms resulting inactivation of ADH release and succeeding anti-diuretic action [21].

Bloor et al. elaborated the effects of TH intake by pregnant and lactating mother [6]. TH is categorised as a category C drug by the Australian Therapeutic Goods Administration Evaluation Committee. These drugs may cause or is alleged to cause unwanted effects (reversible) on the human fetus or the baby, though abnormalities are rare. TH should be cautiously used during conception and organogenesis, explicitly in the first trimester.

5. Co-delivery with other drugs

Opioids are often prescribed with different non-opioids that works by diverse mechanisms to provide a synergistic or additive effect [20]. The purpose is to optimize pain management and reduce drug related adverse effects. Clonidine or other α_2-adrenergic agonists are frequently prescribed together. Clonidine enhances the anti-nociceptive effect of TH and other opioids. It may be possible that 5-HT_3, 5-HT_{1A}, and 5-HT_{2A} receptors, as well as neurokinin-1 and glutamatergic receptors are involved in TH anti-nociception [9]. Similarly, amlodipine (a calcium channel blocker) and TH also enhances the anti-nociceptive activity of TH [8]. Again, combining acetaminophen with TH provides instant and long-lasting pain relief arising from the synergistic effect of the drugs. Cialdai et al. reported that tramadol and dexketoprofen, when taken intra-articularly or orally, showed anti-nociceptive activity at lower doses than required for each drug alone to produce similar effects in monosodium iodoacetate-induced osteoarthritis in rats [22]. TH, when used along with bupivacaine for subarachnoid block for cesarean section, exhibited prolonged period of analgesia with minimum shivering. Moreover, the combination therapy was also safe for labor analgesia and neonate [23].

6. Literatures on tramadol hydrochloride

TH release from hydroxypropyl methyl cellulose and hydrogenated castor oil matrix tablets have been investigated [24]. TH release from hydroxypropyl methyl cellulose matrices was sustained up to 14 h, while that from hydrogenated castor oil matrix TH release was sustained beyond 20 h. The hydrophilic nature of hydroxyl propyl methyl cellulose was responsible for the faster release of TH from the matrix. Hydrogenated castor oil, being hydrophobic in nature was able to slow down the release of TH from the matrix. The hydrophobic polymer formed a hydrophobic coating around the TH particles which retarded the release of TH from the matrix. TH matrix tablets based on different combinations of xanthan gum and guar gum with hydroxypropyl methyl cellulose or combination of the three polymers have been prepared [25]. Burst release of TH from the guar gum matrices has been observed, but no burst effect was seen from the xanthan matrices. The release of TH from the guar gum matrices was faster as compared to the xanthan matrices, indicating that xanthan has better drug release retarding ability than guar gum. TH release from xanthan matrices followed zero order kinetics. Xanthan gum has high erosion and water uptake characteristics. The combination of the three mechanisms (erosion, swelling and diffusion) controls the thickness of the gel layer, producing the zero order release pattern. Incorporation of hydroxypropyl methyl cellulose into xanthan matrices in low amounts made the TH release pattern follow Hixon-Crowell model, due to the high erodability of the xanthan gum. When the percentage of hydroxypropyl methyl cellulose was increased, the release pattern followed Higuchi model. This was due to the formation of a thick gelatinous layer of hydroxypropyl methyl cellulose around the matrix. Guar gum matrices followed first order release kinetics. Guar gum matrices have minimum erosion but high water uptake rate. The combination of the three processes of water uptake, gelatinization and diffusion are responsible for the first order release pattern of TH. Incorporation of hydroxypropyl methyl cellulose in to guar gum matrices made the release pattern follow first order and Higuchi kinetics via Fickian diffusion. Since both hydroxypropyl methyl cellulose and guar gum are water soluble polymers, they dissolve and generated pores within the matrices, from which the drug diffused.

TH matrix tablets based on chitosan and chitosan-graft-poly (2-hydroxyethyl methacrylate-co-itaconic acid) has been prepared [26]. TH release from chitosan matrices was faster than the TH release from chitosan-graft-poly (2-hydroxyethyl methacrylate-co-itaconic acid). The release of TH was more in simulated intestinal fluid than in simulated gastric fluid. This was due to the greater swelling of the matrix in the simulated intestinal fluid. The slow TH release from the grafted copolymer was because of drug-polymer interaction by forming hydrogen

bonding between hydroxyl and carboxyl groups of the grafted polymer and the hydroxyl groups of the drug. Various literatures on TH have been given in Table 4.2.

Table 4.2 Literatures on Tramadol Hydrochloride

Serial No	Formulation excipients	Dosage forms	Major drawbacks	Reference
1	Eudragit RS-100, Ethylcellulose, Carbopol 934P and Polyvinyl Pyrolidone K-90	Matrix tablets	Use of many synthetic release retarding agents	27
2	Carbopol 974P and 934	Matrix tablets	Use of synthetic release retarding agents	28
3	Glyceryl palmitostearate	Matrix tablets	1. Problem during tablet compaction 2. Use of complex procedures	29
4	Carnauba wax (CW) and HPMC K100	Matrix tablets	1. Problem during tablet compaction 2. Use of complex procedures	30
5	Methocel K4M Premium CR or Methocel K100M Premium CR Prosolv SMCC 90 or Disintequik MCC 25	Matrix tablets	Use of complicated procedures for matrix development process.	31

6	Celecoxib	Co-Crystals	1. Use of complex procedures 2. Use of organic solvents	32
7	HPMC E15, PEG 6000, Crosscarmellose sodium, Sodium starch glycolate, Crospovidone	Orally disintegrating films	1. Use of complex procedures 2. Use of organic solvents	33

7. Rationale behind choosing tramadol hydrochloride as the model drug

Tramadol is a centrally acting analgesic and is effective in both clinical and experimental pain management without any associated cardiovascular or respiratory adverse effects [34]. It has a half-life of about 5.5 h and oral administration of 50 mg to 100 mg is required every 4-6 h [24, 27]. The daily maximum oral dose of tramadol is 400 mg [24, 27]. To reduce frequency of dosing, dose related side effects, and enhance patient compliance formulation of sustained/controlled release dosage forms is necessary [24, 27]. Tramadol sustained/controlled release dosage forms are documented in literature [24, 27-30]. Oral administration of tramadol sustained release tablets attains a bioavailability of 87% - 95%, compared with capsules [25]. Long term treatment with tramadol produces satisfactory osteoarthritic, low back, and post-operative pain management with minimum side effects and enhanced patient acceptability [35-36]. Considering all the above factors, formulation of tramadol sustained release hydrogel tablets was undertaken.

References

1. Lavasani H, Sheikholeslami B, Ardakani YH, Abdollahi M, Hakemi L, Rouini MR. Study of the pharmacokinetic changes of Tramadol in diabetic rats. Daru. 2013; 21:17.

2. Lee SH, Cho SY, Lee HG, Choi JI, Yoon MH, Kim WM. Tramadol induced paradoxical hyperalgesia. Pain Phys. 2013;16:41–44.

3. Casella S, Giannetto C, Giudice E, Marafioti S, Fazio F, Assenza A. ADP induced platelet aggregation after addition of tramadol in vitro in fed and fasted horses plasma. Res. Vet. Sci. 2013;94:325–30.

4. Eassa BI, El-Shazly MA. Safety and efficacy of tramadol hydrochloride on treatment of premature ejaculation. Asian J. Androl. 2013;15:138–42.
5. El-Sayed AA, Mohamed KM, Nasser AY, Button J, Holt DW. Simultaneous determination of tramadol, O-desmethyltramadol and N-desmethyltramadol in human urine by gas chromatography-mass spectrometry. J. Chromatogr. B Analyt. Technol. Biomed. Life Sci. 2013;926:9–15.
6. Bloor M, Paech MJ, Kaye R. Tramadol in pregnancy and lactation. Int. J. Obstet. Anesth. 2012;21:163–167.
7. Stoops WW, Lofwall MR, Nuzzo PA, Craig LB, Siegel AJ, Walsh SL. Pharmaco dynamic profile of tramadol in humans: influence of naltrexone pretreatment. Psychopharmacology (Berl). 2012;223:427–438.
8. Modi H, Mazumdar B, Bhatt J. Study of interaction of tramadol with amlodipine in mice. Indian J. Pharmacol. 2013;45:76–79.
9. Andurkar SV, Gendler L, Gulati A. Tramadol antinociception is potentiated by clonidine through alpha (2)-adrenergic and I(2)-imidazoline but not by endothelin ET(A) receptors in mice. Eur. J. Pharmacol. 2012;683:109–115.
10. Ing Lorenzini K, Daali Y, Dayer P, Desmeules J. Pharmacokinetic-pharmacodynamic modelling of opioids in healthy human volunteers, A minireview. Basic Clin. Pharmacol. Toxicol. 2012;110:219–226.
11. Chandra P, Rathore AS, Lohidasan S, Mahadik KR. Application of HPLC for the simultaneous determination of aceclofenac, paracetamol and tramadol hydrochloride in pharmaceutical dosage form. Sci. Pharm. 2012;80:337–351.
12. Garcia-Quetglas E, Azanza JR, Sadaba B, Munoz MJ, Gil I, Campanero MA. Pharmacokinetics of tramadol enantiomers and their respective phase I metabolites in relation to CYP2D6 phenotype. Pharmacol. Res. 2007;55:122–130.
13. Sawynok J, Reid AR, Liu J. Spinal and peripheral adenosine A (1) receptors contribute to antinociception by tramadol in the formalin test in mice. Eur. J. Pharmacol. 2013;714:373–378.
14. Hassanian-Moghaddam H, Farajidana H, Sarjami S, Owliaey H. Tramadol induced apnea. Am. J. Emerg. Med. 2013;31:26–31.
15. Berrocoso E, Mico JA, Ugedo L. In vivo effect of tramadol on locus coeruleus neurons is mediated by alpha2-adrenoceptors and modulated by serotonin. Neuropharmacology. 2006;51:146–53.

16. Jesse CR, Wilhelm EA, Bortolatto CF, Nogueira CW. Evidence for the involvement of the noradrenergic system, dopaminergic and imidazoline receptors in the antidepressant-like effect of tramadol in mice. Pharmacol. Biochem. Behav. 2010;95:344–350.
17. Joshi C, Ambi U, Mirji P. Can we use Tramadol as an anti-shivering agent?. Indian J. Anaesth. 2012;56:91–102.
18. Hsu SK, Yeh CC, Lin CJ, Hsieh YJ. An open label trial of the effects and safety profile of extended-release tramadol in the management of chronic pain. Acta. Anaesthesiol. Taiwan. 2012;50:101–105.
19. Raiger LK, Naithani U, Bhatia S, Chauhan SS. Seizures after intravenous tramadol given as premedication. Indian J. Anaesth. 2012;56:55–57.
20. Pergolizzi Jr JV, van de Laar M, Langford R, Mellinghoff HU, Merchante IM, Nalamachu S. Tramadol/paracetamol fixed-dose combination in the treatment of moderate to severe pain. J. Pain Res. 2012;5:327–346.
21. Lota AS, Dubrey SW, Wills P. Profound hyponatraemia following a tramadol overdose. QJM. 2012;105:397–8.
22. Cialdai C, Giuliani S, Valenti C, Tramontana M, Maggi CA. Comparison between oral and intra-articular antinociceptive effect of dexketoprofen and tramadol combination in monosodium iodoacetate-induced osteoarthritis in rats. Eur. J. Pharmacol. 2013;714:346–51.
23. Subedi A, Biswas BK, Tripathi M, Bhattarai BK, Pokharel K. Analgesic effects of intrathecal tramadol in patients undergoing caesarean section: a randomised, double-blind study. Int. J. Obstet. Anesth. 2013;22:316–321.
24. Tiwari SB, Murthy TK, Pai MR, Mehta PR, Chowdary PB. Controlled Release Formulation of Tramadol Hydrochloride Using Hydrophilic and Hydrophobic Matrix System. AAPS Pharm. Sci. Tech. 2003;4(3):31.
25. Varshosaz J, Tavakoli N, Kheirolahi F. Use of Hydrophilic Natural Gums in Formulation of Sustained-release Matrix Tablets of Tramadol Hydrochloride. AAPS Pharm. Sci. Tech. 2006;7(1):24.
26. Subramanian KG, Vijayakumar V. Synthesis and evaluation of chitosan-graft-poly (2-hydroxyethylmethacrylate-co-itaconicacid) as a drug carrier for controlled release of tramadol hydrochloride. Saudi Pharm. J. 2012;20:263–271.
27. Joshi NC, Ahmad Z, Mishra SK, Singh R. Formulation and Evaluation of Matrix Tablet of Tramadol Hydrochloride. Ind. J. Pharm. Edu. Res. 2004;45:4.

28. Rehman AU, Khan GM, Shah KU, Shah SU, Khan KA. Formulation and Evaluation of Tramadol HCl Matrix Tablets Using Carbopol 974P and 934 as Rate-Controlling Agents. Trop. J. Pharm. Res. 2013;12(2):169.

29**.** Deore RK, Kavitha K, Tamizhmani TG. Preparation and Evaluation of Sustained Release Matrix Tablets of Tramadol Hydrochloride Using Glyceryl Palmitostearate. Trop. J. Pharm. Res. 2010;9(3):275.

30. Deb P, Singha J, Chanda I, Chakraborty P. Formulation Development and Optimization of Matrix Tablet of Tramadol Hydrochloride. Recent Pat. Drug Deliv. Formul. 2017;11:19-27.

31. Komersováa A, Lochaře V, Myslíkováa K, Mužíkováb J, Bartošc M. Formulation and dissolution kinetics study of hydrophilic matrix tablets with tramadol hydrochloride and different co-processed dry binders. Eur. J. Pharm. Sci. 2016;95:36–45.

32. Almansa C, Merce R, Tesson N, Farran J, Tomas J, Plata-Salaman CR. Co-crystal of Tramadol Hydrochloride−Celecoxib (ctc): A Novel API− API Co-crystal for the Treatment of Pain. Cryst. Growth Des. 2017;17:1884−1892.

33. Bhatta HP, Sowmya C, Patnaik HP, Sharma H, Sapkota HP, Wagle N. Formulation and Evaluation of the Tramadol HCl Oral Disintegrating Film by Using The Co-processed Superdisntegrants. Am. J. Pharm. Tech. Res. 2015;5(3):2249-3387.

34. Lehmann KA. Tramadol in acute pain. Drugs. 1997;53(2):25-33.

35.Malonne H, Coffiner M, Fontaine D, Sonet B, Serono A, Peretz A, Vanderbist F. Long-term tolerability of tramadol LP, a new once-daily formulation, in patients with osteoarthritis or low back pain. J. Clin. Pharm. Ther. 2005;30:113-120.

36.Babul N, Noveck R, Chipman H, Roth SH, Gana T, Albert K. Efficacy and safety of extended-release, once-daily tramadol in chronic pain: a randomized 12-week clinical trial in osteoarthritis of the knee. J. Pain Symptom. Manage. 2004;28:59-71.

Chapter 5: Aims and Objectives

The tablet dosage form is the most preferred dosage form for drug delivery. Sustained release matrix tablets are very popular amongst the physicians and patients because it provides prolonged therapeutic drug plasma levels, reduces side effects and treatment cost and enhances patient compliance. Additionally, sustained release tablet matrices can be prepared under simple tableting infrastructure, making it a popular dosage form in the pharmaceutical manufacturing industries also.

Hydrophilic natural polysaccharides have been an efficient matrix material due to its biocompatible, non-toxic, and biodegradable properties. Additionally, they are bio-safe and easily available. When coming in contact with water, these hydrophilic polysaccharides have the unique ability to quickly hydrate and swell and form a viscous layer over the matrix surface. The dispersal of drug from the inflated gelatinous layer is influenced by the viscosity of the inflated layer. The rate of erosion of the swollen layer also determines the drug dissolution from the swollen matrix. Thus, swelling, viscosity, and erosion of the hydrophilic polysaccharide gel layer are the primary determinants of the drug solubilization from the tablet matrix and controlling such parameters will provide the tailored drug dissolution from the matrices.

Natural polysaccharides have diverse chemical structures and functional groups which can take part in different chemical reactions, paving the way to derivatize and modify the natural polysaccharide. The derivatization is primarily done to tailor the physicochemical characteristics of the natural polysaccharide according to the requirements of the dosage form. Carboxymethyltion is a widely used derivatization method which inserts o-carboxymethyl groups into the polysaccharide chains and imparts an anionic nature to the polysaccharide. The anionic carboxymethyl polysaccharide can be used to crosslink with di and trivalent metal cations and form a water insoluble hydrogel, by a process called ionotropic gelation. Cross-linking of polymeric chains is a potent tool to modify the swelling, viscosity and erosion characteristics of the hydrogel layer, and to modulate the drug dissolution from the hydrogel tablet matrix. The swelling, viscosity and erosion characteristics of the hydrogel layer can be modulated by controlling the extent of crosslinking of the polysaccharide polymeric chains with the metal cations. The valency of the ions and variation in the concentration of the ions can alter the swelling, viscosity and erosion characteristics of the hydrogel layer, thus providing an opportunity to the formulation development scientist to modulate the drug dissolution from the polysaccharide hydrogel matrices.

Based on the above hypotheses, the aims of the research work are given below:

1. To carry out pre-formulation studies. The preformulation studies will include compatibility studies of drug and polymer, saturation solubility of drug in distilled water, pH 1.2, and pH 7.4, and determination of melting point of drug/excipients.
2. To synthesize and characterize the carboxymethyl derivative of the natural polysaccharide tara gum.
3. To develop calcium and/or aluminium cross-linked hydrogel matrices and determine the influence of the cross-linking ions on the swelling, viscosity, and erosion characteristics of the hydrogel tablet matrices.
4. To investigate the in-vitro drug dissolution from the calcium and/or aluminium cross-linked hydrogel matrices.

Quite often a single polysaccharide hydrogel matrix may not give the anticipated drug solubilization pattern from the matrix. Blending of two or more polysaccharides may provide the desired hydrophilicity, swelling, viscosity, and erosion profiles of the hydrogel layer, to achieve the tailored drug solubilization pattern from the matrix. In this regard, the development of interpenetrating polymeric network (IPN) and semi-IPN hydrogels have been illustrious in the literature. Again, the robustness and versatility of the hydrogel matrices development process provides an option to fabricate and design the matrix development procedure to attain the specific drug solubilization from the matrices.

Based on the above hypotheses, the aims of the research work are given below:

5. To develop aluminium and calcium cross-linked semi-IPN hydrogel matrices based on tara gum and carboxymethyl tara gum.
6. To investigate the influence of incorporation of extragranular/intragranular tara gum on the swelling, viscosity, and erosion attributes of aluminium and calcium cross-linked semi-IPN hydrogel matrices.
7. To investigate the effect of extragranular/intragranular tara gum on in-vitro drug dissolution from the semi-IPN hydrogel matrices.
8. To carry out *in-vivo* pharmacokinetic study of the best semi-IPN hydrogel matrices.
9. The carry out accelerated stability study of the optimized formulation.

The overall objective of the research work is the development and evaluation of hydrogel matrix tablets using tara gum and/or derivatized tara gum for sustained gastrointestinal delivery of the highly water-soluble drug, tramadol hydrochloride.

Chapter 6: Analytical monitoring of tramadol hydrochloride

1.Preparation of 0.1 (N) HCl (acid solution of pH 1.2)

8.5 ml HCl was carefully measured and added to a volumetric flask initially containing 200 ml of distilled water. Further total volume was made up to 1000 ml. pH meter (Orion 2-Star, Thermo Scientific, US) was used to adjust the pH of the resulting solution at pH 1.2.

2.Preparation of 0.2 (M) tri sodium phosphate dodecahydrate (TSP)

76 grams of TSP were measured and placed into a volumetric flask containing distilled water (500 ml) and made solution. Then total volume was made up to 1000 ml in the flask.

3.Preparation of modified phosphate buffer (MPB) solution pH 7.4

A solution consisting of 200 ml of 0.2 (M) tri-sodium orthophosphate dodecahydrate was introduced into a 700 ml acid solution with a pH of 1.2 to get 900 ml solution with pH 7.4.

4. Determination of λ_{max} of Tramadol hydrochloride in acid solution of pH 1.2

10 mg of Tramadol were dissolved in 10 ml of pH 1.2 solution, and the volume was made up to 100 ml using an acid solution with a pH of 1.2. 2 ml aliquots were taken and made up to 25 ml using an acid solution with a pH of 1.2. The resulting solution was then scanned from 200 to 400 nm using a UV Spectrophotometer (UV 2450, Shimadzu, Japan). UV-spectrum of tramadol in acid solution of pH 1.2 shown in Fig. 6.1.

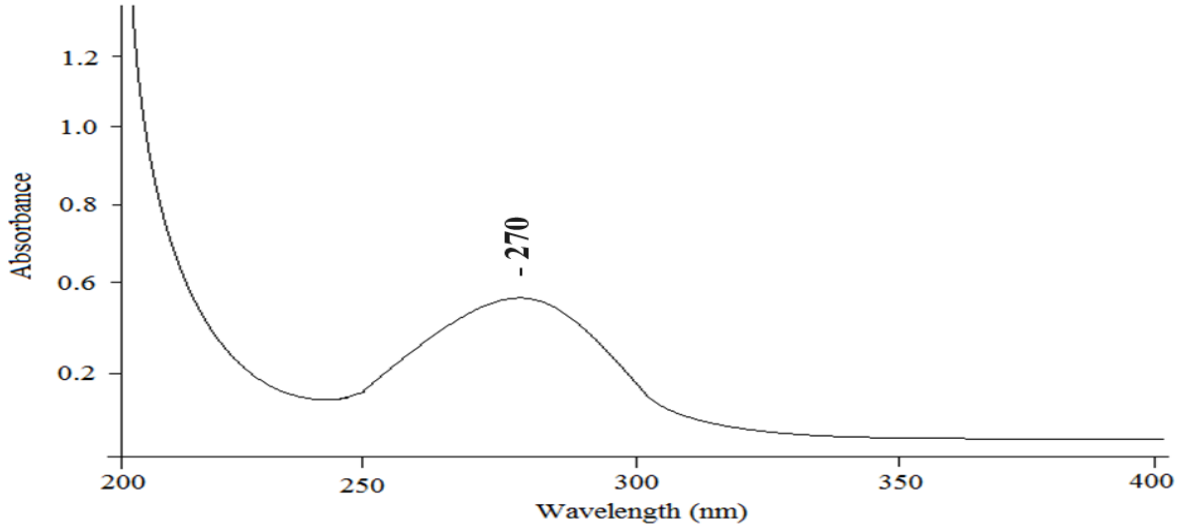

Fig. 6.1. λ_{max} of Tramadol hydrochloride in acid solution of pH 1.2

5. Determination of λ_{max} of Tramadol hydrochloride in phosphate buffer (PB) solution of pH 7.4

10 mg of Tramadol were dissolved in 10 ml of pH 7.4 solution, and the volume was increased to 100 ml using a phosphate solution with a pH of 7.4. 2 ml sample were taken and diluted to 25 ml using a phosphate buffer solution with a pH of 7.4. The resulting solution was then scanned from 200 to 400 nm using a UV Spectrophotometer (UV 2450, Shimadzu, Japan). UV-spectrum of tramadol in PB solution of pH 1.2 shown in Fig. 6.2.

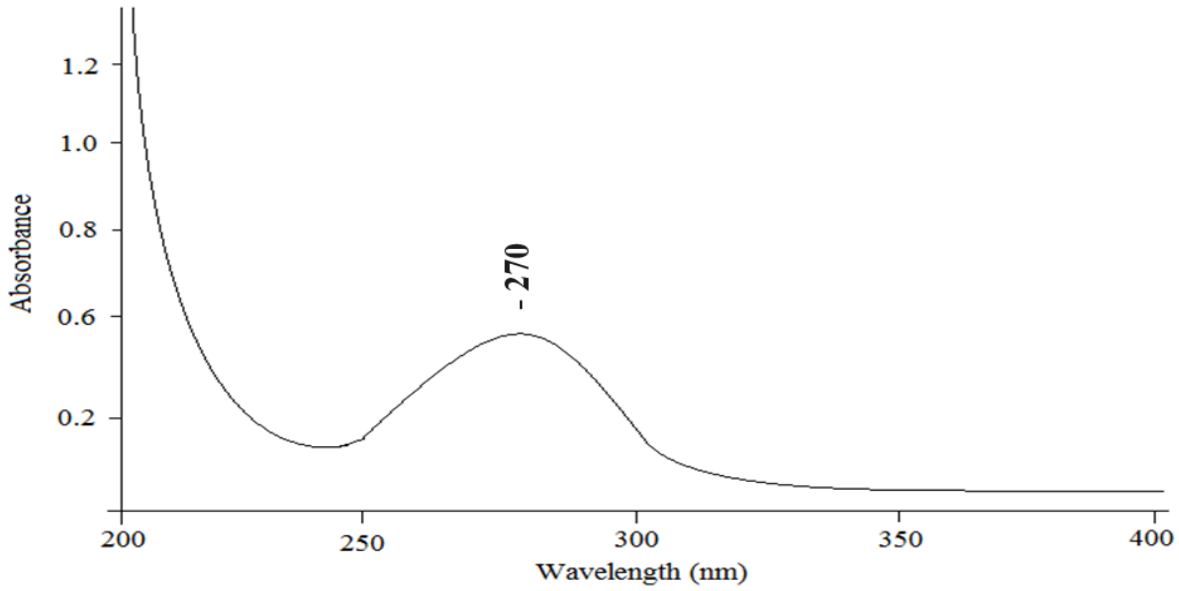

Fig. 6.2. λ_{max} of Tramadol hydrochloride in phosphate buffer (PB) solution of pH 7.4

6. Method development for the estimation of Tramadol hydrochloride in acid solution of pH 1.2

Precisely, 20 mg of tramadol were dissolved in 250 ml of pH 1.2 solution in a 250 ml volumetric flask. Subsequently, aliquots of 0.5, 1.5, 1, 1.5, 2, 2.5 ml were withdrawn from this stock solution and diluted up to 10 ml with acid solution. Absorbance measurements were conducted at 270 nm for each dilution. The observations were recorded three times (Table 6.1). The Fig. 3 show the calibration curve of Tramadol in pH 1.2 solution.

Table 6.1 Data for standard curve of Tramadol hydrochloride in acid solution pH 1.2

Concentration (microgm/ml)	Abs 1	Abs 2	Abs 3	mean±SD (n=3)
0	0	0	0	0
4	0.024	0.024	0.021	0.023±0.001
8	0.045	0.048	0.04	0.044±0.004
12	0.072	0.066	0.065	0.067±0.003
16	0.096	0.09	0.086	0.090±0.005
20	0.118	0.117	0.103	0.113±0.006

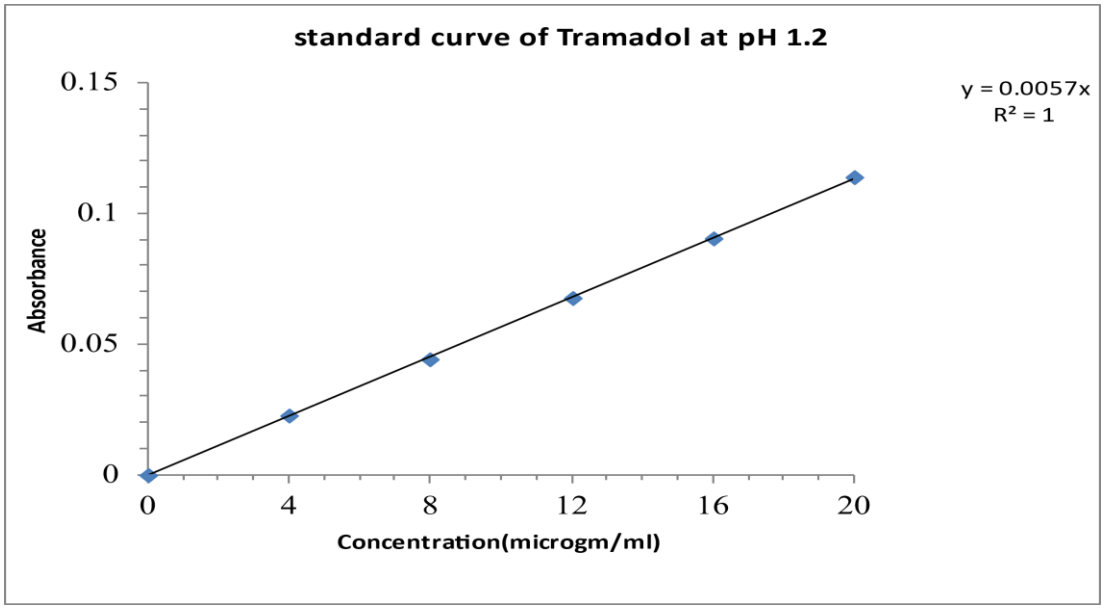

Fig. 6.3. Calibration curve of tramadol hydrochloride in acid solution pH 1.2

7. Method development for the estimation of Tramadol hydrochloride in PB solution of pH 7.4

Precisely, 20 mg of tramadol were dissolved in 250 ml of pH 7.4 solution in a 250 ml volumetric flask. Subsequently, aliquots of 0.5, 1.5, 1, 1.5, 2, 2.5 ml were withdrawn from this stock solution and diluted up to 10 ml with acid solution. Absorbance measurements were conducted at 270 nm for each dilution. The observations were recorded three times (Table 6.2). The Fig. 6.4 show the calibration curve of Tramadol in pH 7.4 solution.

Table 6.2 Data for standard curve of Tramadol hydrochloride in buffer solution pH 7.4

Concentration (microgm/ml)	Abs 1	Abs 2	Abs 3	mean±SD (n=3)
0	0	0	0	0
4	0.021	0.025	0.023	0.023±0.002
8	0.042	0.052	0.045	0.046±0.005
12	0.062	0.077	0.063	0.067±0.008
16	0.084	0.099	0.093	0.092±0.007
20	0.102	0.124	0.109	0.111±0.011

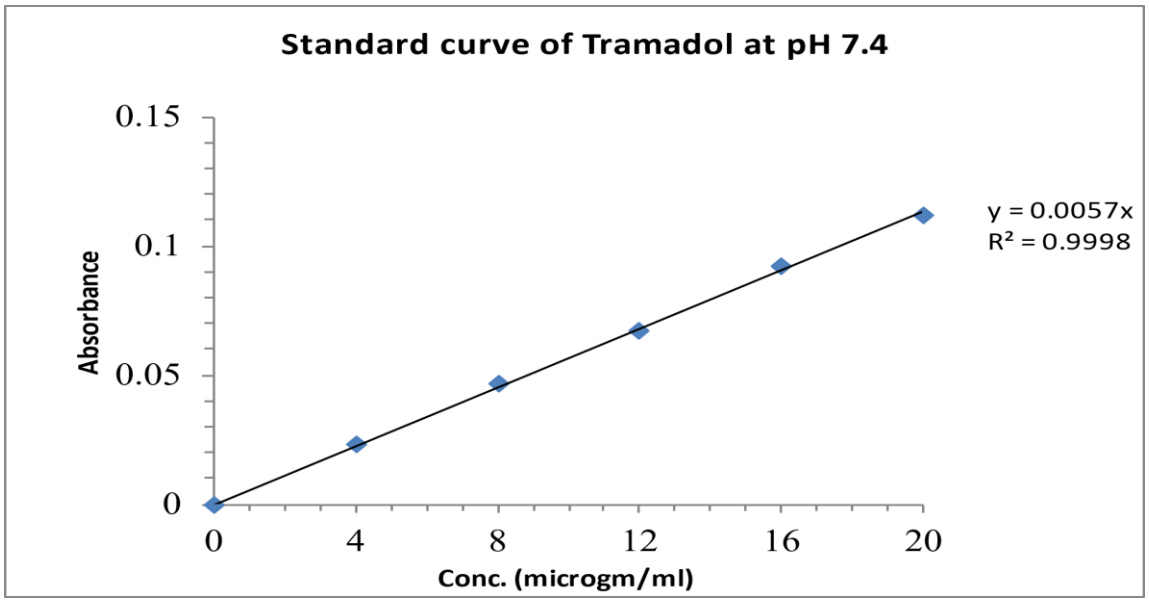

Fig.6.4. Calibration curve of tramadol hydrochloride in buffer solution pH 7.4

8. Determination of solubility of tramadol hydrochloride

Excess amount of Tramadol was added to 0.5 ml double distilled water, pH 1.2 solution and pH 7.4 solution into three different Eppendorf tubes. The eppendorfs were kept in a mechanical shaker for 2-3 hours until equilibrium achieved. Then the saturated solutions were filtered (Whatman filter paper). From the filtrate solutions 50µl aliquot was taken and diluted up to 250 ml with double distilled water, pH 1.2 solution and pH 7.4 solution respectively and all the samples were analysed under UV spectrophotometer at 270nm. Finally, the solubility of tramadol hydrochloride was calculated from the slope of the standard curve of tramadol hydrochloride. Table 6.3 shows the saturation solubility of tramadol hydrochloride in double distilled water, acid solution pH 1.2, and buffer solution pH 7.4.

Table 6.3 Saturation solubility of tramadol hydrochloride at 30ºC

Media	Saturation solubility of tramadol hydrochloride at 30ºC mean±SD (n=3)
Double distilled water	813.40±3.39 mg/ml
Acid solution pH 1.2	870.33±4.2 mg/ml
Buffer solution pH 7.4.	687.58±4.8 mg/ml

Chapter 7: Synthesis, optimization, and characterisation of carboxymethyl tara gum

1. Introduction

Natural polysaccharides are widely used as excipients in pharmaceutical industry because of their non-toxic, non-hazardous and biocompatible nature [1]. However, the natural polysaccharides have uncontrolled hydration, microbial contamination, variation in chemical composition according to the source, and change in viscosity on storage [2-3]. These are serious drawbacks of natural polysaccharides for use as excipients in pharmaceutical formulations.

Modification or derivatization of the natural polysaccharides can overcome the problems associated with the natural polysaccharides. The natural polysaccharides have diverse chemical structure and functional groups. These functional groups can take part in different chemical reactions. Modification of the polysaccharides can create the personalized polysaccharides which can adapt to the specific requirements of the formulation.

Carboxymethylation of the natural polysaccharides is one of such modification technique frequently employed in pharmaceutical and biomedical arena. Carboxymethylation is a base catalyzed reactions which incorporates the carboxylic acid groups onto the polymeric chains [4]. The reaction can be done under mild aqueous environments and does not require any harmful chemical solvents. The carboxymethyl derivative becomes anionic in nature and is more hydrophilic than the native polymer. Due to its anionic nature, the carboxymethyl derivative can interact with specific metal ions to form water insoluble hydrogels. These hydrogels are extensively used in development of sustained release matrices, films, and microparticles.

Tara gum (TG) is a seed endosperm galactomannan non-ionic polysaccharide obtained from *caesalpinia spinose* tree [2]. TG backbone is primarily comprised of a linear main chain of (1–4)- β- d -mannopyranose units joined by (1–6) linkage with α- d -galactopyranose units [2]. TG is a popular stabilizer and thickener in the food industry and is also used as edible films in food packaging industry [5, 6]. Grafted TG based superabsorbent hydrogels have also been synthesized [7]. However, TG is highly hydrophilic and its rheological properties are not suitable for the development of sustained release matrices [8]. Carboxymethylation modifies the rheological, physicochemical, hydrophilic and swelling attributes of the natural polysaccharide [9].

With this context, TG was derivatized to carboxymethyl TG (CMTG) by incorporating *O*-carboxymethyl groups in TG polymeric chains, with an anticipation to introduce ionic nature to TG making it amenable to cross-link with metal ions and also alter its swelling and hydrophilic characteristics.

2. Materials and methods

2.1 Materials

The chemical reagents used in the synthesis of CMTG is presented in Table 7.1.

Table 7.1 Materials used for the synthesis of CMTG

Chemical	Manufacturer
Tara Gum (TG)	IAMPURE Ingredients, India
Sodium hydroxide (NaOH)	Merck Specialities Pvt. Ltd., India
Ethanol	Merck Specialities Pvt. Ltd., India
Mono chloro acetic acid (MCA)	Merck Specialities Pvt. Ltd., India
Methanol	Merck Specialities Pvt. Ltd., India
Hydrochloric acid	Merck Specialities Pvt. Ltd., India
Phenolphthalein	Merck Specialities Pvt. Ltd., India
Distilled water	In-house

2.2 Synthesis of carboxymethyl tara gum

Modification of TG to CMTG was performed in an alkaline milieu by reacting TG with MCA as reported, with modifications [10]. At first, required amount of NaOH was dissolved in cool deionized water and then 5 g of the gum was slowly added to it with stirring and left untouched for uniform hydration. The dispersion temperature was elevated to 60ºC and maintained therein. Then MCA solution was gradually added into the alkaline TG dispersion with constant stirring for 30 min. The resulting dispersion was precipitated using methanol to obtain the carboxymethylated gum and washed with water. The precipitate was air dried, grounded to #72 mesh, and preserved in desiccators until further use. The degree of substitution (DS) of carboxymethylated gum was estimated by potentiometric back titration as per eq. (7.1).

$$DS = \frac{0.162P}{(1 - 0.058P)} \ldots\ldots\ldots (7.1)$$

P = NaOH/g of TG.

2.3 ^{13}C nuclear magnetic resonance (NMR) analysis

The solid state ^{13}C NMR spectral analysis (JEOL ECX 500 MHz NMR spectrometer) of TG and CMTG was carried out to ascertain the modification of the gum. Samples of TG and carboxymethylated TG (50mg each) were put on zirconium made sample holder equipped with

3.2 mm rotor at frequency 10 kHz. Tetramethyl silane (TMS) was used for referencing the spectra and was filled separately in the rotor. Referencing was done externally.

2.4 Fourier transform infrared (FTIR) analysis

Investigation of FTIR spectra of TG and CMTG were done in a FTIR spectrophotometer (RX 1, Perkin Elmer, UK) at 4000–400 cm $^{-1}$. Sample preparation involved sample mixing with potassium bromide in a hydraulic press to convert them into pellets.

2.5 X-ray diffraction (XRD) study

The patterns of X-ray diffraction of TG and CMTG were measured by X-ray diffractometer (D8, Bruker, Germany). The essential specifications are: current 30 mA, scan speed 5º/min, diffraction angle (2θ) 10–80º, and voltage 45Kv.

2.6 Differential scanning colorimetry (DSC) study

DSC thermograms of TG and CMTG were observed in a differential scanning colorimeter (Pyris Diamond TG/ DTA, Perkin Elmer, Singapore), calibrated against indium. Samples was introduced in an air tight aluminium container and heated at 30–400ºC at 10ºC/min, under constant nitrogen flow.

2.7 Subchronic oral toxicity study of the synthesised CMTG

The subchronic oral toxicity study of the synthesised gum was done at TAAB Biostudy Services (Kolkata, India) following OECD 407 procedures for testing of chemicals [9]. Study procedure authorization was done by IAEC, TAAB Biostudy Services (Kolkata, India). Twenty-four healthy wistar rats (6–8 months old) of each sex (non-pregnant and nulliparous females) were arbitrarily chosen and distributed into 4 groups of 6 rats each. The group contained same number of male and female. Rats were caged in polycarbonate cage (50 ± 20 % RH, 22 ± 5ºC and dark/light cycle of 12 h) with regular laboratory food, and enough access of drinking water. The rats were familiarized for seven days before start of experiment. CMTG was given orally at 500, 1000, and 2000 mg/kg dose and vehicle was fed to control group for 28 days. The animals were constantly examined every 30 min for the initial 4 h of CMTG administration and then examined every day for 28 days. The parameters examined were: a) examined daily for presence of any medical symptoms; b) mortality examined day-to-day for the study duration; c) the initial weight of rats and subsequently at 7 day intervals were taken; d) food consumption on weekly basis by each rats; e) the serum biochemical (MICROLAB-300 Semi-Auto Analyzer, Biozone India Scientific, India) and haematological (Medonic M

Series Cell Counter, LABX, India) values of all test groups were found out and interrelated with the control group; f) on the 29th day, the control groups rats and rats that were administered with 2000 mg/kg of CMTG were sacrificed and necropsy of kidneys, heart, liver, lungs and stomach were carried out. After necropsy, the tissues (of the control group and the 2000 mg/kg CMTG treatment group) were fixed in 10 % formalin solution for histopathology studies. After fixation for 24 h, the tissue sections were bathed in running water and dehydrated through a series of graded ethanol solutions (70–99.8 %), cleared in two changes of xylene, and then impregnated and embedded in paraffin blocks at room temperature. The paraffin blocks were sliced at 5 μm, fixed on microscopic glass slides and stained with H&E (hematoxylin and eosin) staining. The tissue samples were then examined and photographed using light microscope.

3. Results and Discussions

3.1 Synthesis and optimization of carboxymethylated tara gum

The structure of TG has abundant OH groups which can be replaced by carboxymethyl moieties. The carboxymethyl TG synthesis was performed in an alkaline milieu by reacting TG with MCA. The reaction occurs in two-steps. In the first step, a highly reactive alkoxide form of TG (TG-ONa) is generated by the reaction of NaOH with TG. In the next step, TG-ONa reacts with MCA, whereby the carboxymethyl moieties are incorporated into TG structural backbone. The two reactions are illustrated below.

$NaOH + TG\text{-}OH = TG\text{-}ONa + H_2O$ (1^{st} step)

$ClCH_2COOH + TG\text{-}ONa = TG\text{-}OCH_2COOH + H_2O$ (2^{nd} step)

A competitive parallel side reaction also takes place between MCA and NaOH, generating sodium glycollate.

$ClCH_2COOH + NaOH = NaCl + HOCH_2COONa$ (side reaction)

The success and efficiency of a carboxymethyl reaction is determined by the DS of the reaction. The DS reflects how much of the OH groups are replaced by the carboxymethyl groups. The DS is primarily dependent on two parameters, the reaction temperature and the ratio of NaOH/MCA. These parameters were optimised to get the highest DS of the CMTG. When the carboxymethylation temperature was maintained at 40ºC and the ratio of NaOH/MCA was varied from 0.35 to 0.50, the DS gradually increased from 0.42 to 0.78. Further increase in the ratio of NaOH/MCA to 0.55, decreased the DS to 0.72. Generation of the TG-ONa is important for the carboxymethyl reaction. Optimum TG-ONa will be generated when there will be

sufficient NaOH. Elevation in the ratio of NaOH/MCA from 0.35 to 0.50, activated the polymer and yielded sufficient TG-ONa [11]. TG-ONa promoted polymer swelling and enhanced the diffusion and permeation of the carboxymethylating agent, MCA [11]. However, when excess NaOH is present (ratio of NaOH/MCA 0.55), the side reaction predominates, which reduces the generation of the TG-ONa as well as the concentration of MCA. This probably reduced the DS to 0.72 when the ratio of NaOH/MCA was elevated to 0.55 [11]. The effect of reaction temperature on the DS of the carboxymethylation reaction was also evaluated. The optimized ratio of NaOH/MCA (0.50) was held constant and the reaction temperature was elevated from 40ºC to 70ºC. The value of DS at 50ºC was 0.81, improved to 0.84 at 60ºC, but declined to 0.69 at 70ºC. Optimum temperatures facilitate relaxation of the polymer chains and subsequent swelling of the polymer. The swelled polymer promotes diffusion and permeation of the carboxymethylating agent MCA, facilitating maximum replacement of the TG-ONa with MCA, thereby increasing DS of the reaction. However, elevated temperature decomposes the polymer chains leading to elimination of the intramolecular water. Elimination of the intramolecular water reduces the OH groups available for reaction and thus brings down the DS [12]. Based on the optimized parameters of the carboxymethylation reaction, the derivatization of TG to CMTG was done at 60ºC and at ratio of NaOH/MCA 0.50.

As there are 3 OH groups (located at C6, C2, and C3 position) per sugar unit of a gum, the theoretically highest DS value would be three [13]. However, the DS of our optimized CMTG is 0.84±0.03 (n=3). Literatures reports that the highest DS of other galactomannans guar gum and locust bean gum have seldom crossed 1 [14-15]. While there are 3 OH moieties/sugar unit in TG, the carboxymethylation substitution reaction generally occurs with the free OH moieties at the primary C6 location of the units. This is because of the feeble steric obstruction at the C6 position as compared to that in the secondary OH moieties at C2 and C3. The high steric impedance at the C2 and C3 positions is responsible for lower DS [16].

3.2 Characterisation of CMTG

The solid state ^{13}C NMR spectra of TG and carboxymethylated TG is displayed in Fig. 7.1. The ^{13}C spectra of TG displayed three specific absorption signals (Fig. 7.1a) at $\delta = 62.10$ ppm for C6 carbon of the mannose unit, $\delta = 72$ ppm for merging of signals of mannan carbon atoms at 2, 3, 4, and 5 position, and $\delta = 101.70$ ppm for C1 mannan carbon atom. Similar ^{13}C spectral signals of TG are reported previously [10]. The solid state ^{13}C spectra of the CMTG are shown in Fig. 7.1b. In addition to the ^{13}C spectral signals of TG, it reveals three extra signals at $\delta =$ 179.1, 169.2, and 167ppm, representing the carbonyl atom of the carboxymethyl groups at 6-

O, 3-O, and 2-O positions respectively. Similar signals for the carbonyl atoms of the carboxymethyl groups are reported earlier [14, 17]. The appearance of the three additional signals in the spectra of CMTG confirms the carboxymethyl reaction at all three locations.

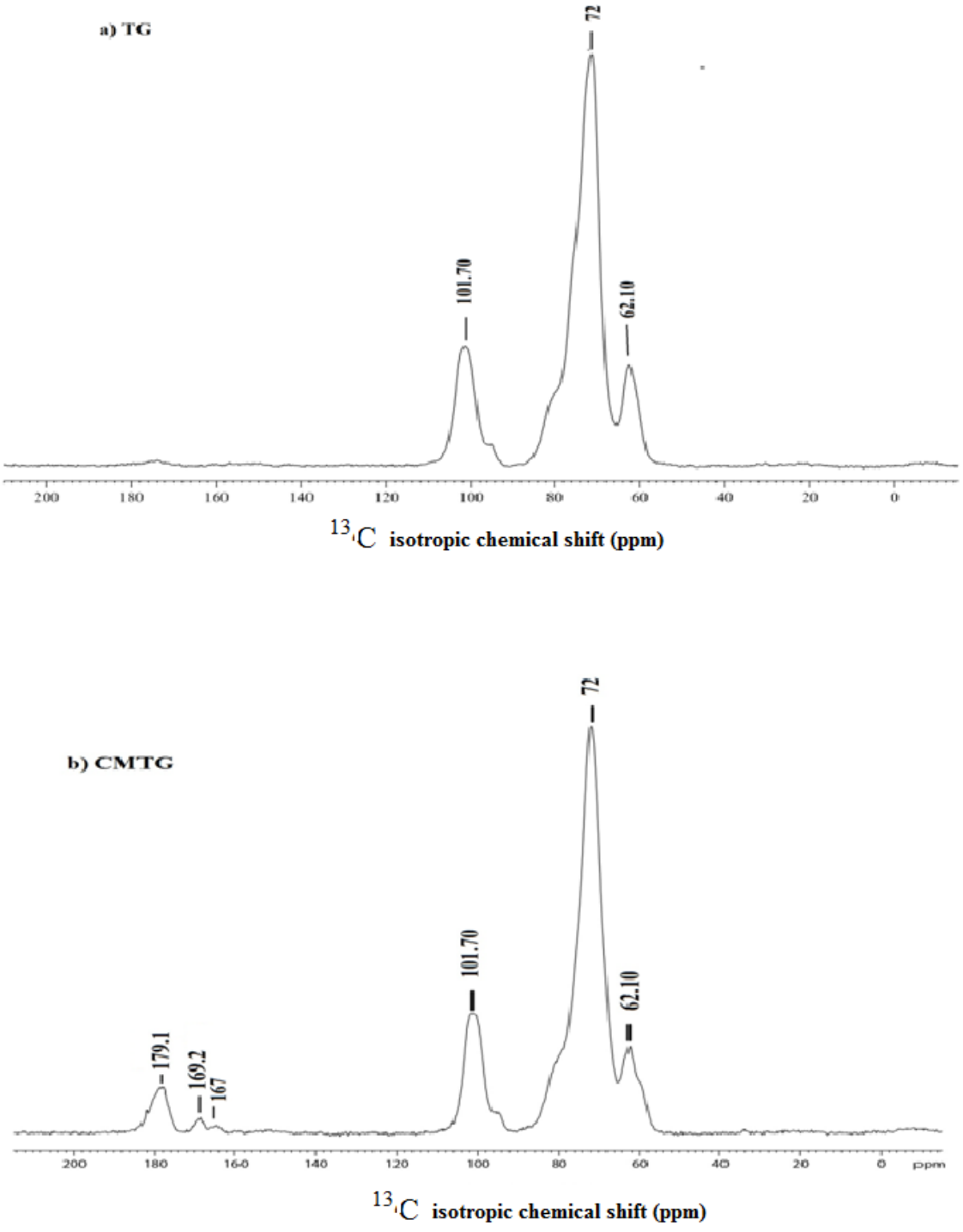

Fig. 7.1. ^{13}C solid state NMR spectra of (a) TG and (b) CMTG

The FTIR spectrum of TG and carboxymethyl TG are shown in Fig.7.2. The IR spectrum of TG (Fig.7.2.) showed a wide peak at 3303 cm^{-1} representing the stretching of the OH moieties

of the gum. The band at 2915 cm^{-1} stands for CH symmetrical stretching and that at 1642 cm^{-1} represents hydroxyl bending vibrations of water. Peak due to bending of H_2C-O-CH_2 is located at 1024 cm^{-1}. The presence of α-D-galactopyranose and β-D-galactopyranose units are confirmed by the absorption peaks at 812 cm^{-1} and 870 cm^{-1} respectively. Literature reports similar IR spectrums of TG [7,18]. Fig. 7.2 depicts the IR spectrum of CMTG. The absorption peaks of the carboxymethylated gum showed up at almost similar wavenumbers as that of TG. Moreover, CMTG displayed characteristics absorption peaks at 1591 cm^{-1} signifying the COO^- asymmetric stretching. Spectrums at 1414 cm^{-1} and 1321 cm^{-1} stands for symmetric stretching of COO^-. The peak intensity at 3303 cm^{-1} appears to be of diminished intensity indicating that the OH groups are substituted with the carboxymethyl groups, ascertaining the insertion of the carboxymethyl groups onto TG structure [14]. Peak intensities at 812 cm^{-1} and 870 cm^{-1} also seems to be reduced. This might be due to molecule breakdown and consequent reduction in the molar mass of the obtained product during the carboxymethyl substitution reaction. The emergence of the additional new peaks in the spectrum of CMTG indicated that the OH groups of TG are substituted by the carboxymethyl moieties. Similar IR spectrum of TG are also reported [19].

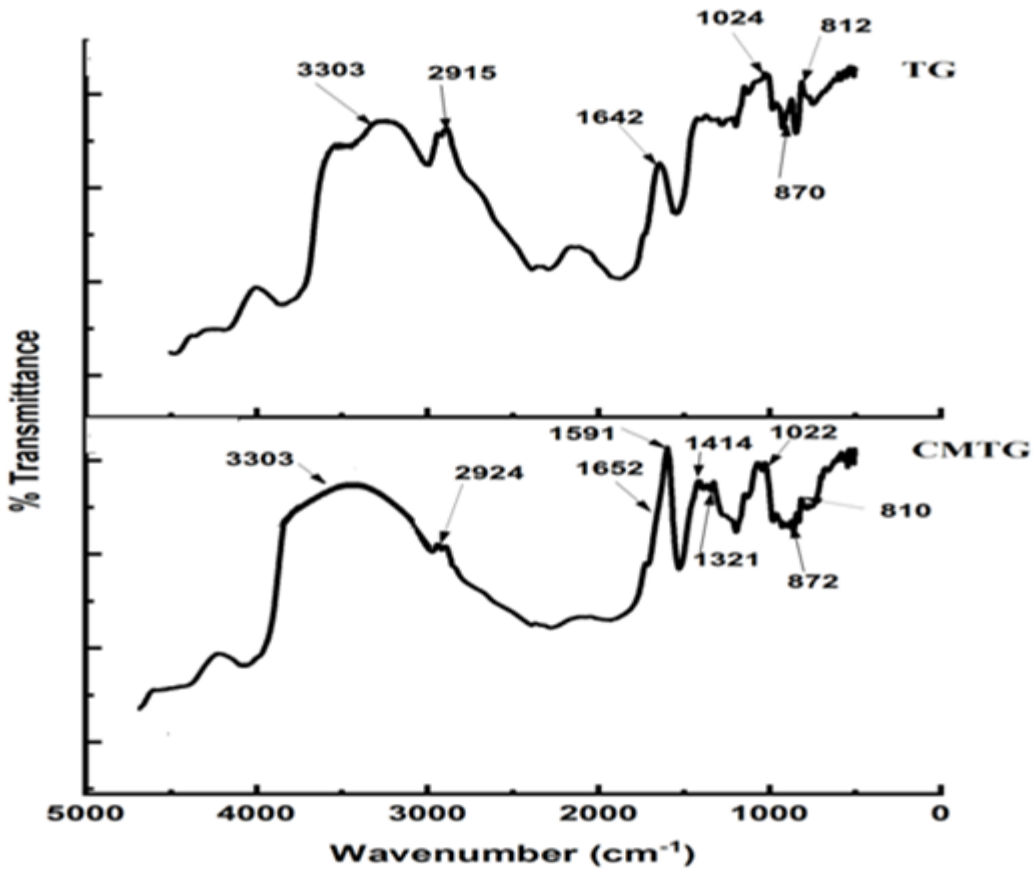

Fig. 7.2. FTIR spectrum of TG and CMTG.

The X-ray diffraction patterns of TG and CMTG are illustrated in Fig. 7.3. The XRD trace of TG indicates its amorphous nature. Similar to TG, the other galactomannan guar gum is also amorphous in nature [20]. The XRD pattern of CMTG also seems like an amorphous hallow, except the appearance of twin intense peaks of intensities 877cps and 484cps at diffraction 2θ 31.68º and 45.40º respectively. Maity et al. have reported the appearance of similar twin intense peaks of almost same intensities (822 cps and 321cps) at the same wavenumbers during the carboxymethylation reaction of xanthan gum [21]. The presence of the two intense peaks in the XRD pattern of CMTG highlighted the slight improvement in crystallinity of TG after the carboxymethylation reaction. A possible explanation of the above phenomena is given below. The carboxymethylation reaction is carried out at a continuous elevated temperature of 50ºC - 60ºC. This high temperature conditions may have improved the organization and orientation of the TG polymeric chains, thereby enhancing the crystallinity of TG [22]. It has also been reported that carboxymethyl gum kondagogu is having improved crystallinity compared to its native form [23].

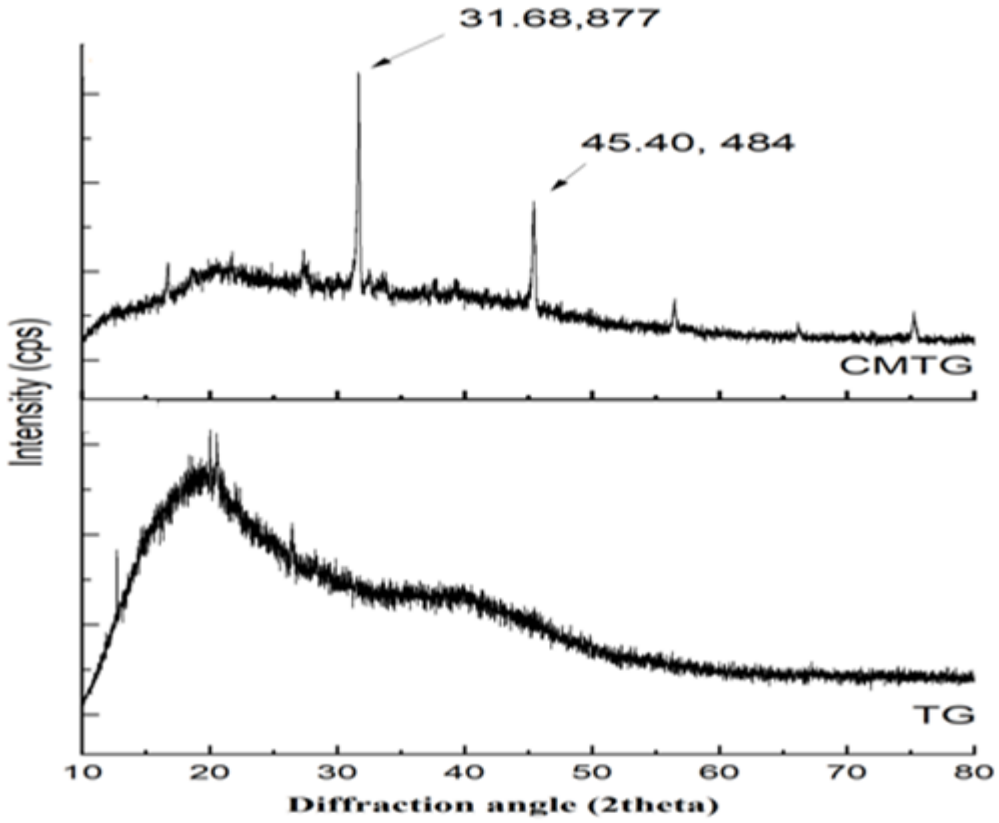

Fig. 7.3. XRD traces of TG and CMTG.

TG and CMTG DSC thermograms are displayed in Fig. 7.4. The thermogram of TG is characterised by the presence of an expanded endotherm at 69ºC assignable to the loss of water from the polymer sample. An exotherm at 306ºC indicates the thermal decomposition or

degradation of the gum. Similar thermal behaviour of TG is available in literature [24]. The DSC curve of CMTG displayed an expanded endothermic event between temperature 70ºC and 120ºC. This event represents water loss from CMTG sample [22,25]. A second exothermic event for CMTG appeared at 259ºC signifying the thermal decomposition or degradation of CMTG [10]. Comparison of the thermal events of the TG and CMTG highlights that the decomposition temperature of CMTG is lower compared to TG. It may be due to the carboxymethylation reaction [26]. The carboxymethylation reaction breaks the inter and intramolecular hydrogen bonding. This facilitates the mobility of chain fragments and hastens the degradation of the modified gum at lower temperature, diminishing its thermal stability.

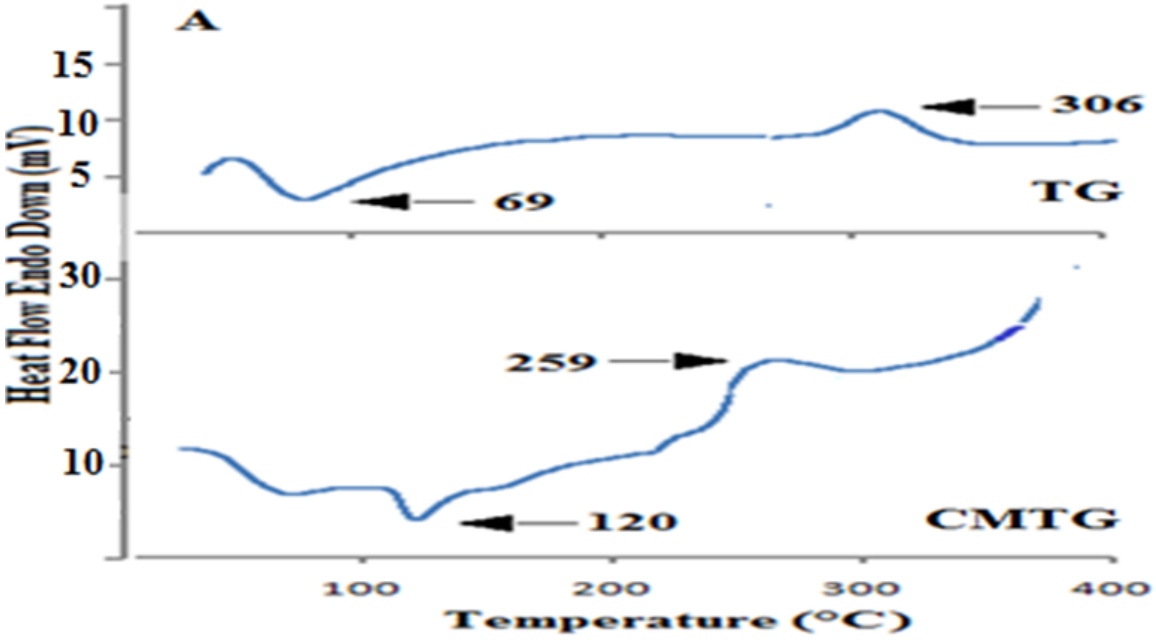

Fig. 7.4. DSC curve of TG and CMTG.

The synthesised gum was evaluated for sub chronic oral toxicity to gather some knowledge about the health risks that may happen following oral intake of the gum. The test outcomes are herein elaborated. The body weights (average) of all dosed group of rats (either sex) didn't exhibited any obvious weight variation throughout the 28 days treating period and the values are analogous with the control group rats. The body weights (average) of all group of rats of either sex of the dosed group are given in Tables 7.2 and 7.3. The food intake of all dosed group was reasonable and no unusual food intake was perceived. The food intake (gm/rat) of all dosed group of rats of both sex is given in Tables 7.4 and 7.5. Minor variations in the figures of different factors under the haematological and serum biochemical studies were detected when the values of dosed groups were interrelated with the test group, and all figures were within the natural medical limits. The haematological and serum biochemical studies are meticulously

shown in Tables 7.6-7.9. The histopathology pictures of kidney, stomach, liver, heart, and lungs of the control group rats and that dosed with the maximum dose of CMTG didn't indicate any symptoms of irregularity (Figure 7.5). As per the outcomes of the subchronic oral toxicity study, it can be concluded that the synthesized CMTG was bereft of any suggestive indications of haematological toxicity, behavioural toxicity, hepatotoxicity and nepherotoxicity in any dose group. Nil lethality in all the dose groups pointed out that the LD_{50} of CMTG is above 2000mg/kg. According to the globally harmonized system (GHS), if the LD_{50} value is higher than 2000 mg/kg dose, then the sample under investigation will fall under "category 5" and the toxicity rating will be "zero". Therefore, CMTG falls under "category 5" and its toxicity rating is "zero".

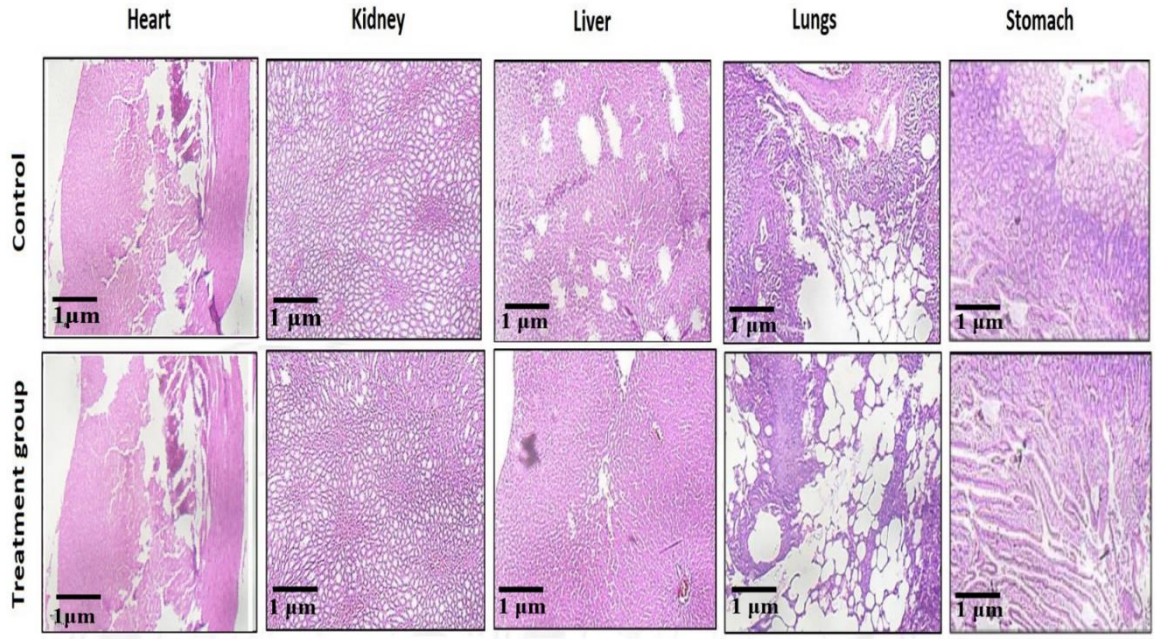

Fig. 7.5. Histopathology images of heart, kidney, liver, lungs, and stomach of the control and the highest dose CMTG treatment group of animals.

Table 7.2 Group mean body weight (gm) of male rats from each treatment group

Gr. No.	Dose mg/kg		Day				
			0	**7**	**14**	**21**	**28**
I	Control	Mean	123.13	125.70	129.17	134.97	140.21
		± SD	1.48	2.18	2.73	2.31	2.02
II	500	Mean	122.0383	123.5836	126.9368	132.4009	138.4609
		± SD	1.5049	1.4847	1.9392	2.4846	2.7068
III	1000	Mean	122.8867	126.856	133.32	138.1175	142.9453
		± SD	1.4948	1.9594	2.2321	2.1412	1.9897
IV	2000	Mean	121.5838	123.2705	126.856	127.5327	132.815
		± SD	1.2726	1.7776	2.3533	2.4644	2.02

Table 7.3 Group mean body weight (gm) of female rats from each treatment group

Gr. No.	Dose mg/kg		Days				
			0	**7**	**14**	**21**	**28**
I	Control	Mean	118.97	122.55	127.18	133.84	136.64
		± SD	1.40	1.80	1.80	2.20	2.64
II	500	Mean	120.98	125.85	131.32	135.83	138.74
		± SD	1.05	1.12	1.58	1.66	4.55
III	1000	Mean	120.44	125.26	130.36	135.01	139.96
		± SD	0.86	1.74	2.03	2.69	2.64
IV	2000	Mean	120.34	125.80	131.74	136.91	141.07
		± SD	2.03	2.06	3.76	3.32	3.17

Table 7.4 Group mean food consumption (g/animal) of male rats from each treatment group

Gr. No.	Dose mg/kg		Day				
			0	**7**	**14**	**21**	**28**
I	Control	Mean	6.94	7.35	7.81	8.15	8.58
II	500	Mean	7.15	7.39	7.78	8.19	8.15
III	1000	Mean	7.20	7.34	7.83	8.05	8.47
IV	2000	Mean	7.25	7.52	7.57	7.83	7.94

Table 7.5 Group mean food consumption (g/animal) of female rats from each treatment group

Gr. No.	Dose mg/kg		Day				
			0	**7**	**14**	**21**	**28**
I	Control	Mean	6.76	6.95	7.07	7.24	7.39
II	500	Mean	6.39	6.75	6.99	7.33	7.73
III	1000	Mean	6.57	6.81	7.08	7.25	7.60
IV	2000	Mean	6.71	7.11	7.23	7.42	7.35

Table 7.6 Group mean haematology of male rats from each treatment group

Gr. No.	Dose mg/kg		Hb (g/dL)	Total RBC (x10/mm^3)	Rt (%)	Platelets (10^3 /µL)	Total WBC (10^3/µL)	Differential %			
								N	L	E	M
I	Control	Mean	15.07	6.58	3.24	4.56	6.81	17.19	74.18	2.11	0.52
		± SD	1.88	0.64	0.79	0.62	1.28	4.07	12.01	1.27	0.57
II	500	Mean	14.78	6.4	3.17	5.23	7.62	13.81	77.82	2.70	0.52
		± SD	1.81	0.98	1.05	1.03	2.67	3.98	8.51	1.20	0.57
III	1000	Mean	14.31	6.34	3.06	5.28	8.50	16.95	79.90	3.28	0.70
		± SD	0.57	0.47	0.93	1.21	1.87	5.67	9.34	1.34	0.54
IV	2000	Mean	14.43	5.82	3.43	5.75	6.36	27.04	76.44	2.42	0.52
		± SD	0.51	0.74	0.91	0.66	0.38	3.14	6.13	1.35	0.57

Hb:Hemoglobin, RBC: Red Blood Corpuscles, Rt: Reticulocyte, WBC: White Blood Corpuscles, N: Neutrophils, L: Lymphocyte, E: Eosinophils, M: Monocytes

Table 7.7 Group mean haematology of female rats from each treatment group

Gr. No.	Dose mg/kg		Hb (g/dL)	Total RBC (x10/mm^3)	Rt (%)	Platelets (10^3 /µL)	Total WBC (10^3/µL)	Differential %			
								N	L	E	M
I	Control	Mean	14.30	6.75	3.27	5.4	8.2	19.3	84.7	2.3	0.5
		± SD	0.55	0.60	0.93	0.96	3.23	5.14	7.68	0.75	0.55
II	500	Mean	13.20	7.34	3.24	5.43	7.63	19.33	78.17	2.33	0.5
		± SD	0.73	0.77	0.91	1.02	1.92	3.14	7.94	0.82	0.55
III	1000	Mean	13.56	6.51	3.66	4.78	7.55	16.33	80.17	2.33	0.67
		± SD	0.70	0.62	0.82	1.13	2.73	3.98	8.52	0.82	0.52
IV	2000	Mean	14.78	6.28	2.63	5.3	6.65	18.67	75.5	2	0.67
		± SD	0.64	0.77	0.57	0.45	1.28	2.8	5.28	0.63	0.52

Table 7.8 Group mean blood chemistry of male rats from each treatment group

Gr. No.	Dose mg/kg		Total Serum Protein (g/dL)	BUN (mg/dL)	SGPT (IU/L)	SGOT (IU/L)	SAP (IU/L)	Blood Sugar (mg/dL)	Creatinine (mg/dL)	Total Bilirubin (mg/dL)
I	Control	Mean	6.76	17.44	61.23	91.75	142.60	93.74	0.76	0.38
		± SD	0.66	3.65	19.82	14.42	4.45	8.74	0.15	0.11
II	500	Mean	6.92	17.44	79.31	96.29	167.97	94.26	0.79	0.51
		± SD	0.62	4.02	2.32	4.44	8.15	6.72	0.19	0.24
III	1000	Mean	7.12	19.88	69.66	94.63	161.95	9 5.92	0.69	0.49
		± SD	0.81	2.22	8.89	1.11	5.95	4.78	0.21	0.25
IV	2000	Mean	7.16	23.10	64.38	90.82	165.27	95.73	0.74	0.44
		± SD	0.80	2.94	4.10	4.50	3.59	3.13	0.27	0.21

BUN: Blood urea nitrogen, SGPT: Serum glutamic pyruvic transaminase, SGOT: Serum glutamic oxaloacetic transaminase, SAP: Serum Amyloid P-Component

Table 7.9 Group mean blood chemistry of female rats from each treatment group

Gr. No.	Dose mg/kg		Total Serum Protein (g/dL)	BUN (mg/dL)	SGPT (IU/L)	SGOT (IU/L)	SAP (IU/L)	Blood Sugar (mg/dL)	Creatinine (mg/dL)	Total Bilirubin (mg/dL)
I	Control	Mean	7.37	19.21	55.94	100.72	126.37	96.42	0.77	0.34
		± SD	0.82	3.57	9.31	26.35	8.51	3.83	0.21	0.12
II	500	Mean	7.20	17.71	52.56	102.04	139.16	106.03	0.73	0.32
		± SD	0.62	3.76	5.38	3.81	3.20	6.87	0.17	0.14
III	1000	Mean	7.37	18.95	56.62	100.34	123.55	99.25	0.94	0.45
		± SD	0.70	6.42	31.06	6.45	6.71	5.90	0.25	0.9
IV	2000	Mean	7.15	23.71	48.97	104.22	126.15	109.22	0.86	0.36
		± SD	0.70	6.93	4.08	4.79	3.87	7.75	0.21	0.11

References

1. Prajapati VD, Jani GK, Moradiya NG, Randeria NP. Pharmaceutical applications of various natural gums, mucilages and their modified forms. Carbohydr. Polym. 2013;92 (2):1685–1699.

2. Mukherjee K, Dutta P, Badwaik HR, Saha A, Das A, Giri TK. Food industry applications of Tara gum and its modified forms. Food Hydrocolloids for Health. 2023;3:100107

3. Mahmoud H, Elella A, Goda ES, Abdallah HM, Abdel- Aziz MM, Gamal H. Green engineering of TMC-CMS nanoparticles decorated graphene sheets for targeting M. Tuberculosis. Carbohydr. Polym. 2023;303:120443.

4. Rakshit P, Giri TK, Mukherjee K. Research progresses on carboxymethyl xanthan gum: Review of synthesis, physicochemical properties, rheological characterization and applications in drug delivery. Int. J. Biol. Macromol. 2024;266(1):131122.

5. Antoniou J, Liu F, Majeed H, Zhong F. Characterization of tara gum edible films incorporated with bulk chitosan and chitosan nanoparticles: a comparative study. Food Hydrocoll. 2015;44:309–319.

6. Chen Y, Xua L, Wang Y, Chen Z, Zhang M, Chen H. Characterization and functional properties of a pectin/tara gum based edible film with ellagitannins from the unripe fruits of Rubuschingii hu. Food Chem. 2020;325:126964.

7. Li B, Shen J, Wang L. Development of an antibacterial superabsorbent hydrogel based on tara gum grafted with polyacrylic acid. Int. J. Environ. Res. Public Health. 2017;4(2):30–35.

8. Ma Q, Wang L. Preparation of a visual pH-sensing film based on tara gum incorporating cellulose and extracts from grape skins. Sens. Actuators B. 2016;235:401–407.

9. Badwaik HR, Kumari L, Maity S, Sakure K, Ajazuddin, Nakhate KT, Tiwari V, Giri TK. A review on challenges and issue with carboxymethylation of natural gums: the widely used excipients for conventional and novel dosage forms. Int. J. Biol. Macromol. 2022;209 (B):2197–2212.

10. Santos MB, dos Santos CHC, de Carvalho MG, de Carvalho CWP, Garcia- Rojas EE. Physicochemical, thermal and rheological properties of synthesized carboxymethyl tara gum (Caesalpinia spinosa). Int. J. Biol. Macromol. 2019;134:595–603.

11. Soni SR, Bhunia BK, Kumari N, Dan S, Mukherjee S, Mandal BB, Ghosh A. Therapeutically effective controlled release formulation of pirfenidone from nontoxic biocompatible carboxymethyl pullulan-poly(vinyl alcohol) interpenetrating polymer networks. ACS Omega. 2018;3:11993–12009.

12. Pushpamalar V, Langford S, Ahmad M, Lim Y. Optimization of reaction conditions for preparing carboxymethyl cellulose from sago waste. Carbohydr. Polym. 2006;64:312–318.

13. Sullad AG, Manjeshwar LS, Aminabhavi TM. Microspheres of carboxymethyl guar gum for in vitro release of abacavir sulfate: preparation and characterization. J. Appl. Polym. Sci. 2011;122:452–460.

14. Kaity S, Ghosh A. Carboxymethylation of locust bean gum: application in interpenetrating polymer network microspheres for controlled drug delivery. Ind. Eng. Chem. Res. 2013;52:10033-10045.

15. Singh R, Maity S, Sa B. Effect of ionic crosslink on the release of metronidazole from partially carboxymethylated guar gum tablet. Carbohydr. Polym. 2014;106:414–421.

16. Rana V, Rai P, Tiwary AK, Singh RS, Kennedy JF, Knill CJ. Modified gums: approaches and applications in drug delivery. Carbohydr. Polym. 2011;83:1031–1047.

17. Chakravorty A, Barman G, Mukherjee S, Sa B. Effect of carboxymethylation on rheological and drug release characteristics of locust bean gum matrix tablets. Carbohydr. Polym. 2016;144:50–58.

18. Shen J, Li B, Zhan X, Wang K. A one pot method for preparing an antibacterial superabsorbent hydrogel with a semi-IPN structure based on tara gum and polyquaternium-7. Polymers. 2018;10:696–707.

19. Santos MB, de Carvalho MG, Garcia-Rojas EE. Carboxymethyl tara gum lactoferrin complex coacervates as carriers for vitamin D3: encapsulation and controlled release. Food Hydrocoll. 2021;112:106347.

20. Pal S, Mal D, Singh RP. Synthesis and characterization of cationic guar gum: a high performance flocculating agent. J. Appl. Polym. Sci. 2007;105:3240–3245.

21. Maity S, Sa B. Ca-carboxymethyl xanthan gum mini-matrices: swelling, erosion and their impact on drug release mechanism. Int. J. Biol. Macromol. 2014;68:78–85.

22. Vendruscolo CW, Ferrero C, Pineda EAG, Silveira JLM, Freitas RA, Jim´enez-Castellanos MR, Bresolin TMB. Physicochemical and mechanical characterization of galactomannan from Mimosa scabrella: effect of drying method. Carbohydr. Polym. 2009;76:86–93.

23. Kumar A, Ahuja M. Carboxymethyl gum kondagogu: synthesis, characterization and evaluation as mucoadhesive polymer. Carbohydr. Polym. 2012;90:637–643.

24. Fernandes RA, Garcia-Rojas EE. Effect of cosolutes on the rheological and thermal properties of Tara gum aqueous solutions. J. Food Sci. Technol. 2021;58:2773–2782.

25. Timilsena YP, Adhikari R, Kasapis S, Adhikari B. Molecular and functional characteristics of purified gum from Australian chia seeds. Carbohydr. Polym. 2016;136:128–136.

26. Gong H, Liu M, Chen J, Han F, Gao C, Zhang B. Synthesis and characterization of carboxymethyl guar gum and rheological properties of its solutions. Carbohydr. Polym. 2012;88:1015–1022.

Chapter 8:

Development and evaluation of single and dual cross-linked hydrogel matrices

1. Introduction

Hydrophilic polysaccharides find extensive use in the development of matrices for sustained drug delivery. These hydrophilic polysaccharides, in contact with water, possess the exclusive ability to absorb water, swell and form a rigid and stiff viscous layer over the matrix surface [1]. Delivery of drug from a viscous stiff and swollen layer is governed by the diffusion of the drug through that layer. The swelling of the hydrophilic polysaccharides also results in relaxation and disentanglement of the polymer chains. The disentanglement and relaxation of the polymeric chains is dictated by the rate of absorption and penetration of water into the core of the polymeric matrix, which in turn is dependent on the viscosity of that polymeric matrix. When the process of disentanglement and relaxation of the polymeric chains continues, the branches of the polymeric chains separate from its parent chain, which is perceived as erosion of the matrix. Polymeric chain erosion also results in delivery of drug from the matrices. It is thus evident that viscosity, swelling and the resulting erosion of the hydrophilic polymeric matrix are the primary factors controlling the drug dissolution from the matrix [1, 2]. Thus, modulation of the swelling, viscosity, and erosion of the matrix will result in tailoring of drug dissolution from the matrix.

Cross-linking of the hydrophilic polysaccharide polymer chains is simple and effective method to control the erosion, swelling, and viscosity of the matrix, and thus the drug dissolution [2]. Anionic polymers can cross-link with selective metal cations to form a true hydrogel layer over the matrix surface. The true hydrogel layer swells less, is rigid and exceptionally viscous, and erodes very slowly, resulting in sustained drug dissolution from the true hydrogel layer.
With this hypothesis, the synthesized CMTG was cross-linked with aluminium and/or calcium ions and the impact of crosslinking ions on the erosion, swelling, and in vitro tramadol hydrochloride dissolution from the matrices is investigated.

2. Materials and methods

2.1 Materials

The ingredients required in this study are given in Table 8.1.

Table 8.1 Chemicals required

Ingredients	Manufacturer
Tramadol Hydrochloride (TH) (gift sample)	IPCA laboratories, Sikkim, India.
Trisodium orthophosphate dodecahydrate	Loba Chemie Pvt. Ltd.
Hydrochloric acid	Merck Specialities Pvt. Ltd., India
Calcium chloride ($CaCl_2$)	Merck Specialities Pvt. Ltd., India
Aluminium chloride ($AlCl_3$)	Loba Chemie Pvt. Ltd.
Magnesium stearate	Loba Chemie Pvt. Ltd.

2.2 Development of hydrogel matrices

The hydrogel matrices composition is shown in Table 8.2. CMTG and TH (# 72 grade) were blended homogeneously and then slowly triturated with cross-linking solutions to form a wet cohesive mass. The wet cohesive mass was put through # 18 screen and dried in an oven. The dried mass was once again put through # 23 mesh to get the granules and again dried. The granules were then blended with magnesium stearate (lubricant) and compressed in a flat faced 6 mm punch automatic tablet punching machine (RIMEK, Karnavati Engineering Ltd., India).

Table 8.2 Hydrogel matrices composition

Formulation code	Quantity of CMTG (mg)	Amount of TH(mg)	Quantity of $CaCl_2$ (mg)	Quantity of $AlCl_3$ (mg)	Weight % of crosslinkions in the matrix (% w/w)	Weight of matrix (mg) (CMTG+ $CaCl_2$/ $AlCl_3$)	Weight % between $AlCl_3$/ $CaCl_2$ (% w/w)	Mag St (mg)	Hardness (Kg/cm^2)
F1	225	100	-	-	0%	225	-	2	4
F2	218.25	100	-	6.75	3%	225	-	2	4
F3	211.5	100	-	13.5	6%	225	-	2	4
F4	204.75	100	-	20.25	9%	225	-	2	4
F5	198	100	-	27	12%	225	-	2	4
F6	218.25	100	6.75	-	3%	225	-	2	4
F7	211.5	100	13.5	-	6%	225	-	2	4
F8	204.75	100	20.25	-	9%	225	-	2	4
F9	198	100	27	-	12%	225	-	2	4
F10	191.25	100	33.75	-	15%	225	-	2	4
F11	204.75	100	14.175	6.075	9%	225	30/70 ($CaCl_2$/$AlCl_3$)	2	4
F12	204.75	100	10.125	10.125	9%	225	50/50 ($CaCl_2$/$AlCl_3$)	2	4
F13	204.75	100	6.075	14.175	9%	225	70/30 ($CaCl_2$/$AlCl_3$)	2	4
F14	198	100	18.9	8.1	12%	225	30/70 ($AlCl_3$/$CaCl_2$)	2	4

F15	198	100	13.5	13.5	12%	225	50/50 ($AlCl_3$/$CaCl_2$)	2	4
F16	198	100	8.1	18.9	12%	225	70/30 ($AlCl_3$/$CaCl_2$)	2	4

2.3 Characterization of the hydrogel matrix tablets

2.3.1 Weight Variation Test

20 tablets were precisely weighed in an electronic balance (SPT-200, Prime Technologies, India). The individual tablet weight was matched with the average tablet weight.

2.3.2 Crushing Strength (hardness) of hydrogel matrices

Hardness of the matrices was examined in a Monsanto Tablet Hardness Tester (Campbell Electronics, Mumbai, India), and mean hardness of 10 tablets was taken.

2.3.3 Friability Test

Weight of 10 matrices were noted and put in the friabilator drum (EF2, Electro Lab, Mumbai, India) and rotated at 25±1 rpm. Following 100 revolutions, the matrices were cleaned, de-dusted and reweighed. The weight loss (percentage) was determined.

2.3.4 TH content of the hydrogel tablets

3 tablets were crushed individually in a mortar and pestle and finely grounded. The grounded mass was then transferred in to 250 ml pH 7.4 volumetric flask and mechanically shaken for 24 h. After 24 h, the solution was filtered and following adequate dilutions was spectrophotometrically (UV-2450, Shimadzu, Japan) analysed at 270 nm for determining the TH content in the hydrogel tablets.

2.4 Erosion and swelling of the hydrogel tablets

The percentage erosion and swelling of the unloaded hydrogel tablets were determined in USP II dissolution instrument. One hydrogel tablet was precisely weighed (W_0, initial hydrogel tablet weight) (SPT-200, Prime Technologies, India) and put inside a net basket and the whole assembly was immersed in dissolution solution. At hourly time intervals, the net basket assembly was taken out from the dissolution solution, freed from the surface water using a tissue paper and then the hydrogel tablets were weighed precisely (W_t, matrix weight at the particular time interval). The hydrogel matrix was then kept inside a hot air oven for drying until constant weight and then the final constant weight of the matrix (W_f) was noted accurately.

The percentage erosion and swelling of the hydrogel matrix was determined following Eq. (8.1) & Eq. (8.2) [2].

$$\% \, Swelling = \frac{W_t - W_0}{W_0} \times 100 \ldots\ldots\ldots\ldots\ldots\ldots\ldots\ldots (8.1)$$

$$\% \, Erosion = \frac{W_0 - W_f}{W0} \times 100 \ldots\ldots\ldots\ldots\ldots\ldots\ldots\ldots . (8.2)$$

2.5 *In-vitro* dissolution of TH

In-Vitro TH dissolution from hydrogel matrices were determined as per IP 2018 procedure in an USP II dissolution instrument (TDT-06P, Electrolab, India). One matrices were submerged in a glass beaker filled with 700 ml pH 1.2. After 2 h, the media pH was elevated to pH 7.4 by addition of 200 ml 0.2 (M) trisodium ortho phosphate dodecahydrate solution and dissolution continued for the next 10 h. Aliquots were taken out at hourly intervals and refilled with the same volume of the respective dissolution media. Aliquots were analysed in a spectrophotometer (UV-2450, Shimadzu, Japan) at 270 nm and the TH dissolved from the hydrogel tablets were determined from calibration curve plotted at the individual dissolution solution. Dissolution of TH hydrogel tablets were done in triplicates.

2.6 Fourier transform infrared (FTIR) analysis

Investigation of FTIR spectra of TH and TH hydrogel matrices were done in a FTIR spectrophotometer (RX 1, Perkin Elmer, UK) at 4000–400 cm^{-1}. Sample preparation include sample mixing with potassium bromide in a hydraulic press to convert them into pellets.

2.7 X-ray diffraction (XRD) study

The patterns of X-ray diffraction of TH and TH hydrogel matrices were measured by X-ray diffractometer (D8, Bruker, Germany). The essential specifications are: scan speed 5º/min, current 30 mA, diffraction angle (2θ) 10–80º, and voltage 45Kv.

2.8 Differential scanning colorimetry (DSC) study

DSC thermal curves of TH and TH hydrogel matrices were observed in a differential scanning colorimeter calibrated against indium (Pyris Diamond TG/ DTA, Perkin Elmer, Singapore). Samples was introduced in a sealed aluminium bottle and heated at 30–400ºC at 10ºC/min, under nitrogen atmosphere.

2.9 Determination of Viscosity

Dispersions simulating the hydrogel matrix formulae were prepared and left for 24 h for homogenous hydration. The viscosities of the dispersions were determined using S 61 spindle in a viscometer (DV-E, Brookfield Engg. Inc., USA) at 37ºC.

2.10 Scanning electron microscopy (SEM)

Surface structure of selected matrices before and following 6 h dissolution was observed in a scanning electron microscope (SU3800, Hitachi, Japan) at 15 Kv. The matrices were mounted onto stubs and gold-sputter coated to render them electrically conductive.

2.11 Diffusion coefficient of TH

The equivalent spherical diameter (cm) of hydrogel matrix tablets was found out from the equation $d = (6r_ch)^{1/3}$, where d, h, and r_c represents the equivalent spherical diameter, height (cm), and radius of the hydrogel tablets. The diffusion coefficients (cm^2/s) were determined following Eq. (8.3) [3].

$$D_c = \pi \times (\frac{r\theta}{6M_\infty})^2 \ldots\ldots\ldots\ldots\ldots\ldots\ldots (8.3)$$

Where θ = gradient of the straight line of the $M_t/M\alpha$ v/s $t^{1/2}$ plot.

M_α = TH loaded in the hydrogel matrices.

M_t = TH dissolved in t s.

r = equivalent spherical radius of the hydrogel matrices.

2.12 Water penetration (intrusion) velocity

The percent swelling data was used to compute the velocity of penetration (intrusion) of water into the hydrogel matrices following the process defined as per Eq. (8.4) [1].

$$V = \frac{1}{2\rho A} \times \frac{d_w}{d_t} \ldots\ldots\ldots\ldots\ldots\ldots (8.4)$$

Where V stands for water penetration (intrusion) velocity, ρ for the density of water (37°C), A for the hydrogel tablets surface area and dw/dt denotes the gradient of the % swelling v/s time plots.

2.13 Swelling and TH dissolution mechanism

Power law equation (8.5) was utilized to define the mechanism & kinetics of TH dissolution from hydrogel matrices [2].

$$\frac{M_t}{M_\infty} = kt^n \ldots\ldots\ldots\ldots\ldots\ldots\ldots\ldots\ldots (8.5)$$

Where $M_t/M\alpha$ = portion of TH dissolved at time t, n= diffusional exponent, k= rate constant

For tablet matrices, n=0.5 signifies Fickian diffusion, 0.5<n<1.0 is suggestive of anomalous or non-Fickian diffusion, n=1.0 suggests case II and n>1.0 characterizes super case II transport process [2].

The swelling kinetics was found out similarly, where the swelling results for initial 3 h, when the matrix swelling predominated, was plotted to the power law equation.

2.14 Mean dissolution time (MDT)

The MDT (min) was calculated from Eq. (8.6) [4]. The power law Eq. (8.5) was utilized for gathering the n and k values.

$$MDT = \left(\frac{n}{n+1}\right) k^{\left(-\frac{1}{n}\right)} \ldots\ldots\ldots\ldots\ldots\ldots\ldots\ldots (8.6)$$

2.15 Statistical Analysis

ANOVA (GraphPad Prism 3.0) was done to ascertain the statistical importance of the data gathered from erosion, swelling, and TH dissolution study. The difference was reckoned significant when $p<0.05$.

3 Results and discussion

3.1 TH compatibility in hydrogel matrices

The excipient-TH compatibility was judged by FTIR, DSC, and XRD studies. The FTIR spectrum of TH and TH hydrogel tablets are illustrated in Fig. 8.1. The spectrum of TH demonstrated a peak at 3306 cm^{-1} representing OH stretching. Subsequent peaks at 3062 cm^{-1} and 2929 cm^{-1} stands for aromatic CH ring stretching and methyl group CH stretching. The peak at 2859 cm^{-1} is because of CH_2 stretching. Additional peaks at 1586 cm^{-1}, 1259 cm^{-1}, and 753 cm^{-1} represents C=C (aromatic) stretching, CN stretching, and substituted benzene ring stretching respectively. Similar IR signals of TH have been reported by Deb et. al. [5]. The IR signals for TH hydrogel matrices appeared at almost similar wavenumbers as that of TH, indicating the TH compatibility in the hydrogel tablets.

The DSC curves of TH and TH hydrogel tablets are described in Fig. 8.2. The intense endotherm at 180ºC is the melting point of TH. The stretched endotherm at 200ºC-260ºC signified total degradation/decomposition of TH. Related DSC events of TH are available in literature [5]. The DSC thermal events of TH hydrogel matrices revealed an expanded endotherm at 70ºC representing water loss and an exotherm at 260ºC indicating CMTG decomposition. The stretched exotherm originating at 190ºC and culminating at 210ºC represents the melting of $AlCl_3$ [6]. The sharp endotherm at 180ºC which appeared in the thermal event of TH, got reduced in the thermal curve of TH matrices. The reduced intensity of the melting endotherm of TH in the hydrogel matrices may indicate the molecularly dispersed TH in the CMTG polymeric matrices or TH conversion to amorphous form during matrix development.

To precisely determine the state of TH in the cross-linked CMTG matrix, XRD analysis of TH and TH hydrogel matrices was done (Fig. 8.3.). The TH X-ray diffraction patterns showed

reflections at 15.20°, 16.40°, 18.23°, 21.28°, 24.09°, 26.68°, 29.23°, 30.56°, 40.31° and 41.82° 2θ. The TH hydrogel matrices showed similar 2θ reflection as that of TH, however, with reduced intensities. Reduced XRD intensities of TH hydrogel matrices may indicate the diminished crystallinity of TH in the CMTG matrix. It can be anticipated from the XRD and DSC results that TH have not gone through any solid-state change in the CMTG matrices, but the crystallinity of TH has diminished in the matrices.

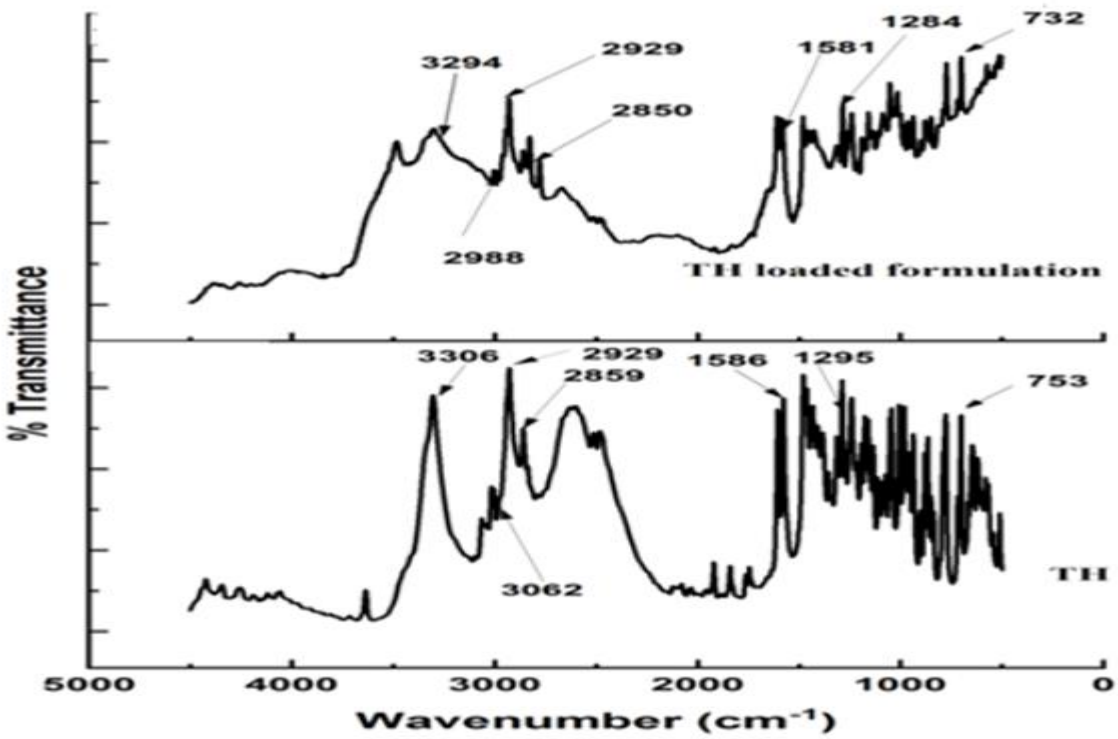

Fig.8.1. FTIR spectrum of TH and TH hydrogel matrices.

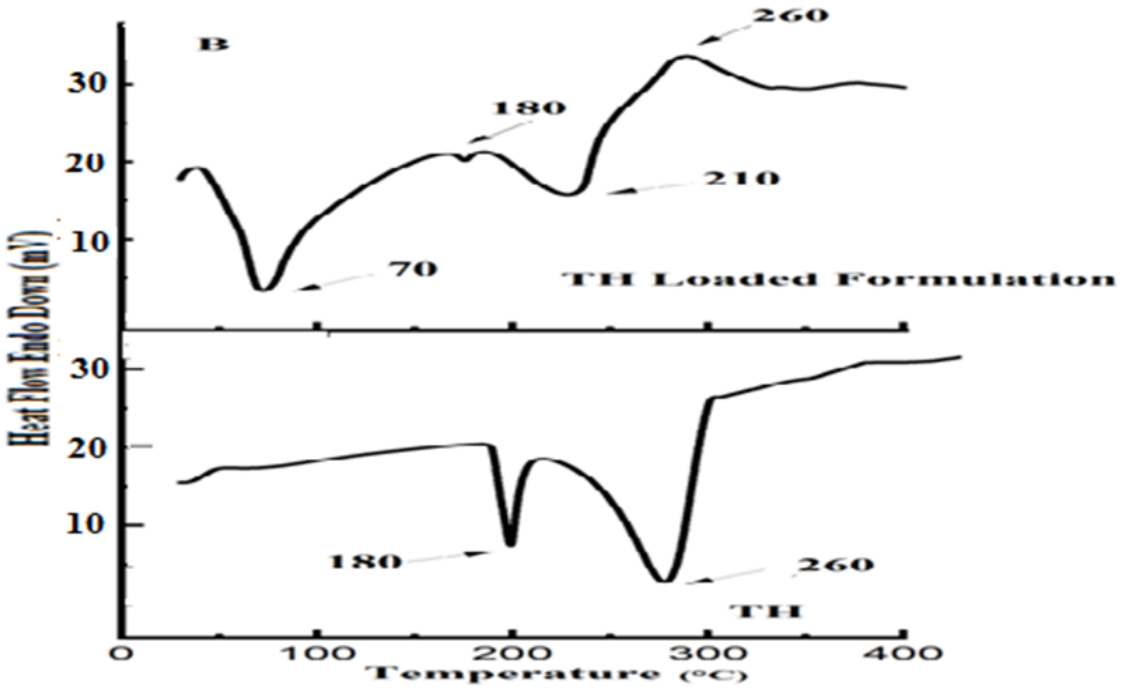

Fig.8.2. DSC thermal curves of TH and TH hydrogel matrices.

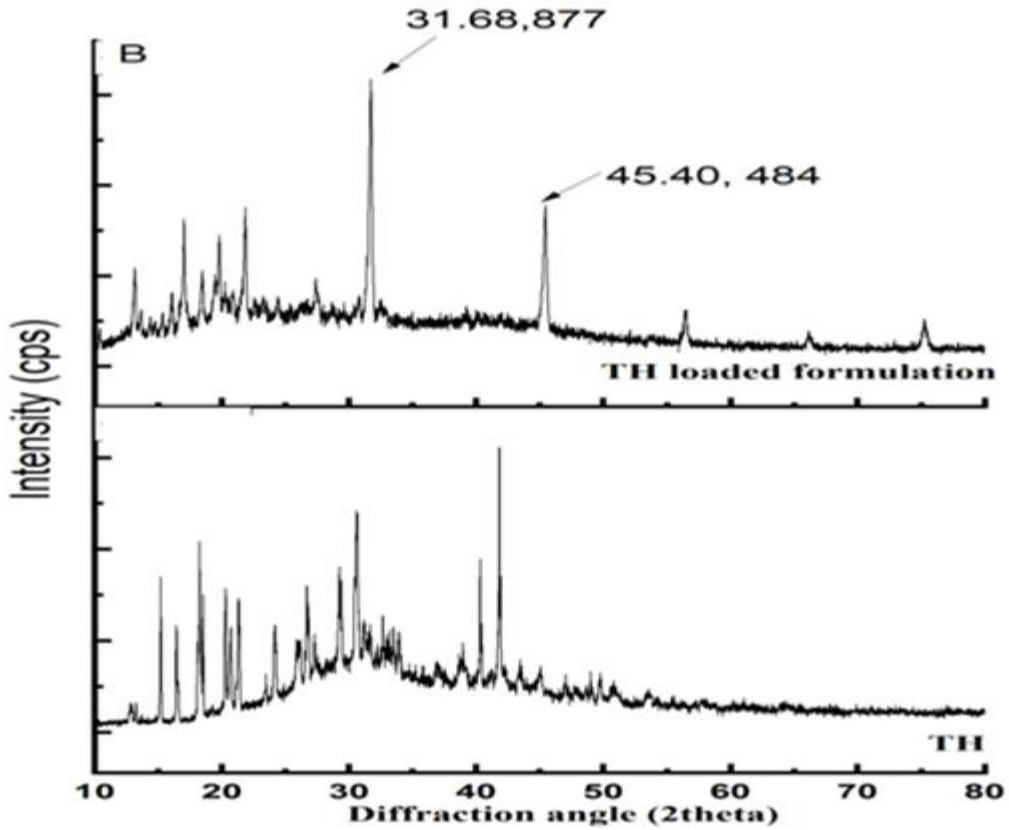

Fig. 8.3. XRD reflections of TH and TH hydrogel matrices.

3.2 Characterisation of CMTG hydrogel matrices

Weight variation test of the hydrogel matrices showed that weight of all the 20 matrices were within the ±5% of the mean matrices weight [7]. The friability of the hydrogel matrices was between 0.45%-0.84% and within the IP 2018 pharmacopoeial limit. The TH content of each hydrogel matrices was within 96%-102% of the loaded TH.

3.3 Swelling, erosion of the single metal ion cross-linked hydrogel matrices

The dynamic erosion, swelling pattern of aluminium cross-linked (Al-CMTG) matrices are illustrated in Fig. 8.4. Al-CMTG matrices swelled immediately to various extents in pH 1.2 acid solution, and subsequently the swelling progressively reduced demonstrating mass loss (erosion) of the matrices. Uncross-linked CMTG matrices F1 swelled 381% after 2 h in pH 1.2 acid solution, thereafter the swelling gradually declined (194% after 8 h). The erosion of uncross-linked CMTG matrices F1 showed an early burst erosion (34% at 2 h), following which the erosion gradually increased with time (69% at 8 h). $AlCl_3$ incorporation in the hydrogel matrices changed the erosion and swelling characteristics of the matrices substantially. Accentuating $AlCl_3$ concentration in the hydrogel matrices from 3-9% w/w (F2-F4) declined the erosion and swelling characteristics ($p<0.05$). But, further elevation in $AlCl_3$ concentration to 12% w/w (F5) stimulated the matrix erosion, although the swelling declined. Reduced water intrusion velocity through the thick polymeric or gel-like matrices was the cause of fall in swelling rate of the hydrogel matrices with the rise in $AlCl_3$ concentration. Elevation in the $AlCl_3$ amount in the matrices effected the decline of water intrusion velocity. The stiff hydrogel layer slowed down matrix dissolution and decrease in the percentage erosion of the hydrogel matrices with the rise in the $AlCl_3$ concentration. Similar erosion and swelling profiles have been documented for calcium-carboxymethyl guar gum matrices [1]. Swelling of a hydrophilic polymer follows Fickian diffusion process. The swelling data of all hydrogel matrices have been plotted as per equation 8.5, up to 3 h of swelling, when swelling predominated over erosion. The swelling kinetics very nearly followed Fickian diffusion, as revealed by the n_s values (Table 8.3**).**

Table 8.3 Specifications of the swelling study

Formulation code	Swelling Exponent (n_s)	Swelling kinetic constant (ks) (h^{-1}) (mean±SD, n=3)	Swelling rate (%/$t^{\wedge 1/2}$) (mean±SD, n=3)	Water Penetration velocity (cm/sec)
F1	0.501	2.457±0.54	279.9±5.9	0.0131
F2	0.478	2.302±0.36	194.9±4.7	0.0099
F3	0.462	2.181±0.24	156.3±5.1	0.0071
F4	0.447	2.091±0.21	135.2±3.9	0.0053
F5	0.420	2.04±0.18	122.8±4.5	0.0048
F6	0.489	2.425±0.84	261.6±2.07	0.0110
F7	0.480	2.406±0.96	253.8±3.63	0.0084
F8	0.467	2.356±0.75	239.5±3.54	0.0073
F9	0.450	2.294±0.63	229.5±4.02	0.0052
F10	0.432	2.156±0.84	219.5±5.04	0.0040

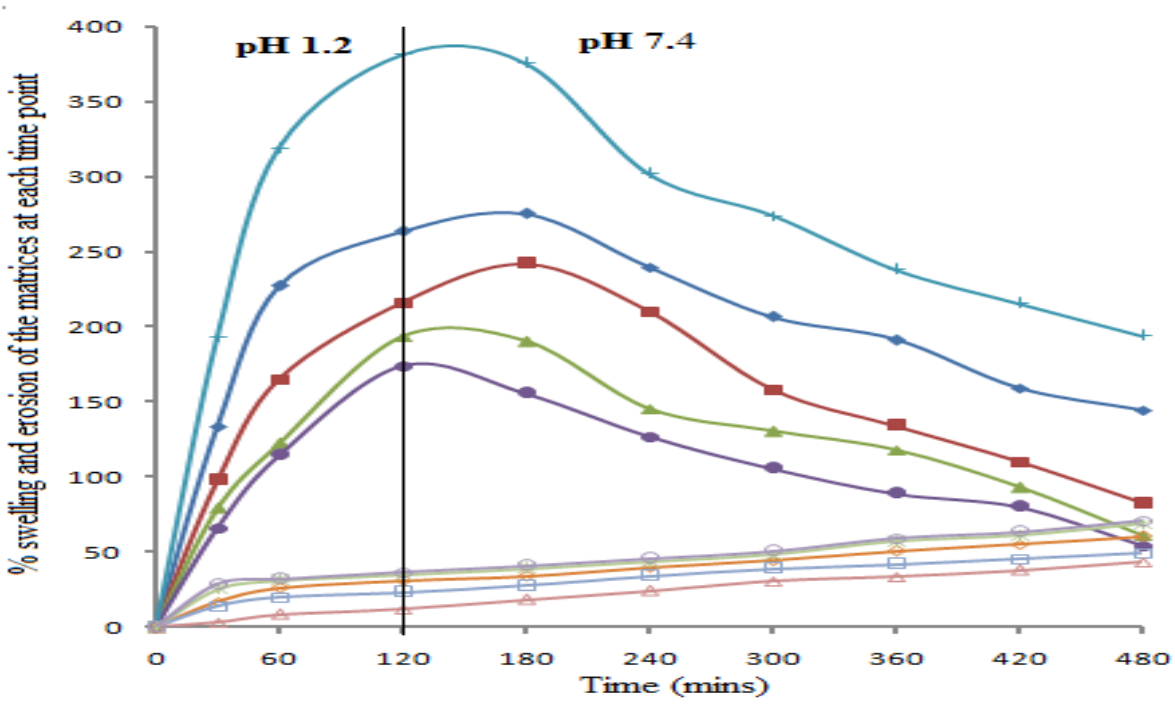

Fig. 8.4. Swelling (bold markers) and erosion (hollow markers) characteristics of hydrogel matrices in pH 1.2 acid solution for 2 h followed by pH 7.4 alkaline solution up to 8 h. % (w/w) $AlCl_3$ in hydrogel matrices: 0% (✳), 3% (♦), 6% (■), 9% (▲) and 12% (●).

The erosion and swelling characteristics of calcium ion cross-linked CMTG matrices are illustrated in Fig. 8.5. Like aluminuim ions, calcium ions also changed the erosion, swelling characteristics of the matrices substantially (Fig. 8.5.). Elevation in the Ca^{2+} ions concentration in the hydrogel matrices from 3-12% w/w (F6-F9) declined the erosion and swelling ($p<0.05$). But additional rise in the Ca^{2+} ions concentration to 15% w/w (F10) escalated the matrix erosion, however the swelling declined. Like Al-CMTG matrices, the water intrusion velocity declined through the calcium cross-linked dense and viscous hydrogel layer, resulting in decline in swelling of the matrices. The fall in erosion was attributable to the development of firm hydrogel layer with lesser matrix dissolution rate. Ca-CMTG matrices swelling kinetics followed Fickian diffusional kinetics (Table 8.3).

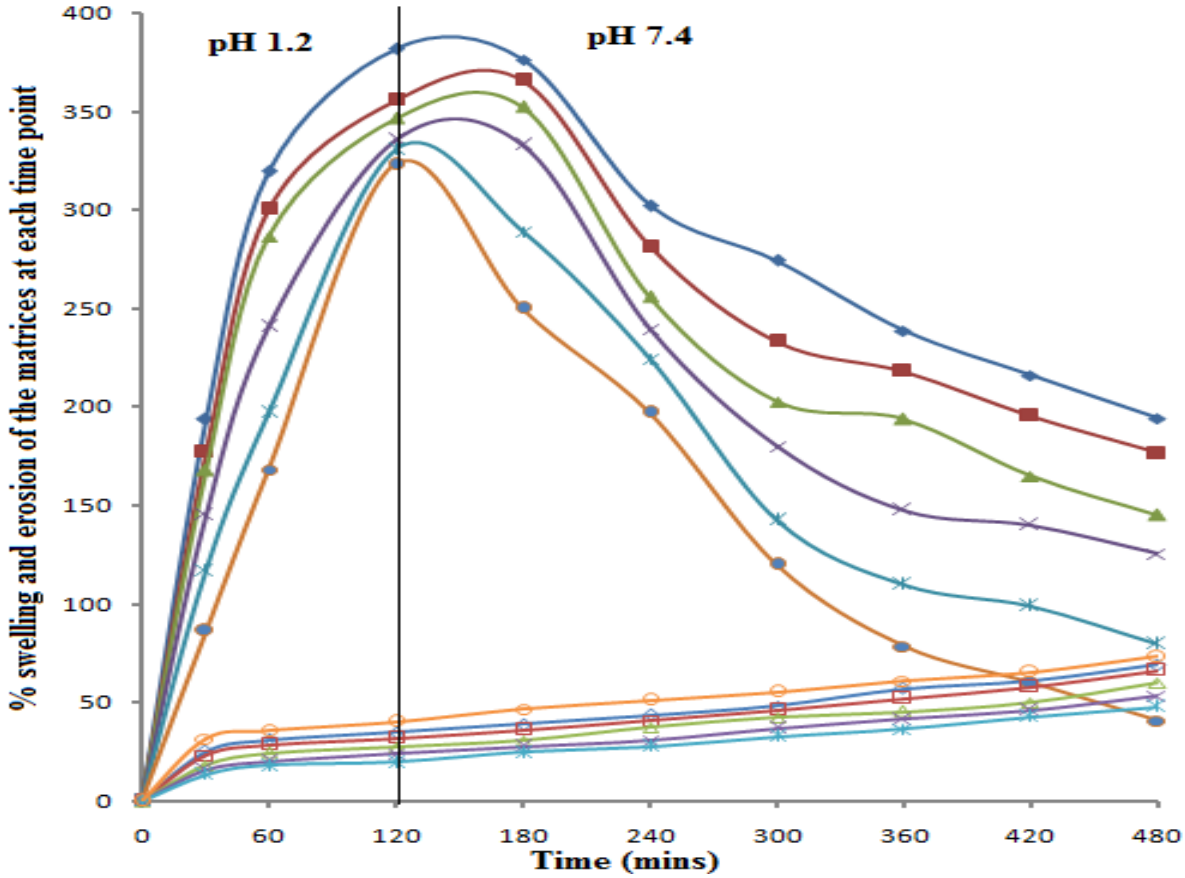

Fig. 8.5. Swelling (bold markers) and erosion (hollow markers) characteristics of hydrogel matrices in pH 1.2 acid solution for 2h followed by pH 7.4 alkaline solution up to 8h. % (w/w) $CaCl_2$ in matrices: 0% (♦), 3% (■), 6% (▲), 9% (×), 12% (✳) and 15% (●).

Analysis of the erosion and swelling characteristics of Ca and Al-CMTG matrices formulated with equal percentage weight of the respective cross-linking ions revealed that % erosion and

swelling of Al-CMTG matrices was low at every time points when matched with Ca-CMTG matrices (Table 8.3). This can be explained by the variance in the water intrusion velocity rates between Ca-CMTG and Al-CMTG matrices formulated with equal amounts of cross-linking ions (Table 8.3). The water intrusion velocity of Al-CMTG hydrogel matrices was low compared to Ca-CMTG hydrogel matrices. The outcomes are in perfect accordance with the outcomes of Reddy et al [8]. They documented that the swelling rate of aluminium-alginate beads were low in comparison to calcium-alginate beads, because reduced H_2O uptake percentage by aluminium alginate beads in comparison to calcium alginate beads. The outcomes were also bolstered by the photographs of matrices F1 (uncross-linked CMTG matrix), matrices F4 (cross-linked with 9%w/w $AlCl_3$) and matrices F8 (cross-linked with 9%w/w $CaCl_2$) captured at various times between 0-12 h (Fig. 8.6). The photographs give a strong suggestion that the erosion and swelling characteristics of F1 matrices was the maximum, followed by F8 matrices and minimum by F4 matrices. At 0 h, the CMTG (F1) and Ca-CMTG (F8) matrices revealed no changes, but a thin hydrogel layer over the Al-CMTG (F4) matrix was evident immediately when F4 matrices contacted with dissolution solution. After 2 h, swelling process was noted in all hydrogel matrices, moreover a slimy gel layer seemed to appear over the Ca-CMTG matrix surface and a relatively strong and noticeable hydrogel layer developed around Al-CMTG (F4) matrices. At 4 h, both swelling and erosion was observed with CMTG (F1) and Ca-CMTG (F8) matrices, but the hydrogel over the Al-CMTG (F4) matrices became firm and denser as time elapsed and the matrix core was integrated. After 6 h and 8 h, erosion was evident in both matrices, but the Al-CMTG (F4) matrices didn't indicate any sign of erosion. Finally, at 12 h, a substantial change was noted in all matrices. The F1 matrices got totally eroded, noteworthy erosion was noted in F8 matrices although the hydrogel was visible, but the hydrogel of F4 matrices was still stiff and dense and the core matrices was unbroken and clearly visible.

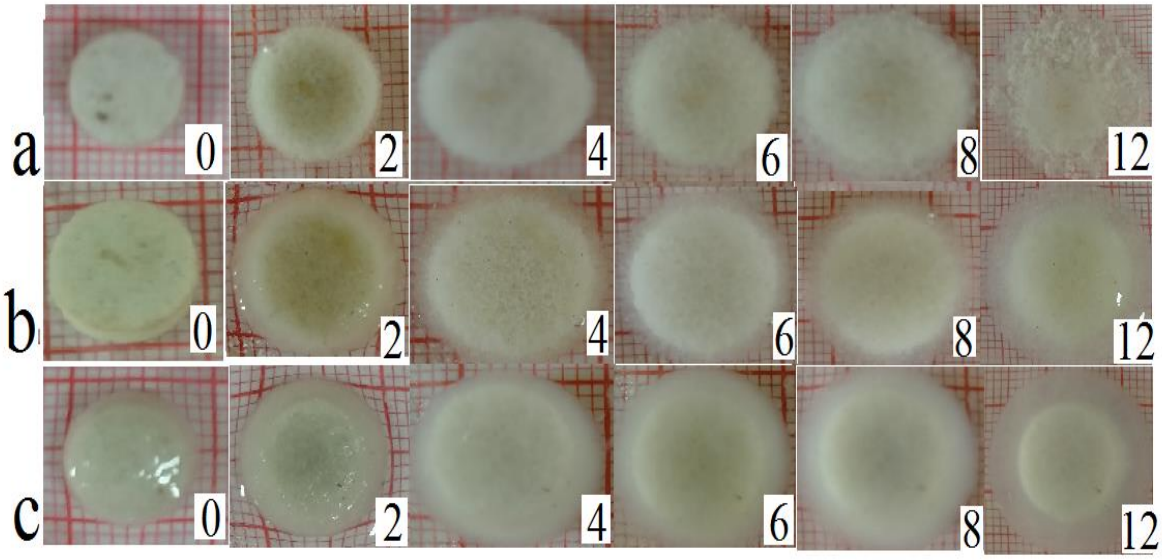

Fig. 8.6. Photographs of matrix F1 (row a), F4 (row c) and F8 (row b) captured at various time points of 0h, 2h, 4h, 6h, 8h and 12h.

3.4 In-Vitro TH dissolution from single metal ion cross-linked hydrogel matrices

The *in vitro* TH dissolutions from uncross-linked CMTG and Al-CMTG matrices formulated with different percentage weight of $AlCl_3$ are illustrated in Fig. 8.7. An immediate rapid TH release (33% - 23%) was seen in the initial 30 min of dissolution. The TH dissolution was uniform following the immediate dissolution. No sudden alteration in TH dissolution was noted when the dissolution solution pH was brought to pH 7.4, following 2 h of TH dissolution. Matrices F1, formulated with CMTG only liberated 46% and 96% of TH at 2 h and 8 h respectively. Aluminium ion cross-linking of the CMTG matrices significantly changed the TH dissolution pattern. Increase in $AlCl_3$ concentration in the matrices from 3% w/w (matrices F2) to 9% w/w (matrices F4) decreased the TH dissolution rate. However, elevation in the $AlCl_3$ amount to 12% w/w (matrices F5) increased the TH dissolution rate significantly ($p<0.05$). TH dissolution from hydrogel matrices F2-F5 varied in the following manner: after 2 h in pH 1.2 acid media -F2(42%)> F3(38%)> F4(36%)< F5(50%) and at 8 h- F2(87%)> F3(81%)> F4(72%)< F5(99%). The AUCs dropped for matrices F1 to F4, and then again augmented for matrices F5 considerably (Table 8.4) ($p<0.05$). MDT for matrices F1 to F4 augmented and then declined for matrices F5 ($p<0.05$) (Table 8.4). The TH dissolution characteristics was simultaneous with erosion, swelling characteristics of the hydrogel matrices.

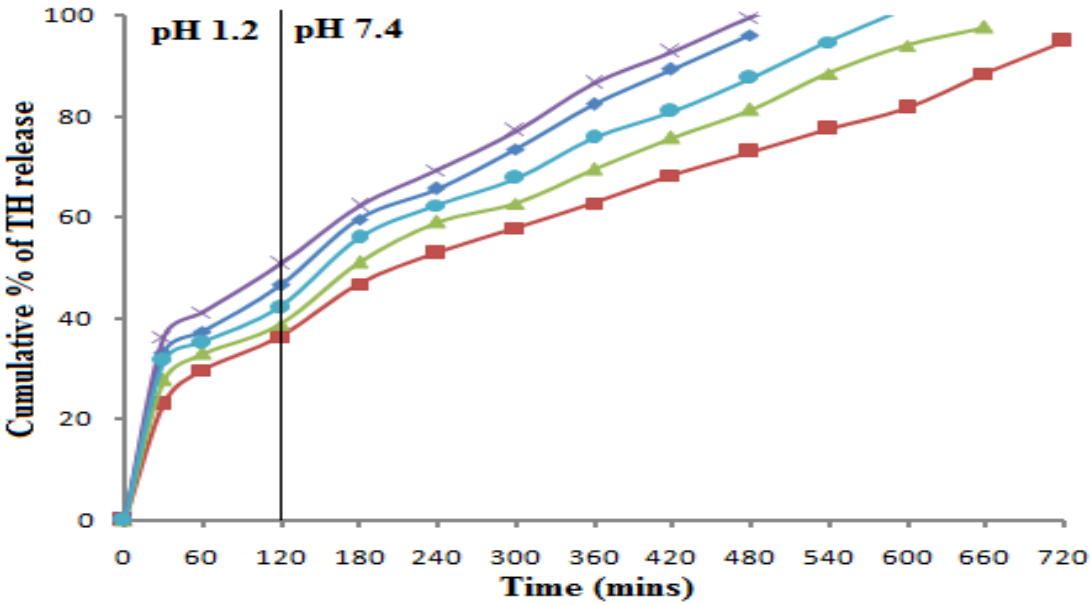

Fig. 8.7. TH dissolution from hydrogel matrices. % (w/w) $AlCl_3$ in matrices: 0% (♦ , F1), 3% (● , F2), 6% (▲ , F3), 9% (■ , F4) and 12% (× , F5), n = 3.

Table 8.4 TH Release specifications

Formulation Code	Mean Dissolution Time (MDT), (min) (mean±SD, n=3)	Diffusion coefficient (cm^2/s)	AUC($\%h^{-1}$) (mean±SD, n=3)
F1	2.957±0.33	$1.19*10^{-07}$	96.13±1.32
F2	3.482±0.27	$1.16*10^{-07}$	81.35±2.31
F3	3.732±0.18	$1.13*10^{-07}$	79.59±3.03
F4	4.335±0.21	$1.10*10^{-07}$	73.23±2.82
F5	2.981±0.33	$1.2*10^{-07}$	95.30±3.33
F6	3.017±0.21	$1.18*10^{-07}$	92.33±2.34
F7	3.474±0.18	$1.15*10^{-07}$	87.38±1.33
F8	3.847±0.24	$1.13*10^{-07}$	85.36±1.80
F9	4.156±0.15	$1.12*10^{-07}$	74.75±2.43
F10	2.93±0.27	$1.17*10^{-07}$	100.44±3.33

In contact with water a hydrophilic polymer swells due to simple relaxation of polymer chains and pressure generated by the intruding water. Subsequently, a dense viscous film of the polymer with poor mechanical strength is generated over the hydrogel matrices surface by simple intermingling of the polymeric chain. As time elapses, the dense viscous film gets

diluted with the dissolution solution and erosion or dissolution of the polymer initiates from the exposed matrix surface, facilitating further invasion of the dissolution solution to hydrate the core of the matrix. The drug particles, along with the polymer, starts to solubilize and move into the dissolution solution [9]. The amount of polymer contained in the matrix determines the viscosity of the swollen viscous layer, which in turn controls the drug diffusion from that layer [10]. Since matrices F1 is made up of almost 70% w/w of CMTG, a dense and viscous polymer layer was generated over the exposed matrix surface having enough mechanical strength to function as an obstruction to drug diffusion. $AlCl_3$ incorporation to the hydrogel matrices F2-F5 produced Al^{3+} ions due to $AlCl_3$ solubilization in water. The Al^{3+} ions and the available CMTG carboxylic groups reacted to cross-link the polymeric chains of CMTG. Similar ionic cross- linking between Al^{3+} and CMC and Ca^{2+} and gellan gum/ alginate have been described in literature [11-13]. This cross-link restricts the polymer chain mobility ensuing in the growth of a stiff viscous hydrogel layer over the exposed matrices surface [9]. Elevation in $AlCl_3$ concentration elevates the cross-link density to generate superior gel strength and condense macromolecular mesh network size, ultimately reducing the TH diffusion. Accordingly, a fall in TH dissolution was observed. The TH diffusion coefficient through the hydrogel layer of the Al-CMTG matrices was calculated by Fickian diffusion model following equation III. Decrease in TH diffusion coefficient was observed when $AlCl_3$ concentration was elevated up to 9%w/w ($p<0.05$) (Table 8.4). However, at 12% w/w $AlCl_3$, the TH diffusion coefficient increased. It seems that $AlCl_3$ incorporation in the hydrogel matrices may have modified the viscosity of the hydrogel layer because a drug's diffusion coefficient through a gel layer is governed by the viscosity of that hydrogel layer. Increase in viscosity of the hydrogel lowers the drug diffusion coefficient. Analysis of viscosity of the CMTG solutions containing different concentration (same as that of the hydrogel matrices composition) of $AlCl_3$ solution revealed that the viscosity of the hydrogel increased up to 9%w/w $AlCl_3$ in the hydrogel matrices, past which (12%w/w $AlCl_3$) the viscosity declined (Fig. 8.8). The above observations were also bolstered by SEM surface morphology micro-images of the matrices taken at multiple time points (Fig. 8.9). The F1 and F4 matrices surface structures before dissolution and following 6 h of dissolution confirmed the effect of Al^{3+} ions on elevating the mechanical strength and cross-linking density of the hydrogel layer. The F1 and F4 matrices surface structures before dissolution are demonstrated in Fig. 8.9 (a & b). The surface of matrices F4 (Fig.8. 9b) is denser, compact and smooth and devoid of any perforations and pores, compared to the surface of matrices F1 (Fig. 8.9a). The dissimilar surface structures are due to different cross-link densities of the matrices F1 and F4. The hydrogel layer of the

matrix F4 being cross-linked by Al^{3+} ions, have higher cross-link density compared to the uncross-linked matrix F1 hydrogel layer. This made the surface of matrix F4 appear dense and tight and bereft of any cracks or pores. Kaity et al. also reported that cross-linked polymer matrices have dense surface structures with less pores [14]. The surface structures of matrices F1 and F4 following 6 h of dissolution is represented in Fig. 8.9 (c & d respectively). The surface of matrix F4, even following 6 h of dissolution (Fig. 8.9d), appeared dense and compact, whereas that of matrix F1 (Fig. 8.9c) is loose with many perforations and cracks. The Al^{3+} cross-linked matrix F4 have greater cross-link density and impedes the mobility of the polymer chains as compared to uncross-linked matrices F1. Restricted mobility of the polymer chains makes the hydrogel layer stiff and rigid. The TH release through the hydrogel matrices simulated perfectly with the SEM microimages. TH dissolution from F1 matrices was faster compared to matrices F4. However, a higher concentration of Al^{3+} ions (12%w/w, F5) resulted in deterioration of the tensile strength and viscosity of the gel layer, promoting faster TH diffusion and dissolution. Faster TH dissolution from matrices F5 (formulated with 12% w/w $AlCl_3$) was attributed to increased percentage erosion, decreased viscosity of the matrix hydrogel layer, and rapid TH diffusion through the hydrogel layer. Related observations have been reported [11, 15]. The authors reported that elevation in the calcium ions concentration up to a definite level declined the drug dissolution from matrices. But, further elevation in the calcium ions concentration expedited the drug dissolution. The observations have been linked to either the weak gel strength of the polymeric matrix resulting from non-homogeneous cross-linking in calcium pectinate matrices or the channelling property of the additional (than necessary for efficient crosslink) calcium ions present in the matrix. The rapid TH dissolution from the hydrogel matrices is either due to TH high water solubility or some TH at the tablet surface dissolves prior to the formation of gel layer. Rapid drug dissolution from polymeric matrices is well acknowledged in literature. A rapid TH dissolution from guar gum and HPMC matrices have been documented by Tiwari et al [16]. They ascribed the rapid dissolution due to TH high water solubility. Surface erosion facilitated burst dissolution is also reported in literature [17].

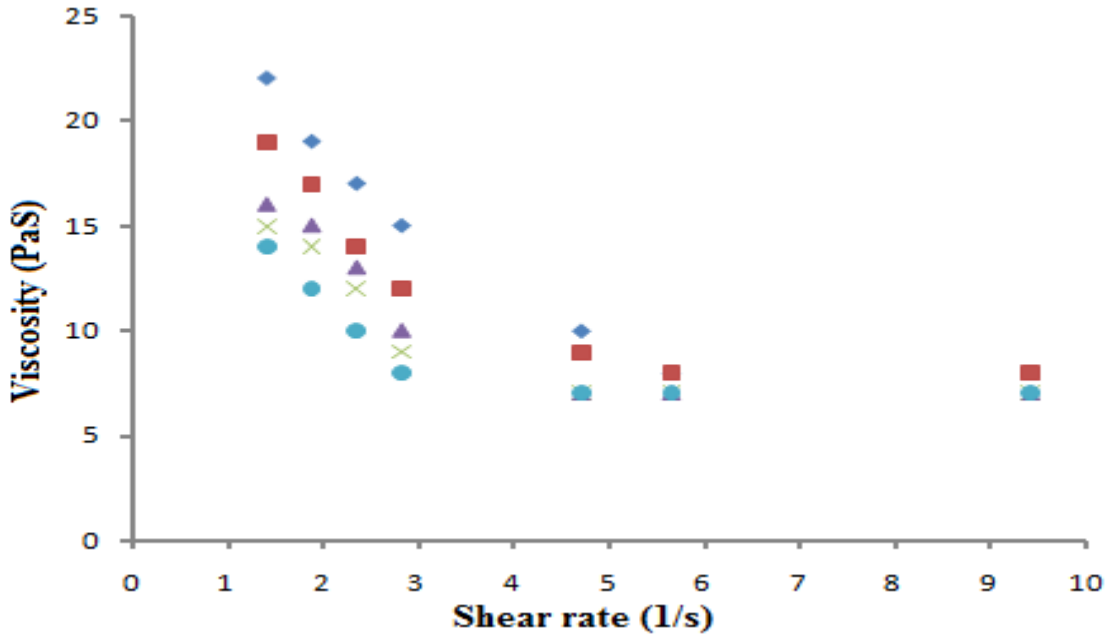

Fig. 8.8. Viscosities of different CMTG solutions. % (w/w) $AlCl_3$ in matrices: 0% (●), 3% (▲), 6% (■), 9% (♦) and 12% (×).

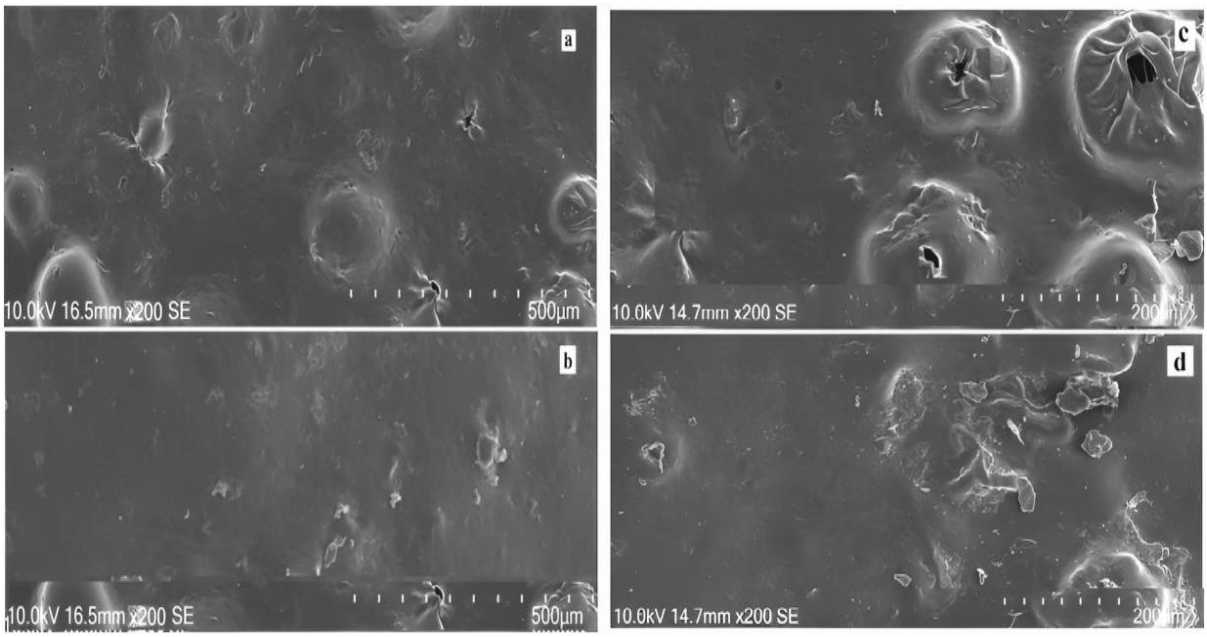

Fig. 8.9. SEM microimages of matrices: before dissolution a (F1) & b (F4), 6 h following dissolution c (F1) & d (F4).

The TH dissolution from calcium cross-linked CMTG matrices are illustrated in Fig. 8.10. Like Al-CMTG matrices, Ca-CMTG exhibited an initial rapid TH dissolution (22%-33%, governed by the Ca^{2+} ions concentration in the matrices) from the matrices, following which TH dissolution was steady until complete dissolution. Accentuating $CaCl_2$ concentration from 3% w/w (F6 matrices) to 12% w/w (F9 matrices) in the matrices, attenuated the TH dissolution from the matrices. Though further elevation in $CaCl_2$ concentration to 15% w/w (matrices F10)

significantly augmented TH dissolution rate ($p<0.05$). TH dissolution from hydrogel matrices F6-F10 altered in the following fashion: at 2 h in pH 1.2 acid media–F6(40%)> F7(39%)> F8(37%)> F9(31%)< F10(41%) and at 8 h-F6(97%)> F7(91%)> F8(82%)> F9(77%)< F10(102%). AUCs declined for matrices F6 to F9, and then again amplified for matrices F10 (Table 8.4) ($p<0.05$). MDT for matrices F6 to F9 augmented and then declined for matrix F10 ($p<0.05$) (Table 8.4). Like Al-CMTG matrices, increase in Ca^{2+} from 3%w/w (F6) -12% w/w (F9) augmented the viscosity and declined the TH diffusion through the matrices hydrogel layer, which ensued in decline of TH dissolution. However, at 15% w/w of Ca^{2+} ion in the matrices (F10), the hydrogel viscosity dwindled and TH diffusion coefficient augmented, accounting for faster TH dissolution.

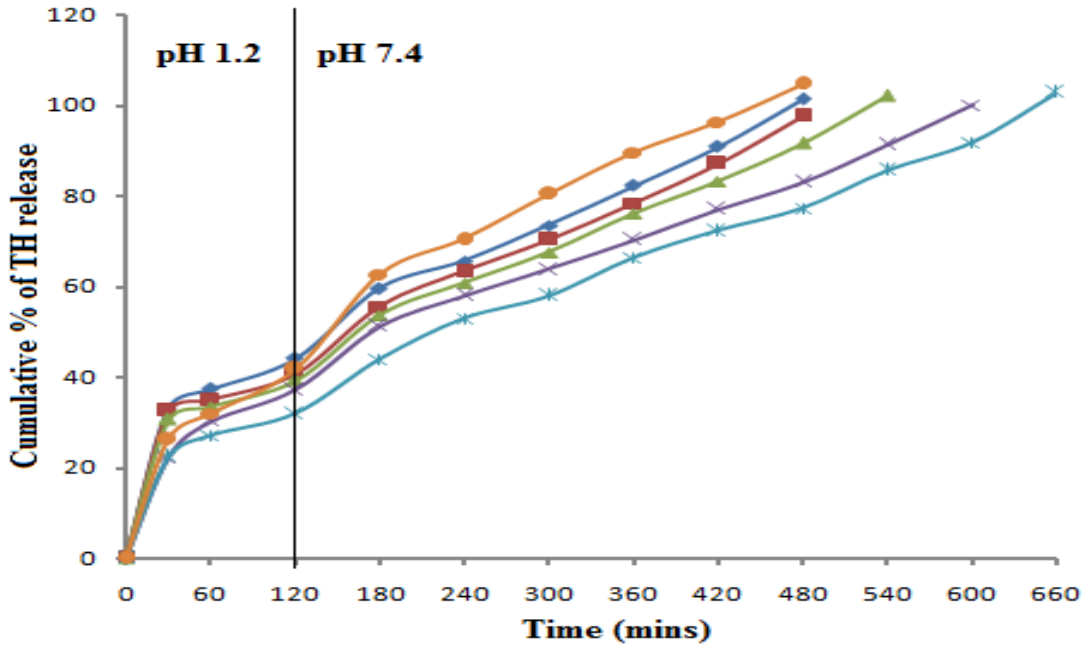

Fig. 8.10. TH dissolution from tablet matrices. % (w/w) $CaCl_2$ in matrices: 0% (♦ ,F1), 3% (■ , F6), 6% (▲, F7), 9% (×, F8), 12% (✳ , F9) and 15% (● , F10), n = 3.

Critical analysis of TH dissolution pattern from Al and Ca cross-linked CMTG matrices showed significant variances in TH dissolution from the matrices. Firstly, at the equal percentage weight of cross-linking ions, TH dissolution from Ca-CMTG matrices was faster compared to Al-CMTG matrices. Secondly, Al-CMTG matrices F4 (9% w/w $AlCl_3$) provided the most sustained TH dissolution, whereas, the Ca-CMTG matrices F9 (12% w/w $CaCl_2$) released TH in the most sustained manner. And lastly, matrices F4 gave more sustained TH dissolution compared to matrices F9. These observations are elucidated below. The cation concentration and valency strongly influences the drug dissolution profile from cross-linked

matrices [18-19]. Al^{3+} ions have an additional positive ion than Ca^{2+} ions, promoting a more efficient cross-linking with CMTG carboxylic groups. This Al-CMTG cross-linked network has superior cross-linking density compared to the Ca-CMTG cross-linked structure. As deliberated previously, surge in the cross-link density elevates the viscosity and declines the TH diffusion through the matrix hydrogel layer and therefore the TH dissolution. Fig. 8.8 and Fig. 8.11 denotes that viscosity of Al-CMTG dispersions is higher than Ca-CMTG dispersions having the equal amounts of cross-linking ions. Likewise, the TH diffusion coefficient from Al-CMTG matrices is lower than Ca-CMTG matrices having the equal amounts of Al^{3+}/Ca^{2+} ions. This results in slower TH dissolution from Al-CMTG hydrogel matrices as compared with Ca-CMTG matrices. Again, one Al^{3+} ion can cross-link with three CMTG carboxylic groups, but one Ca^{2+} ion could cross-link with two CMTG carboxylic groups. Hence, the CMTG carboxylic acid groups will get saturated and thus will be more efficacious at much lower concentration of the Al^{3+} ions compared to calcium ions. This is the reason behind matrices F4 giving a more sustained TH dissolution as compared to matrices F9.

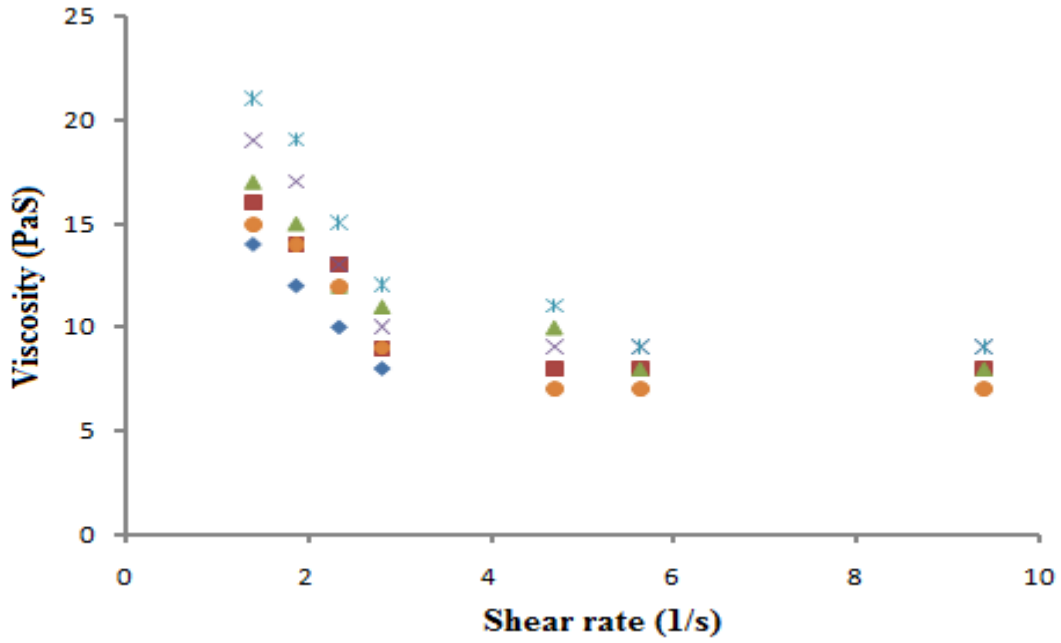

Fig. 8.11. Viscosities of different CMTG solutions. % (w/w) $CaCl_2$ in matrices: 0% (♦), 3% (■), 6% (▲), 9% (×), 12% (✳) and 15% (●).

Fig. 8.12 shows the TH dissolution from the optimized F4 matrices and a marketed commercial tablet TRD-CONTIN® (TH 100 mg). TH dissolution from F4 matrices and commercial tablet in pH 1.2 acid media almost overlapped and merged with each other and difference was not significant ($p>0.05$). However, TH dissolution from F4 matrices and marketed commercial tablet in pH 7.4 buffer media was reckoned significant ($p<0.05$). The figure illustrates that TH

dissolution from optimized F4 matrices was more sustained and slower as compared to marketed tablet in pH 7.4 buffer media. Thus, the developed matrices had a better sustained dissolution pattern as compared to the marketed commercial tablet.

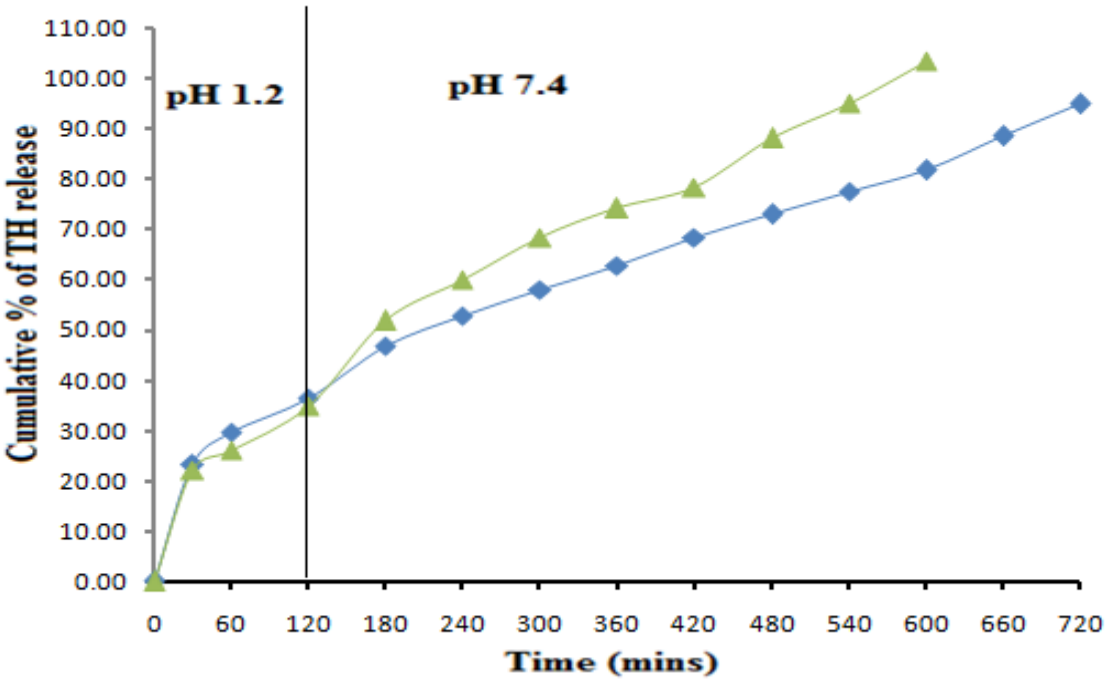

Fig. 8.12. Comparison of TH dissolution from hydrogel matrices F4 and a commercial marketed tablet TRD-CONTIN®. Marketed formulation (▲), F4 (♦), n = 3.

3.5 In-Vitro TH dissolution from dual metal ion cross-linked hydrogel matrices

Al-CMTG matrices F4 (9% w/w $AlCl_3$) and Ca-CMTG matrices F9 (12% w/w $CaCl_2$) gave the most sustained TH dissolution form the matrices. Development of dual cross-linked (Al^{3+} and Ca^{2+}) hydrogel matrices was done at the already optimized concentrations of the cross-linking ions.

TH dissolution from CMTG hydrogel matrices cross-linked with different weight ratios of Ca^{2+} and Al^{3+} ions (F11-F13, where the overall cross-linking ion concentrations was maintained at 9% w/w of the matrices) are demonstrated in Fig. 8.13. A burst TH dissolution (approximately 22%-24%) within 30 min of dissolution was noted from formulations F11-F13. After the rapid dissolution, TH dissolution was steady and uniform and no abrupt alteration in TH dissolution was perceived when the pH of dissolution solution was brought to pH 7.4 after 2 h of dissolution. The Al^{3+} cross-linked CMTG matrices F4 released 33% and 81% of TH following 2 h & 10 h of dissolution respectively. Substituting $AlCl_3$ with increasing amounts of $CaCl_2$ in the matrices effected substantial variations in TH dissolution pattern. Raising the concentration

of Ca^{2+} ions from 30%w/w (matrices F11) to 70%w/w (matrices F13) (where the overall cross-linking ion concentrations was maintained at 9% w/w) in the hydrogel matrices substantially expedited the TH dissolution from the matrices ($p<0.05$). TH dissolution from hydrogel matrices F11-F13 augmented in the following fashion: after 2 h in pH 1.2 acidic dissolution solution-37%(F11)<40%(F12)<44%(F13) and after 10 h- 86%(F2)< 92%(F3)<101%(F4). The MDT and AUCs values also significantly augmented for the matrices F11-F13 (Table 8.5) ($p<0.05$).

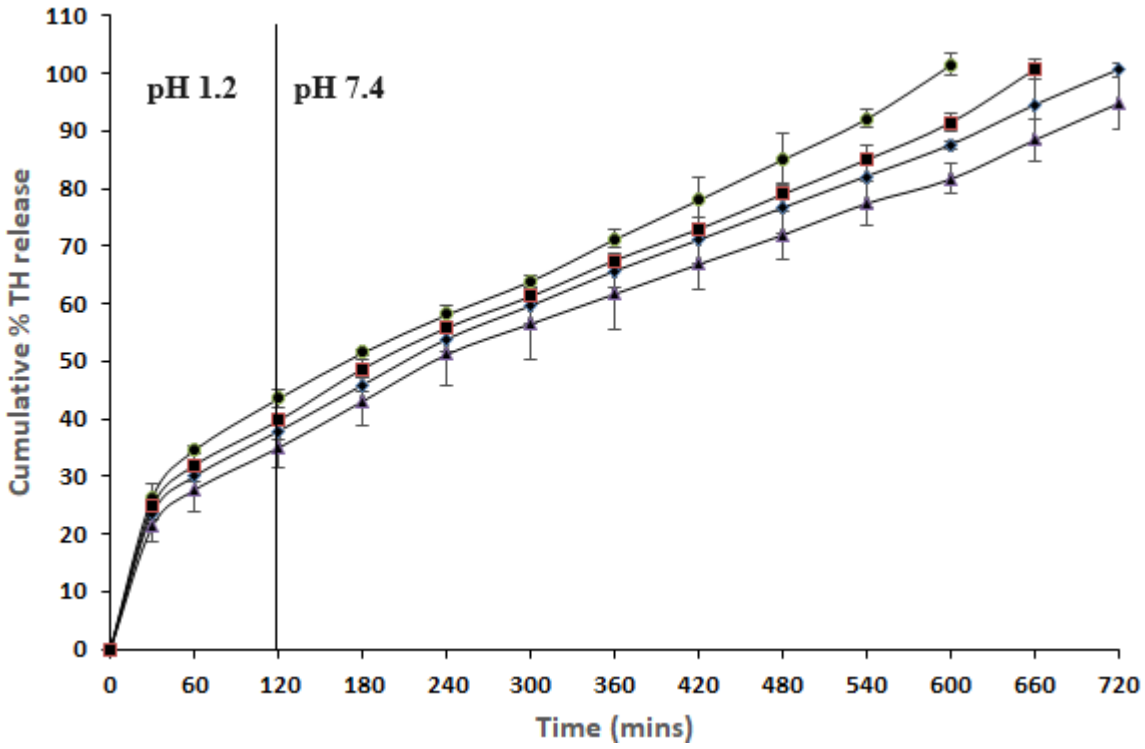

Fig. 8.13. TH dissolution from dual cross-linked hydrogel matrices. F4 (▲), F11 (♦), F12 (■), F13 (●).

Table 8.5 TH dissolution specifications

Formulation code	Mean dissolution time (MDT), (min)	Diffusion coefficient (cm^2/s)	AUC ($\%h^{-1}$)
F11	3.73±0.15	$1.21*10^{-07}$	76.14±1.38
F12	2.98±0.36	$1.23*10^{-07}$	79.19±2.25
F13	2.77±0.18	$1.25*10^{-07}$	82.15±3.35
F14	4.5±0.27	$1.07*10^{-07}$	72.14±1.53
F15	4.71±0.15	$1.02*10^{-07}$	69.18±2.52
F16	2.6±0.81	$1.18*10^{-07}$	78.58±3.60

Al^{3+}/Ca^{2+} ions were generated by the dissociation of $AlCl_3/CaCl_2$ in aqueous media during wet massing and also at the time of *in vitro* dissolution study. The ions react with CMTG carboxylic groups to cross-link the polymer chains. This cross-link restrains the polymeric chains and ensues in the growth of a dense, highly viscous and firm hydrogel layer around and over the surface of hydrogel matrices [9]. The rigidity, viscosity and firmness of the hydrogel layer is dictated by the degree of cross-linking, which is again influenced by the cross-linking ions concentration and valency [18-19]. Previous literature indicates that viscosity and firmness of the hydrogel layer increases with the augmentation in the cross-linking ions concentration [20]. Literature also indicates that a trivalent ion is capable of cross-linking more powerfully and effectually as compared to a divalent ion [20-21]. The Al^{3+} ion cross-linked hydrogel layer has improved mechanical strength and superior cross-link density as compared to Ca^{2+} ion cross-linked hydrogel layer [21]. Matrices F4 was cross-linked with Al^{3+} ions at 9 % w/w concentration. In matrices F11-F13, the Al^{3+} ions were progressively substituted with the divalent Ca^{2+} ions, maintaining the overall cross-linking ion concentrations at 9% w/w. Progressive substitution of Al^{3+} ions with Ca^{2+} ions may have steadily dwindled the F11-F13 matrices gel layer stiffness, thickness, and viscosity. Drug diffusion through hydrogel layer bears a reverse connection with that hydrogel layer viscosity [10]. The TH diffusion coefficient through the hydrogel layer of matrices F11-F13 was determined by the Fickian diffusion model (Eq. 8.3). The TH diffusion coefficient from matrices F4 was the lowest, and steadily augmented for matrices F11-F13, with the augmentation in Ca^{2+} ions concentration in the matrices (Table 8.5). Examination of viscosities of dispersions simulating the matrices F4, F11-F13 composition showed that matrix F4 has the highest viscosity, and as the Ca^{2+} ions concentration was augmented, the dispersion viscosity declined (Fig. 8.14). Photographs of the

gel layer thickness (Fig. 8.15) of matrices F4 (row a) and matrices F13 (row b) captured at 3 h, 6 h, 9 h, and 12 h following dissolution also bolstered the Ca^{2+} ions effected decline in hydrogel layer stiffness and viscosity. A stiff, highly rigid and viscous hydrogel layer in water (dissolution medium) will slowly crumble and erode down and will stay intact for an extended duration as compared with a less rigid and viscous hydrogel layer. After 3 h, hydrogel layer formation over the core of the matrices F4 and F13 have taken place (Fig. 8.15). But the hydrogel layer of matrices F4 is rigid and dense than that for matrices F13. After 6 h, the hydrogel layer in matrices F4 and F13 becomes prominent, but the hydrogel layer in matrices F4 is thicker than that in matrices F13. Besides, it appears visually that the F13 matrices hydrogel layer is flexible and soft, but for F4 it is dense and rigid. After 9 h, matrices F13 hydrogel layer has begun to degenerate/disintegrate, but no evidence of erosion/disintegration of the F4 hydrogel layer is seen, in fact, it is totally integrated and more obvious. After 12 h, F13 hydrogel layer has totally crumbled/eroded and substantial mass loss in the matrix was perceptible. However, the F4 hydrogel layer was still rigid and thick and the matrix core was intact and visible clearly. SEM surface structures of matrices F4 and F13 originally before dissolution and following 6 h of dissolution also showed Ca^{2+} ion induced decline in gel layer rigidity, viscosity and cross-link density. Fig. 8.16 portrays that the matrices F4 surface (Fig. 8.16a) is compact and denser as compared to the matrices F13 surface (Fig. 8.16b). Additionally, matrices F4 surface is irregular but that of F13 is even. This is because of superior crosslink density in matrices F4 as compared to matrices F13. It is documented that at elevated cross-linking density, hydrogel membrane surface is denser and rough [22]. Surface structures of matrices F4 and F13 following 6 h of dissolution are shown in Fig. 8.16 (c & d) respectively. The matrices F13 surface (Fig. 8.16d) has developed quite a few pores and perforation, but the matrices F4 was still dense and bereft of any perforations & pores, again attributed to the Ca^{2+} ion effected decline in cross-link density for matrices F13. Since the cross-link density for matrices F13 is lower than that of matrices F4, the matrices F13 surface has developed holes and perforations, but the matrices F4 surface mostly smooth and holes/pores are lacking. TH dissolution from the hydrogel matrices blended perfectly with the SEM surface microimages. TH dissolution from matrices F4 was slower as compared to matrices F13.

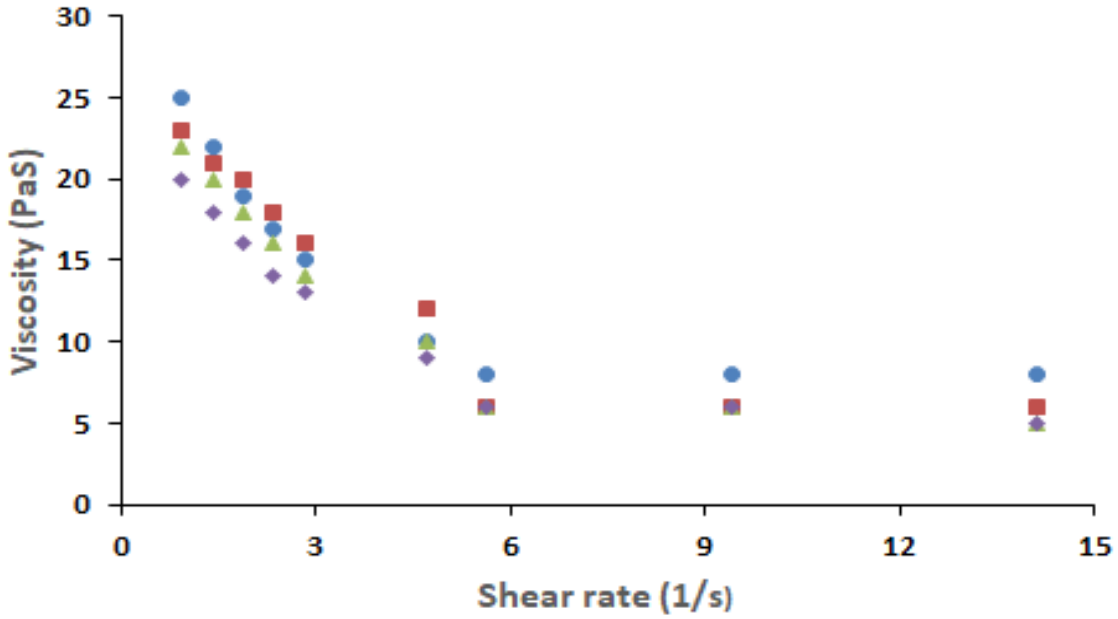

Fig. 8.14. Viscosities of CMTG solutions simulating matrices F4 (●), F11 (■), F12 (▲), F13 (♦).

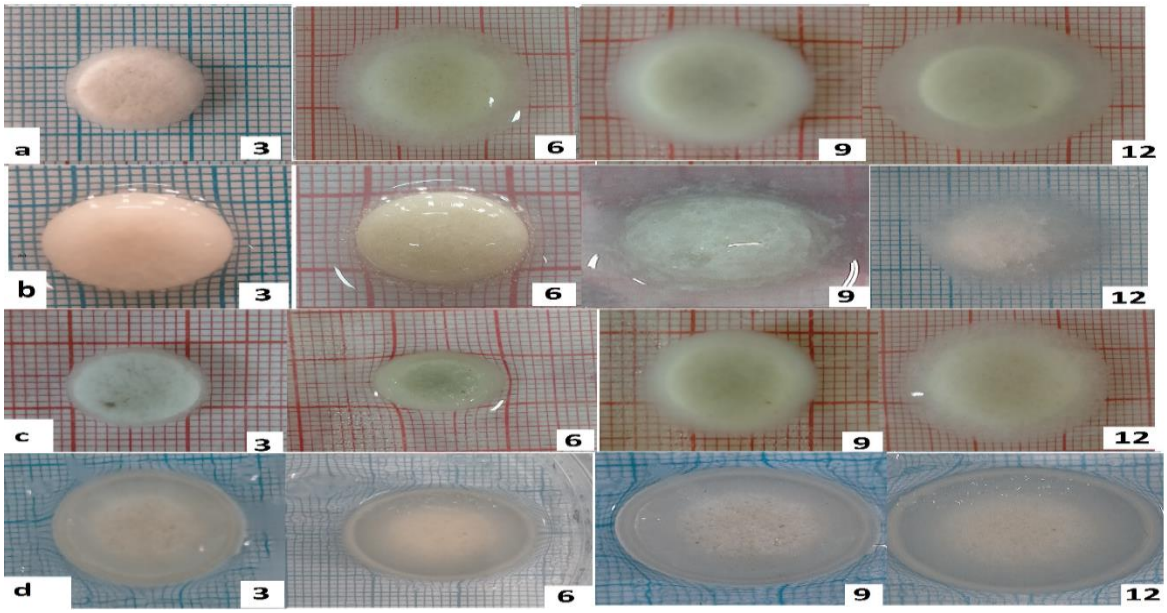

Fig. 8.15. Photoimages of matrices F4 (row a), F13 (row b), F9 (row c), and F15 (row d) at time intervals of 3 h, 6 h, 9 h, and 12 h.

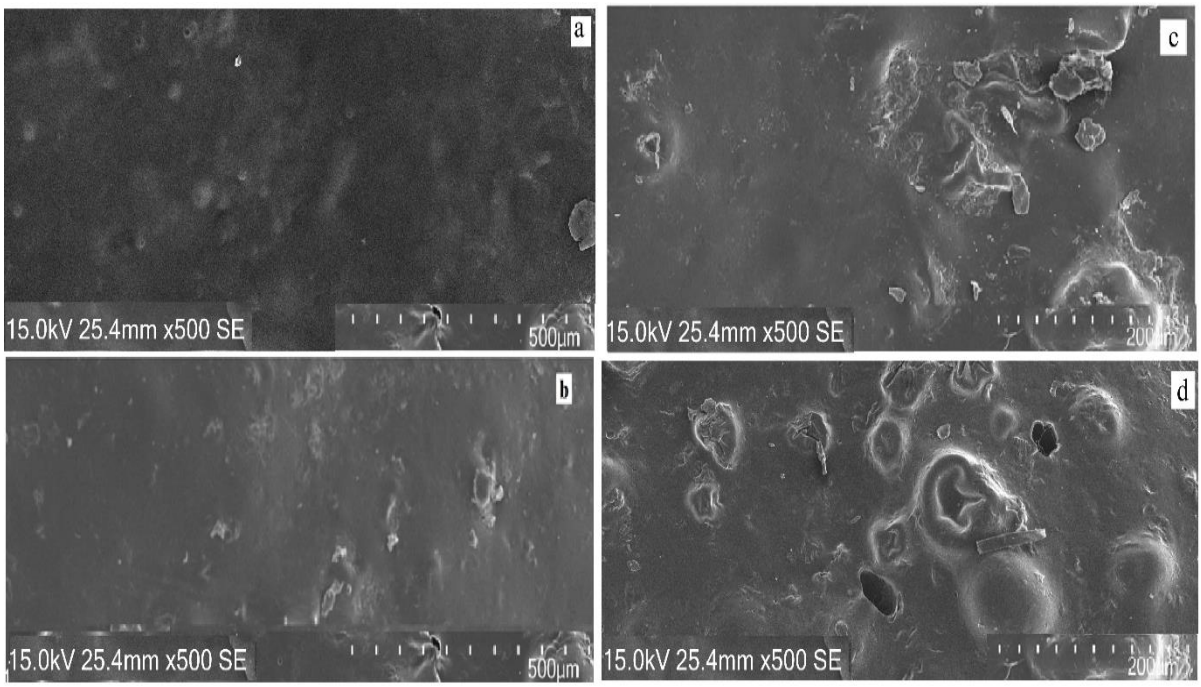

Fig. 8.16. SEM photomicrographs of matrices: before dissolution F4 (a) & F13 (b), following 6 h of dissolution F4 (c) & F13 (d).

TH dissolution from CMTG hydrogel matrices cross-linked with different weight ratios of Ca^{2+} and Al^{3+} ions (where the overall cross-linking ion concentrations was maintained at 12% w/w) are demonstrated in Fig. 8.17. Similar to matrices F11-F13, matrices F14-F16 also displayed an initial rapid TH dissolution (18%-30%) during the initial 30 min of dissolution, after which TH dissolution was gradual and uniform. Ca^{2+} ions cross-linked matrix F9 liberated 33% and 91% of TH following 2 h and 10 h of dissolution respectively. Substituting $CaCl_2$ with increasing amounts of $AlCl_3$ in the matrices effected substantial variations in TH dissolution pattern. Raising the concentration of Al^{3+} ions from 30%w/w (matrices F14) to 50%w/w (matrices F15) (where the overall cross-linking ion concentrations was maintained at 12% w/w) in the hydrogel matrices substantially impeded the TH dissolution from the matrices ($p<0.05$). However, further augmentation in $AlCl_3$ concentration to 70%w/w (matrices F16) (where the overall cross-linking ion concentrations was maintained at 12% w/w), substantially increased the TH dissolution rate ($p<0.05$). TH dissolution from the hydrogel matrices F14-F16 changed in the following fashion: after 2 h -30%(F14)>27%(F15)<42%(F16) and after 10 h-86%(F14)>75%(F15)<99%(F16). The AUCs declined for the formulations F14-F15 and then substantially increased for F16 (Table 8.5) ($p<0.05$). Similarly, MDT increased for matrices F14-F15, and then declined for matrices F16 (Table 8.5) ($p<0.05$).

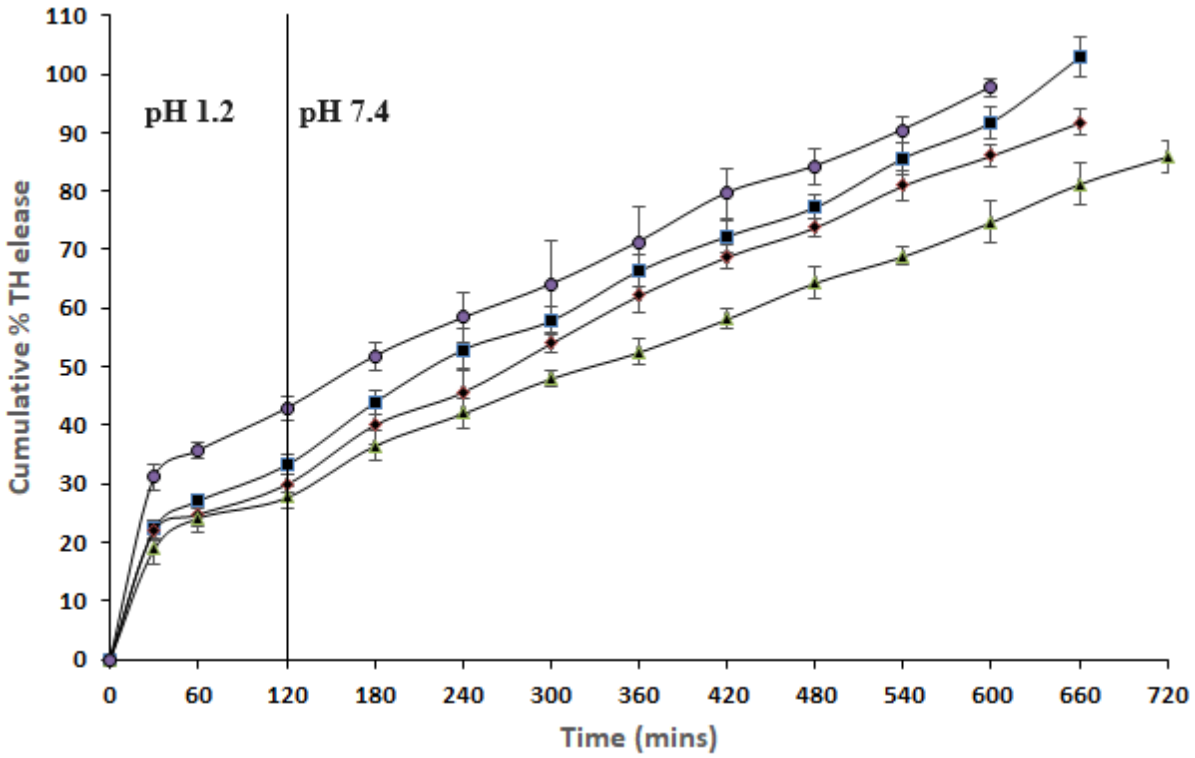

Fig. 8.17. TH dissolution from dual cross-linked hydrogel matrices. F9 (■), F14 (♦), F15 (▲), F16 (●).

In matrices F11-F13, a trivalent Al^{3+} was progressively substituted with a divalent Ca^{2+}, however, in matrices F14-F16, the divalent Ca^{2+} ion was progressively substituted with the trivalent Al^{3+}. As previously deliberated, trivalent ions cross-link more efficiently and generate a hydrogel layer of superior cross-link density as compared to divalent ions. Elevation in the Al^{3+} ions concentration in matrices F14-F15 generates a more viscous and stiff hydrogel layer, which dwindles the TH diffusion coefficient through the hydrogel layer resulting in slower TH dissolution (Table 8.5). Examination of viscosities of dispersions simulating the composition of matrices F9, F14-F16 revealed that the dispersion viscosity of matrices F9, F14-F15 progressively enhanced as the Al^{3+} ions concentration in the matrices is augmented (Fig. 8.18). Photographs of the gel layer thickness (Fig. 8.15) of matrices F9 (row c) and matrices F15 (row d) captured at 3 h, 6 h, 9 h, and 12 h following dissolution also bolstered the Al^{3+} ions effected elevation in hydrogel layer stiffness and viscosity. At 3 h, hydrogel layer formation is clearly visible around the core of matrices F9 and F15. However, the hydrogel layer in F15 was rigid and dense as compared to a slimy hydrogel layer in F9. At 6 h & 9 h, the gel layer thickness of both matrices F9 and F15 has enlarged, but in F15 the gel layer is thicker, stiffer and denser, while in F9 it is soft and thin. Lastly, at 12 h, although the F9 hydrogel layer was perceptible but erosion and disintegration have initiated (loose packed gel layer). However, for F15, the

hydrogel layer was even more firm, dense and rigid and the core of the matrix was intact and prominent. SEM surface structure micro-images of matrices F9 and F15 initially before dissolution and following 6 h dissolution also showed Al^{3+} ion effected upsurge in gel layer stiffness/viscosity and cross-link density. Fig. 8.19 describes that the surface of matrices F15 (Fig.8.19b) is irregular with foldings and wrinkles, while that of F9 (Fig. 8.19a) is even. This is due to superior cross-link density in the F15 matrices hydrogel layer in comparison to the F9 matrices gel layer. It is documented that at elevated crosslink density, microcapsules have rough and dense surface with foldings in it [23]. Surface structures of matrices F9 and F15 following 6 h of dissolution are displayed in Fig. 8.19 c & d respectively. As observed, pores have developed in the F9 matrices surface, but the F15 matrices surface was still dense and tight and bereft of any perforations/pores, again attributable to the Al^{3+} ion effected accentuation in cross link density for matrices F15. Higher cross-link density in matrices F15 made its surface even and devoid of cracks and perforations, while poor cross-link density in matrices F9 have generated surface perforations and fissures. TH dissolution pattern also perfectly simulated with the SEM surface micro-images. TH dissolution from matrices F15 was slower as compared to matrices F9. Reddy et. al. documented similar outcomes where curcumin dissolution from Ca^{2+} and Al^{3+} ions cross-linked (at ratio 1:1) composite beads were more sustained as compared to curcumin dissolution from only Ca^{2+} ions cross-linked composite beads (overall cross-linking ion concentration were same) [8]. The authors accredited that such variances in curcumin dissolution was because of generation of more stiff and firm hydrogel network in Al^{3+}- Ca^{2+} cross-linked composite beads as compared to that in Ca^{2+} cross-linked composite beads. However, when the concentration of Al^{3+} ions was 70%w/w (overall concentrations of the cross linking ions maintained at 12% w/w) as in matrices F16, the solution viscosity declined resulting in higher TH diffusion coefficient through the hydrogel layer and eventually faster TH dissolution (Table 8.5). Fall in gel layer/dispersion viscosity for matrices F16 is due non-homogenous cross linking at such elevated cross-linking ion concentration. Similar reports are available in literature from calcium-pectinate matrices [15]. Faster TH dissolution from F16 matrices may again be due to the channeling effect of the cross-linking ions which are surplus than that necessary for optimum cross link [24].

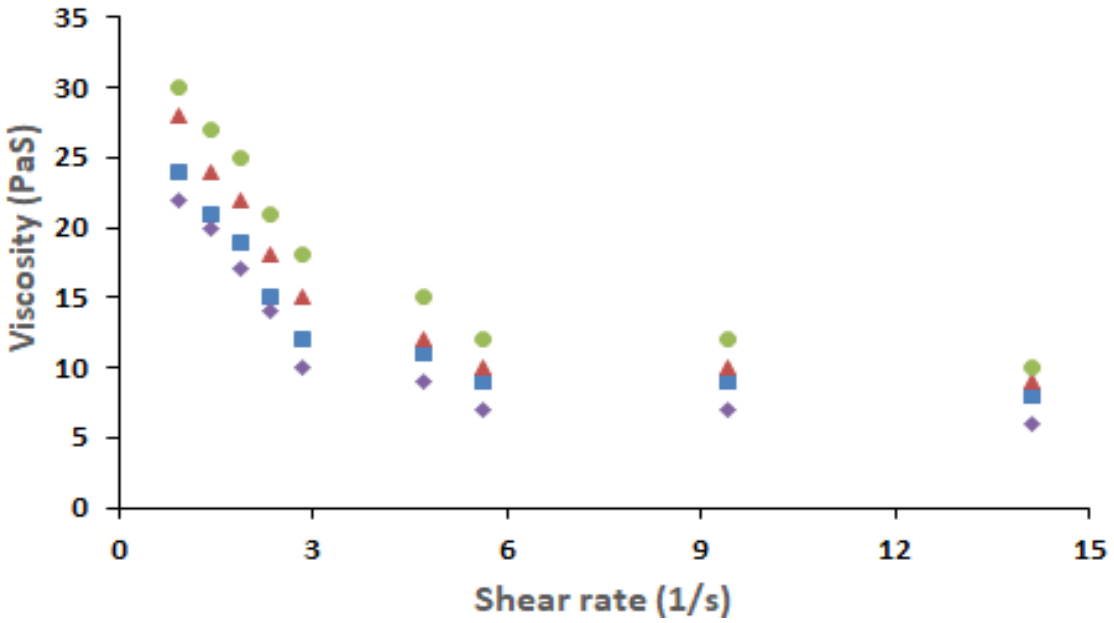

Fig. 8.18. Viscosities of CMTG solutions simulating matrices F9 (■), F14 (▲), F15 (●), F16 (♦).

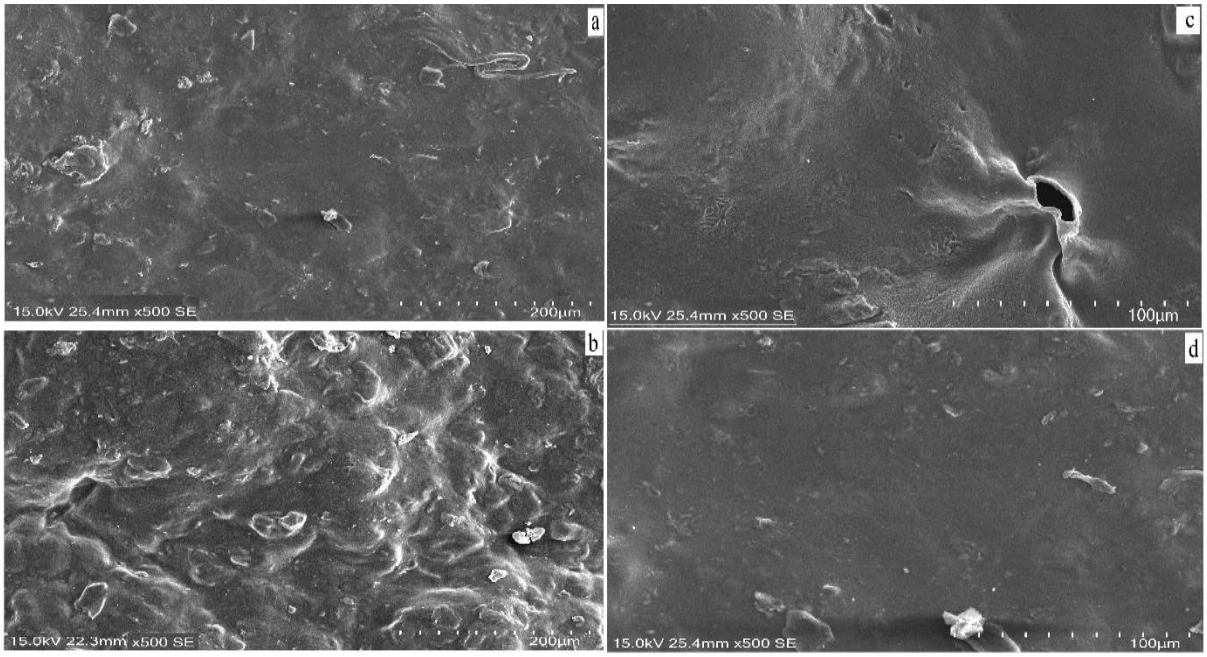

Fig. 8.19. SEM photomicrographs of matrices: before dissolution F9 (a) & F15 (b), following 6 h of dissolution F9 (c) & F15 (d).

3.6 TH dissolution mechanism specifications

The drug dissolution data from a matrix (up to 60 %) is usually plotted to power law equation. Since our matrices gave burst TH dissolution within 30 min of dissolution, the dissolution data from 1 h to 60% TH dissolution was plotted in power law expression to get the TH dissolution mechanism. Prior research also testified plotting of dissolution data from 1 h to 60% drug

dissolution associated with burst dissolution [1]. The TH dissolution from uncross-linked, Al^{3+} and/or Ca^{2+} cross-linked CMTG matrices obeyed Fickian diffusion (R^2 values 0.955-0.989) with release exponent (n) values less than 0.5 (Table 8.6). For water soluble drugs, the drug dissolution mechanism is governed by diffusion [25]. The solvent penetration rate and solute diffusion through such systems is much greater than the polymer chain disentanglement/relaxation [25].

Table 8.6 TH dissolution mechanism

Formulation code	Kinetic Constant (k)	Release exponent (n)	Co-relation coefficient (r^2)
F1	1.599	0.341	0.969
F2	1.580	0.342	0.972
F3	1.555	0.356	0.975
F4	1.507	0.392	0.987
F5	1.618	0.327	0.977
F6	1.571	0.324	0.986
F7	1.551	0.358	0.922
F8	1.472	0.444	0.978
F9	1.442	0.454	0.955
F10	1.532	0.487	0.949
F11	1.584	0.415	0.989
F12	1.591	0.402	0.976
F13	1.599	0.419	0.979
F14	1.418	0.421	0.937
F15	1.388	0.419	0.955
F16	1.567	0.317	0.974

3.7 Conclusion

Al^{3+} and/or Ca^{2+} cross-linked CMTG matrices were developed for sustained TH dissolution. TH compatibility in matrices was verified by XRD, FTIR, and DSC examination. The impact of Al^{3+} / Ca^{2+} ions on erosion, swelling, and TH dissolution were explored. Elevation in cross-linking ions concentration until a specific concentration declined the erosion and swelling of the matrices, reducing TH dissolution from the matrices. Beyond a certain amount of cross-linking ions, matrix erosion increased, and so was the TH dissolution. The cross-linking ions

enriched the hydrogel layer viscosity, which hindered the intrusion of water and consequently the TH diffusion coefficient. Al-CMTG matrices had better cross-linking density, generated a rigid, firmer, and denser hydrogel layer as compared to Ca-CMTG matrices. When the overall concentration of the cross-linking ions was maintained at a certain concentration, elevation in the concentration of the trivalent Al^{3+} ions decreased TH dissolution from the matrices. The reverse phenomenon was observed with the Ca^{2+} ions. Photographs of the matrices, SEM surface structure microimages of the matrices perfectly simulated with TH dissolution behaviour. TH dissolution from the matrices obeyed Fickian diffusion mechanism. We conclude from the research that Al^{3+} and Ca^{2+} ion cross-linked CMTG matrices could be used for sustained dissolution of a highly water soluble drug.

References

1. Singh R, Maity S, Sa B. Effect of ionic crosslink on the release of metronidazole from partially carboxymethylated guar gum tablet. Carbohydr. Polym. 2014;106:414–421.

2. Maity S, Sa B. Ca-carboxymethyl xanthan gum mini-matrices: swelling, erosion and their impact on drug release mechanism. Int. J. Biol. Macromol. 2014;68:78–85.

3. Li P, Dai YN, Zhang JP, Wang AQ, Wei Q. Chitosan-alginate nanoparticles as a novel drug delivery system for nifedipine. Int. J. Biomed. Sci. 2008;4(3):221–228.

4. Wei X, Sun N, Wu B, Yin C, Wu W. Sigmoidal release of indomethacin from pectin matrix tablets: effect of in situ crosslinking by calcium cations. Int. J. Pharm. 2006;318 (12):132–138.

5. Deb P, Singha J, Chanda I, Chakraborty P. Formulation development and optimization of matrix tablet of tramadol hydrochloride. Recent Pat. Drug Deliv. Formul.2017;11:19–27.

6. Hartman M, Trnka O, Sÿolcova O. Thermal decomposition of aluminum chloride hexahydrate. Ind. Eng. Chem. Res. 2005;44:6591–6598.

7. Indian Pharmacopoeia, vol. I, The Indian Pharmacopoeia Commission, Government of India, Ghaziabad, 2010.

8. Reddy OS, Subha MCS, Jithendra T, Madhavi C, Chowdoji Rao K. Curcumin encapsulated dual cross linked sodium alginate/montmorillonite polymeric composite beads for controlled drug delivery. J. Pharm. Anal. 2021;11:191–199.

9. Collett J, Moreton C. Modified release peroral dosage forms, in: M.E. Aulton (Ed.), Pharmaceutics: The Science of Dosage Form Design. 2nd ed. Churchill Livingstone, 2002, pp. 189–305.

10. Mughal MA, Iqbal Z, Neau SH. Guar gum, xanthan gum, and HPMC can define release mechanisms and sustain release of propranolol hydrochloride. AAPS Pharm. Sci. Tech. 2011;12:77–87.

11. Mandal S, Basu SK, Sa B. Sustained release of a water-soluble drug from alginate matrix tablets prepared by wet granulation method. AAPS Pharm. Sci. Tech. 2009;10(4):1348–1356.
12. Wang P, Luo ZG, Xiao ZG, Ahmed Saleh SM. Impact of calcium ions and degree of oxidation on the structural, physicochemical, and in-vitro release properties of resveratrol-loaded oxidized gellan gum hydrogel beads. Int. J. Biol. Macromol. 2022;196:54–62.
13. Mukherjee K, Kundu T, Sa B. Al^{3+} ion cross-linked matrix tablets of sodium carboxymethyl cellulose for controlled release of aceclofenac: development and in-vitro evaluation. Der. Pharm. Lett. 2012;4(6):1633–1647.
14. Kaity S, Issac J, Ghosh A. Interpenetrating polymer network of locust bean gum-poly (vinyl alcohol) for controlled release drug delivery. Carbohydr. Polym. 2013;94:456–467.
15. Sungthongjeen S, Sriamornsak P, Pitaksuteepong T, Somsiri A, Puttipipatkhachorn S. Effect of degree of esterification of pectin and calcium amount on drug release from pectin-based matrix tablets. AAPS Pharm. Sci. Tech. 2004;5:1–8.
16. Tiwari SB, Murthy TK, Pai MR, Mehta PR, Chowdary PB. Controlled release formulation of tramadol hydrochloride using hydrophilic and hydrophobic matrix systems. AAPS Pharm. Sci. Tech. 2003;4(3):E31.
17. Varshosaz J, Tavakoli N, Kheirolahi F. Use of hydrophilic natural gums in formulation of sustained-release matrix tablets of tramadol hydrochloride. AAPS Pharm. Sci. Tech. 2006;7:E168–E174.
18. Das MK, Senapati PC. Furosemide-loaded alginate microspheres prepared by ionic crosslinking technique: morphology and release characteristics. Indian J. Pharm. Sci. 2008;70(1):77–84.
19. Bajpai SK, Sharma S. Investigation on swelling/degradation behavior of alginate beads cross-linked with Ca^{2+} and Ba^{2+} ions. React. Funct. Polym. 2004;59(2):129–140.
20. Nokhodchi A, Tailor A. In situ cross-linking of sodium alginate with calcium and aluminum ions to sustain the release of theophylline from polymeric matrices. IL Farmaco. 2004;59:999–1004.
21. Mukherjee K, Dutta P, Giri Tk. Al^{3+}/Ca^{2+} cross-linked hydrogel matrix tablet of etherified tara gum for sustained delivery of tramadol hydrochloride in gastrointestinal milieu. Int. J. Biol. Macromol. 2023;232:123448.
22. Kulkarni RV, Sreedhar V, Mutalik S, Setty CM, Sa B. Interpenetrating network hydrogel membranes of sodium alginate and poly(vinyl alcohol) for controlled release of prazosin hydrochloride through skin. Int. J. Biol. Macromol. 2010;47:520–527.

23. Kulkarni RV, Mangond BS, Mutalik S, Sa B. Interpenetrating polymer network microcapsules of gellan gum and egg albumin entrapped with diltiazem–resin complex for controlled release application. Carbohydr. Polym. 2011;83:1001–1007.
24. Mukherjee K, Chakraborty S, Sa B. Quick/slow biphasic release of a poorly water soluble antidiabetic drug from bi-layer tablets. Int. J. Pharm. Pharm. Sci. 2015;7(11):250–258.
25. Bruschi ML. Mathematical models of drug release, in: Strategies to Modify the Drug Release From Pharmaceutical Systems. Elsevier Ltd. 2015;63–86.

Chapter 9: Development and evaluation of intragranular/extragranular semi-IPN hydrogel matrices

1. Introduction

Hydrophilic polysaccharides find extensive use as matrix materials for development of sustained drug delivery dosage forms. The dosage forms may be hydrogel particles, matrix tablets, bilayer tablets, microparticles, compression coated tablets etc. Recently, hydrophilic tablet matrices have been illustrious as evidenced by numerous publications and applications in drug delivery. The success of hydrophilic tablet matrices is attributed to its effortless processibility using modest, reproducible, and cost-effective tablet manufacturing process [1]. Additionally, the robustness and flexibility of the tablet manufacturing process opens newer avenues for fabricating the matrix development process to obtain the specific drug dissolution from the hydrophilic tablet matrices. Apart from fabricating the matrix development process, the erosion, swelling, hydrophilicity, and viscous nature of the matrix can also be modulated to get the specific drug solubilization characteristics [2, 3]. Cross-linking of polymeric chains also modulates the erosion, swelling, and viscous nature of the matrix delivery agent [2, 3].

Quite often, a sole polymer matrix may not fulfill the divergent necessities of a drug delivery agent. To overcome such problems, blending of polymers have been explored so that the tailored functional properties and drug dissolution from the matrices can be achieved. Blending of polymers provides the specific functional requirements from the delivery agents in terms of erosion, swelling, hydrophilicity, and viscous nature of the matrix. When both the polymers in the blend are cross-linked by a common cross-linking ion, they form an interpenetrating polymer network (IPN) structure [4, 5]. And when one polymer is cross-linked and the other is straight, it forms a semi-IPN structure [6, 7].

In the previous chapter we have developed and optimized dual cross-linked CMTG matrices. Matrices containing equal weight ratios of the cross-linking ions (when the overall cross-linking ion concentrations was maintained at 12% w/w of the matrices) gave the most prolonged tramadol hydrochloride delivery from the matrices. Tramadol dissolution from the dual cross-linked matrices after 2 h, 6 h, and 12 h of dissolution was 28%, 53%, and 86% respectively. With an aim to further prolong TH delivery from the matrices, TG was incorporated onto the matrices. This chapter deals with the development of a one of its kind, novel matrix development process which utilizes both the wet granulation and direct compression method of matrix development. TG was incorporated both within and outside the dual cross-linked CMTG granules and its effect on erosion, swelling and TH dissolution from the matrices was investigated.

2. Materials and methods

2.1. Materials

The ingredients required in this study are given in Table 9.1.

Table 9.1 Ingredients required

Ingredients required	Manufacturer
Tramadol Hydrochloride (TH) (gift sample)	IPCA laboratories, Sikkim, India.
Tara gum (TG)	IAMPURE ingredients, India
Trisodium orthophosphate dodecahydrate	Loba Chemie Pvt. Ltd.
Hydrochloric acid	Merck Specialities Pvt. Ltd., India
Calcium chloride ($CaCl_2$)	Merck Specialities Pvt. Ltd., India
Aluminium chloride ($AlCl_3$)	Loba Chemie Pvt. Ltd.
Magnesium stearate	Loba Chemie Pvt. Ltd.

2.2 Development of hydrogel matrices

The hydrogel matrices composition is shown in Table 9.2. CMTG, TG and TH (# 72 grade) were blended homogeneously and then slowly triturated with cross-linking solutions to form a wet cohesive mass. The wet cohesive mass was put through # 18 screen and dried. The dried mass was once again put through # 23 mesh to get the granules and again dried. The granules were then blended with magnesium stearate (lubricant) and compressed in a flat faced 6 mm punch in automatic tablet punching machine (RIMEK, Karnavati Engineering Ltd., India). This was the method of preparation of matrices F1-F4. For matrices F5-F8, TG was not mixed with TH and CMTG. TG was incorporated to the # 22 mesh granules and blended homogenously. Thereafter, lubricant was added to the granules and compressed as usual. Hardness of the tablets were maintained at 4 kg/cm^2.

Table 9.2 Hydrogel matrices composition

Formulation code	Amount of TH (mg)	Quantity of CMTG (mg)	Quantity of TG (mg)		Quantity of $AlCl_3$ (mg)	Quantity of $CaCl_2$ (mg)	Weight of matrix (CMTG/TG + $CaCl_2$/$AlCl_3$)	Weight % of crosslinkions in the matrix (% w/w)	Weight % between CMTG /TG	Weight % between $AlCl_3$ / $CaCl_2$ (% w/w)	Mag St (mg)
			Intra granular TG	Extra granular TG							
F1	100	188.1	9.9	-	13.5	13.5	225	12%	95/05	50/50	2
F2	100	178.2	19.8	-	13.5	13.5	225	12%	90/10	50/50	2
F3	100	168.3	29.7	-	13.5	13.5	225	12%	85/15	50/50	2
F4	100	158.4	39.6	-	13.5	13.5	225	12%	80/20	50/50	2
F5	100	188.1	-	9.9	13.5	13.5	225	12%	95/05	50/50	2
F6	100	178.2	-	19.8	13.5	13.5	225	12%	90/10	50/50	2
F7	100	168.3	-	29.7	13.5	13.5	225	12%	85/15	50/50	2
F8	100	158.4	-	39.6	13.5	13.5	225	12%	80/20	50/50	2

2.3 Characterization of the hydrogel matrix tablets

2.3.1 Weight Variation Test

Tablets, 20 in numbers, were precisely separately weighed in an electronic balance (SPT-200, Prime Technologies, India). The individual tablet weight was matched with the average tablet weight.

2.3.2 Crushing Strength (hardness) of hydrogel matrices

Hardness of the matrices was examined in a Tablet Hardness Tester (Monsanto type) (Campbell Electronics, Mumbai, India), and mean hardness of 10 tablets was taken.

2.3.3 Friability Test

Weight of 10 matrices were noted and put in the friabilator drum (EF2, Electro Lab, Mumbai, India) and rotated at 25±1 rpm. Following 100 revolutions, the matrices were cleaned, de-dusted and reweighed. The weight loss (percentage) was determined.

2.3.4 TH content of the hydrogel tablets

3 tablets were crushed individually in a mortar and pestle and finely grounded. The grounded mass was then transferred in to 250 ml pH 7.4 volumetric flask and mechanically shaken for 24 h. After 24 h, the solution was filtered and following adequate dilutions was spectrophotometrically (UV-2450, Shimadzu, Japan) analysed at 270nm for determining the TH content in the hydrogel tablets.

2.4 Erosion and swelling of the hydrogel tablets

The percentage erosion and swelling of the unloaded hydrogel tablets were determined in USP II dissolution instrument. One hydrogel tablet was precisely weighed (W_0, initial hydrogel tablet weight) (SPT-200, Prime Technologies, India) and put inside a net basket and the whole assembly was immersed in dissolution solution. At hourly time intervals, the net basket assembly was taken out from the dissolution solution, freed from the surface water using a tissue paper and then the hydrogel tablets were weighed precisely (W_t, matrix weight at the particular time interval). The hydrogel matrix was then kept inside a hot air oven for drying until constant weight and then the final constant weight of the matrix (W_f) was noted accurately. The percentage erosion and swelling of the hydrogel matrix was determined following Eq. (9.1) & Eq. (9.2) [3].

$$\% \, Swelling = \frac{W_t - W_0}{W_0} \times 100 \ldots\ldots\ldots\ldots\ldots\ldots\ldots (9.1)$$

$$\% \, Erosion = \frac{W_0 - W_f}{W0} \times 100 \ldots\ldots\ldots\ldots\ldots\ldots\ldots (9.2)$$

2.5 *In-vitro* dissolution of TH

In-Vitro TH dissolution from hydrogel matrices were determined as per IP 2018 procedure in an USP II dissolution instrument (TDT-06P, Electrolab, India). One matrices were submerged in a glass beaker filled with 700 ml pH 1.2. After 2 h, the media pH was elevated to pH 7.4 by addition of 200 ml 0.2 (M) trisodium ortho phosphate dodecahydrate solution and dissolution continued for the next 10 h. Aliquots were taken out at hourly intervals and refilled with the same volume of the respective dissolution media. Aliquots were analysed in a spectrophotometer (UV-2450, Shimadzu, Japan) at 270 nm and the TH dissolved from the

hydrogel tablets were determined from calibration curve plotted at the individual dissolution solution. Dissolution of TH hydrogel tablets were done in triplicates.

2.6 Fourier transform infrared (FTIR) analysis

Investigation of FTIR spectra of TH and TH hydrogel matrices were done in a FTIR spectrophotometer (RX 1, Perkin Elmer, UK) at 4000–400 cm^{-1}. Sample preparation include sample mixing with potassium bromide in a hydraulic press to convert them into pellets.

2.7 X-ray diffraction (XRD) study

The XRD of TH and TH hydrogel matrices were measured by X-ray diffractometer (D8, Bruker, Germany). The essential specifications are: scan speed 5º/min, current 30 mA, diffraction angle (2θ) 10–80º, and voltage 45Kv.

2.8 Differential scanning colorimetry (DSC) study

DSC thermal curves of TH and TH hydrogel matrices were observed in a differential scanning colorimeter calibrated against indium (Pyris Diamond TG/ DTA, Perkin Elmer, Singapore). Samples was introduced in a sealed aluminium bottle and heated at 30–400ºC at 10ºC/min, under nitrogen atmosphere.

2.9 Determination of Viscosity

Dispersions simulating the hydrogel matrix formulae were prepared and left for 24 h for homogenous hydration. The viscosities of the dispersions were determined using S 61 spindle in a viscometer (DV-E, Brookfield Engg. Inc., USA) at 37ºC.

2.10 Scanning electron microscopy (SEM)

Surface structure of selected matrices before and following 6 h dissolution was observed in a scanning electron microscope (SU3800, Hitachi, Japan) at 15 Kv. The matrices were mounted onto stubs and gold-sputter coated to render them electrically conductive.

2.11 Diffusion coefficient of TH

The equivalent spherical diameter (cm) of hydrogel matrix tablets was found out from the equation $d = (6r_ch)^{1/3}$, where d, h, and r_c represents the equivalent spherical diameter, height (cm), and radius of the hydrogel tablets. The diffusion coefficients (cm^2/s) were determined following Eq. (9.3) [8].

$$D_c = \pi \times (\frac{r\theta}{6M_\infty})^2 \ldots\ldots\ldots\ldots\ldots\ldots\ldots (9.3)$$

Where θ = gradient of the straight line of the $M_t/M\alpha$ v/s $t^{1/2}$ plot.

M_α = TH loaded in the hydrogel matrices.

M_t = TH dissolved in t s.

r = equivalent spherical radius of the hydrogel matrices.

2.12 Water penetration (intrusion) velocity

The percent swelling data was used to compute the velocity of penetration (intrusion) of water into the hydrogel matrices following the process defined as per Eq. (9.4) [2].

$$V = \frac{1}{2\rho A} \times \frac{d_w}{d_t} \ldots\ldots\ldots\ldots\ldots\ldots (9.4)$$

Where V stands for water penetration (intrusion) velocity, ρ for the density of water (37°C), A for the hydrogel tablets surface area and dw/dt denotes the gradient of the % swelling v/s time plots.

2.13 Swelling and TH dissolution mechanism

Power law equation (9.5) was utilized to define the mechanism & kinetics of TH dissolution from hydrogel matrices [9].

$$\frac{M_t}{M_\infty} = kt^n \ldots\ldots\ldots\ldots\ldots\ldots\ldots\ldots\ldots (9.5)$$

Where $M_t/M\alpha$ = portion of TH dissolved at time t, n= diffusional exponent, k= rate constant

For tablet matrices, n=0.5 signifies Fickian diffusion, 0.5<n<1.0 is suggestive of anomalous or non-Fickian diffusion, n=1.0 suggests case II and n>1.0 characterizes super case II transport process [9].

The swelling kinetics was found out similarly, where the swelling results for initial 3 h, when the matrix swelling predominated, was plotted to the power law equation.

2.14 Mean dissolution time (MDT)

The MDT (min) was calculated from Eq. (9.6) [10]. The power law Eq. (9.5) was utilized for gathering the n and k values.

$$MDT = \left(\frac{n}{n+1}\right) k^{\left(-\frac{1}{n}\right)} \ldots\ldots\ldots\ldots\ldots\ldots (9.6)$$

2.15 Determination of volume of the matrices

The volume of the unloaded matrices was determined with the aid of slide calipers (CD-6CSX, Mitutoyo, Japan). The thickness (height) and diameter (millimetres, mm) of the matrices were determined correctly and then submerged in pH 1.2 dissolution media. The dissolution media pH was adjusted to pH 7.4 after 2 h. At definite time periods of 1 h, 2 h, 3 h, 5 h, and 8 h the matrices were cautiously taken out from the dissolution solution and then the thickness (height) and diameter were again measured correctly. The matrices were again put into the dissolution medium. The matrices volume was determined from the following formulae.

$$V = \pi \times r^2 \times h \ldots\ldots\ldots\ldots\ldots\ldots (9.7)$$

Where V represents the matrices volume with height (thickness) h and radius r.

2.16 In-Vivo Pharmacokinetic study

The in-vivo pharmacokinetics of the optimized final hydrogel matrices was done at TAAB Biostudy Services (Kolkata-32, India). Study protocol was sanctioned by IAEC, TAAB Biostudy Services (Kolkata-32, India). The study was done on12 healthy New Zealand white rabbits (1-2kg). Overnight (12h) fasting of the rabbits with plenty access to water were done prior to dosing. The rabbits were divided into 2 groups of 6 each: reference group receiving 9 mg oral solution of TH and the test group receiving optimized hydrogel matrices (F7) equivalent to 9 mg TH orally [11]. 0.5ml blood was taken by retro-orbital puncture at 0.5, 1, 2, 3, 6, 8, 12 and 24 h and stored in centrifuge tube (heparinized). The tubes were centrifuged (5000 rpm, 10 min) then plasma collected and stored at -20°C till analysed.

2.17 Estimation of TH in rabbit plasma

Estimation of concentration of TH in rabbit plasma was done by LC-MS/MS (API 4000 Q-trap, Toronto, Canada). API 4000 Q trap triple quadrapole mass spectrometry detection system was utilized for TH analysis. Propranolol was the internal standard. Methanol: phosphate buffer (pH 3) was the mobile phase delivered at ambient temperature at 1 ml/min. At 1.35 ng/ml, TH was detected. Internal standard and chromatographic separation of TH was done by means of a Thermo ODS C_{18} column (250mm×4.6mm, 6.5µm particle size). Acetonitrile protein precipitation method was use to process the blood samples. To 0.5 ml acetonitrile was added 0.1 ml of blood sample and cyclomixed (10mins) to extract TH. It was then centrifuged (5 min, 6000 rpm) and collection of the supernatant was done. Filtration of the solution was done through 0.45µ filter and 20 µl was injected into HPLC system. 50 µl of internal standard and 150 µl rabbit plasma were transferred into 1.5 ml microcentrifuge tubes. Deproteinization of the samples was done by addition of acetonitrile (300µl). The samples were vortexed (5 min) and centrifuged (5min, 6000 rpm).

2.18 Pharmacokinetic parameters

The analysis of pharmacokinetic parameters was done by SPSS WinNonlin 8.1 software. The parameters studied were: plasma half-life ($t_{1/2}$), peak plasma TH concentration (C_{max}), time to reach C_{max} (T_{max}), AUC $_{0\text{-}24h}$, $AUC_{0\text{-}\infty}$, and elimination rate constant (K_{el}).

2.19 Accelerated stability studies

Stability study was performed on the optimized hydrogel matrices F7 to evaluate the effect of relative humidity and temperature on the physical characteristics and *in vitro* TH dissolution from the hydrogel matrices. The accelerated stability studies have been carried out as per European Medicines Agency (EMA) guidelines, with minor modifications [12]. The conditions

of the study were 40±2°C at RH 75±5% for 3 months. The physical characteristics and in vitro TH release from the hydrogel matrices prior to and after conduction of the stability study were compared.

2.20 Statistical Analysis

ANOVA (GraphPad Prism 3.0) was done to ascertain the statistical importance of the data gathered from erosion, swelling, and TH dissolution study. The difference was reckoned significant when $p<0.05$.

3 Results and discussion

3.1 TH compatibility in hydrogel matrices

The excipient-TH compatibility was judged by FTIR, DSC, and XRD studies. The FTIR spectrum of TH and TH hydrogel tablets are illustrated in Fig. 9.1. The spectrum of TH demonstrated a peak at 3306 cm^{-1} representing OH stretching. Subsequent peaks at 3062 cm^{-1} and 2929 cm^{-1} stands for aromatic CH ring stretching and methyl group CH stretching. The peak at 2859 cm^{-1} is because of CH_2 stretching. Additional peaks at 1586 cm^{-1}, 1259 cm^{-1}, and 753 cm^{-1} represents C=C (aromatic) stretching, CN stretching, and substituted benzene ring stretching respectively. Similar IR signals of TH have been reported by Deb et. al. [13]. The IR signals for TH hydrogel matrices appeared at almost similar wavenumbers as that of TH, indicating the TH compatibility in the hydrogel tablets.

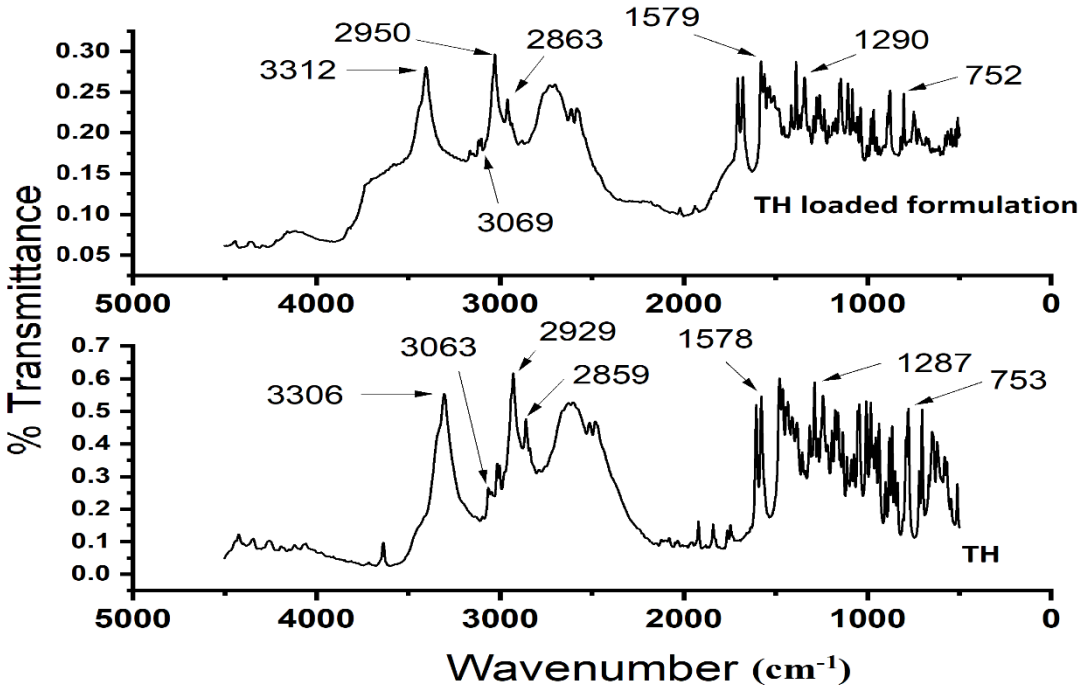

Fig. 9.1. FTIR spectrum of TH and TH hydrogel matrices.

The DSC curves of TH and TH hydrogel tablets are described in Fig. 9.2. The intense endotherm at 180ºC is the melting point of TH. The sharp endotherm at 260ºC signified total

degradation/decomposition of TH. Related DSC events of TH are available in literature [13]. The DSC thermal events of TH hydrogel matrices revealed an expanded endotherm at 69ºC representing water loss and an exotherm at 255ºC indicating CMTG decomposition. The sharp endotherm at 192ºC represents the melting of $AlCl_3$ [14]. The stretched exotherm at 306ºC signifies thermal degradation/decomposition of TG [15]. The DSC thermal curve of the TH matrices didn't show any thermal event at the melting point of TH, indicating the conversion of TH into amorphous form during matrix preparation.

The TH X-ray diffraction patterns (Fig. 9.3) showed reflections at 15.20°, 16.40°, 18.23°, 21.28°, 24.09°, 26.68°, 29.23°, 30.56°, 40.31° and 41.82° 2θ. The TH hydrogel matrices didn't show such characteristics 2θ reflections of TH. The appearance of dual intense peaks at 2θ 45.40º and 31.68º with intensities 484 cps and 877 cps respectively are the characteristics reflections of CMTG. It can be anticipated from the XRD and DSC results that TH was converted to amorphous form during matrix preparation. Maity et. al. documented that crystalline prednisolone was converted to amorphous form during matrix development [16]. Similar result was also documented when capecitabine was loaded in poly (ethylene oxide-g-acrylamide) and chitosan IPN structure [17].

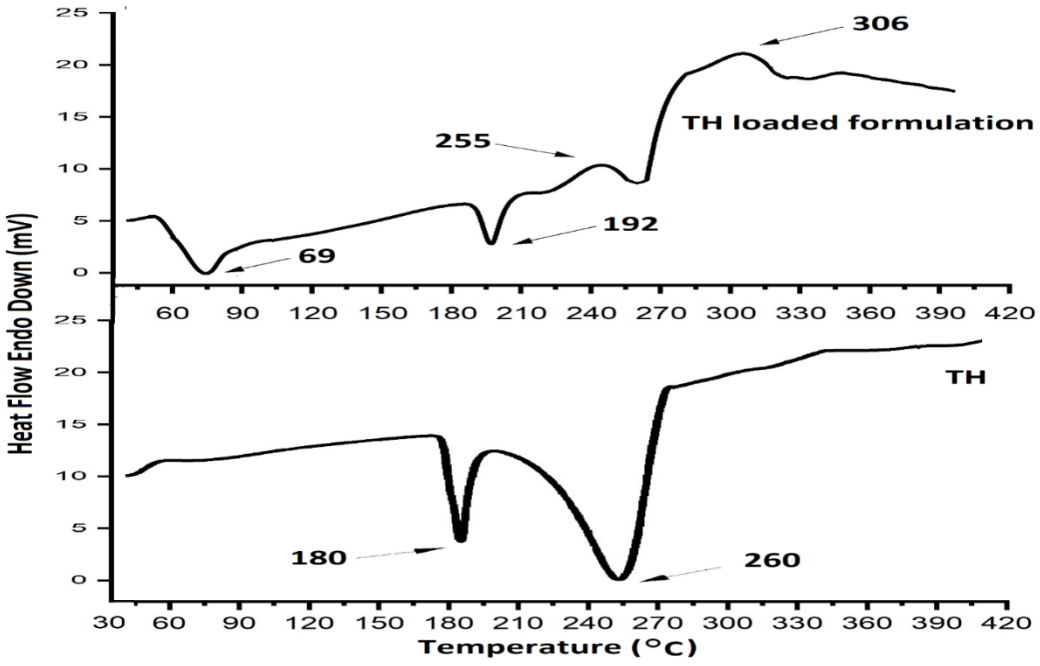

Fig. 9.2. DSC thermal curves of TH and TH hydrogel matrices.

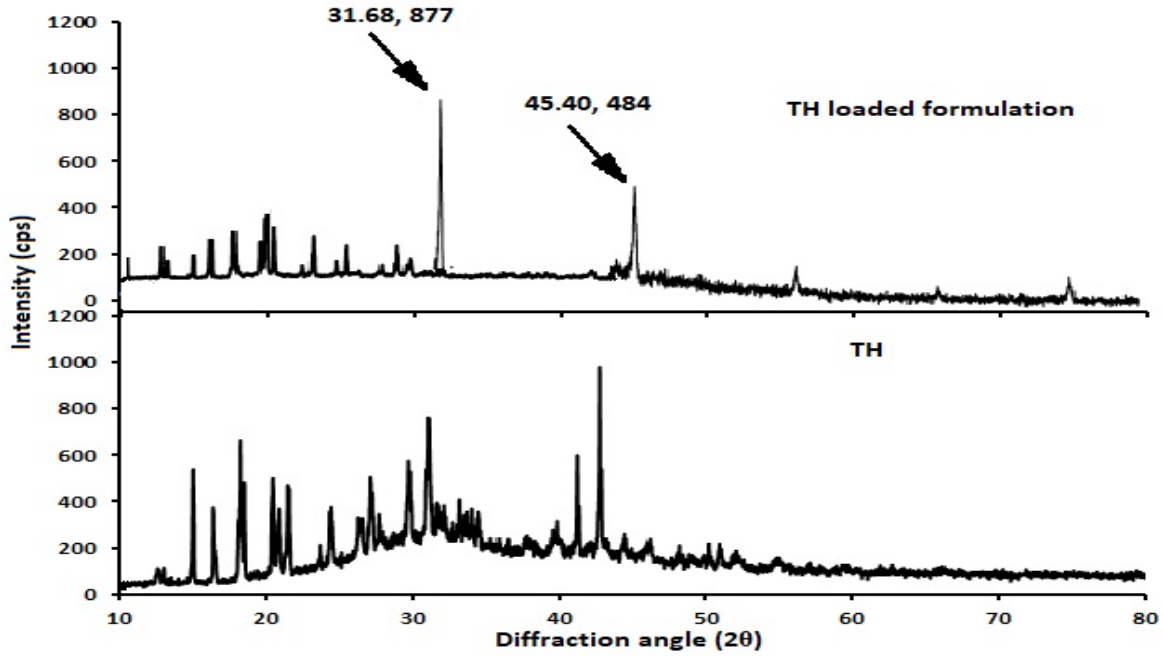

Fig. 9.3. XRD reflections of TH and TH hydrogel matrices.

3.2 In vitro TH dissolution from dual metal ion cross-linked semi-IPN hydrogel matrices

In the previous chapter we have reported the optimization of the cross-linking ions concentration in the matrices. The overall cross-linking ions concentration in the matrices as well as the weight ratio between the Ca^{2+} and Al^{3+} in the matrices have been optimized. Matrices containing equal weight ratios of the cross-linking ions (when the overall cross-linking ion concentrations was maintained at 12% w/w of the matrices) gave the most sustained tramadol hydrochloride delivery from the matrices. TH dissolution from the optimized dual cross-linked matrices was 86% following 12 h of dissolution. With the purpose to further prolong TH dissolution from the matrices, TG was incorporated to the optimized dual cross-linked hydrogel matrices. Accordingly, semi-IPN hydrogel matrices of CMTG and TG have been prepared. The erosion, swelling, and TH dissolution from the semi-IPN matrices have been investigated. Keeping all the variables (ratio between Al^{3+}/Ca^{2+} ions and polymer: cross-linker) of the dual cross-linked hydrogel matrices constant, CMTG was progressively substituted with TG in the matrices. Weight percentage of TG was 5% w/w, 10% w/w, 15% w/w, and 20% w/w of the total polymer for semi-IPN matrices F1-F4 respectively. The *in vitro* TH dissolution from matrices F1-F4 are illustrated in Fig. 9.4. Incorporation of TG onto the dual cross-linked matrices produced substantial changes in the *in vitro* TH dissolution profile. Matrices F1-F4 provided burst TH dissolution (21%-30%) within 30 min of dissolution. The TH dissolution was uniform following the burst dissolution. No immediate alteration in TH

dissolution was noted when the dissolution solution pH was brought to pH 7.4, following 2 h of TH dissolution. TH dissolution progressively augmented with the elevation in the TG weight percentage in the matrices. TH dissolution from matrices F1-F4 increased in the following fashion: following 2 h in pH 1.2 dissolution solution- F1 (31%)<F2 (33%)< F3 (36%)< F4 (40%) and following 10 h of dissolution- F1 (79%)<F2 (82%)< F3 (86%)< F4 (91%). Mean Dissolution Times (MDT) and AUCs progressively increased for matrices F1-F4 (Table 9.3) ($p<0.05$). Augmentation in TH dissolution with the elevation in TG weight percentage in the matrices can be explained from the erosion and swelling of the matrices.

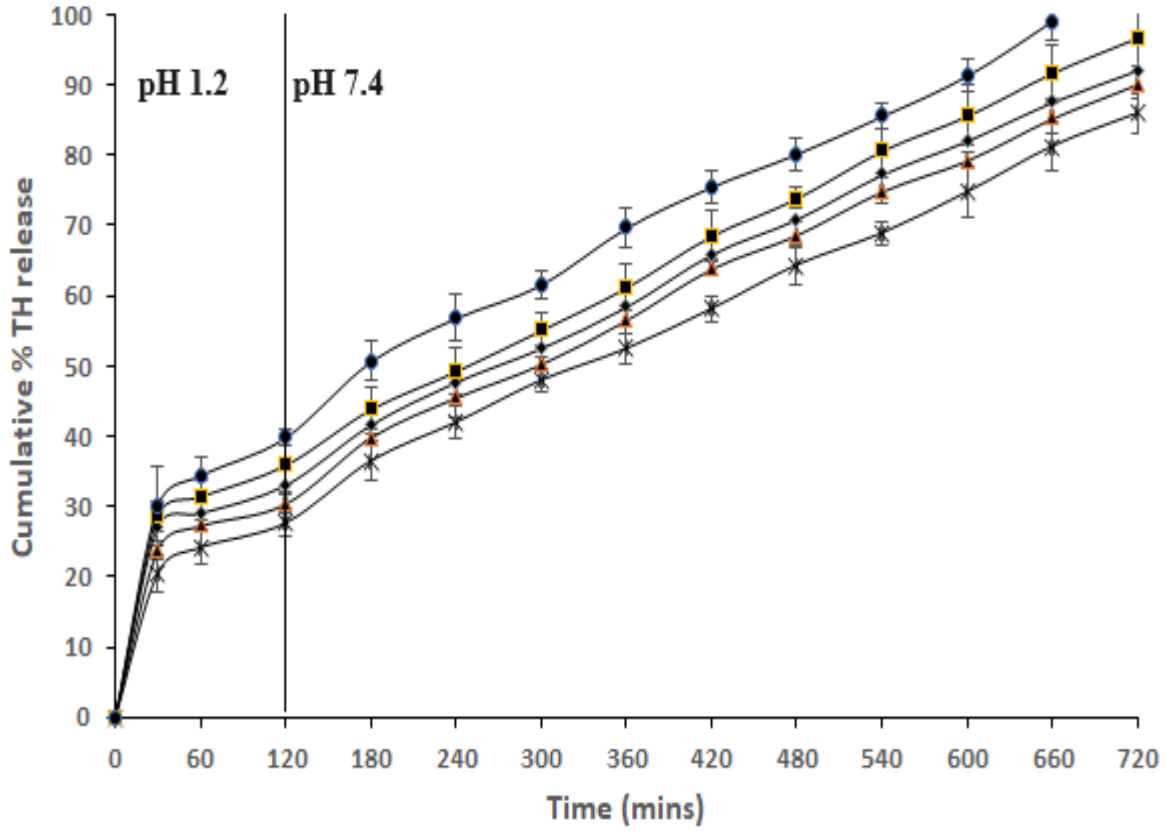

Fig.9.4. TH dissolution from semi-IPN hydrogel matrices. F15 (×), F1 (▲), F2 (♦), F3 (■), F4 (●).

Table 9.3 Release specifications (mean±SD, n=3)

Formulation code	Mean dissolution time (MDT), (min)	Diffusion coefficient (cm^2/s)	AUC ($\%h^{-1}$)
F1	4.54±0.12	$1.15*10^{-07}$	72.23±4.23
F2	4.41±0.06	$1.16*10^{-07}$	74.46±5.25
F3	4.43±0.27	$1.17*10^{-07}$	76.97±3.36
F4	3.78±0.33	$1.20*10^{-07}$	79.25±3.39
F5	4.83±0.18	$1.18*10^{-08}$	53.32±4.23
F6	4.94±0.15	$1.13*10^{-08}$	48.22±4.50
F7	5.03±0.26	$1.06*10^{-08}$	44.43±2.25
F8	4.19±0.27	$1.13*10^{-07}$	73.22±3.24

The dynamic erosion and swelling of the semi-IPN matrices F1-F4 have been illustrated in Fig. 9.5. Matrices F1-F4 swelled immediately to various extents in pH 1.2 dissolution solution, attained an equilibrium swelling state at around 5 h, following which swelling progressively declined as time elapsed indicating loss in matrix mass. Swelling of the optimized dual cross-linked matrices F15 (previous chapter) was 90%, 126%, and 82% after 2 h, 5 h, and 8 h of swelling study. The F15 matrix erosion indicated steady elevation in percentage erosion with time (10%, 22%, and 35% at 2 h, 5 h, and 8 h respectively). Progressive substitution of CMTG with TG in the matrices, effected substantial changes in the percentage erosion and swelling of the semi-IPN matrices. Progressive elevation in TG weight percentage significantly augmented the percentage erosion and swelling of the semi-IPN matrices ($p<0.05$). Percentage swelling of the matrices F1, F2, F3, and F4 following 2 h in pH 1.2 dissolution solution was 98%, 106%, 118%, and 129%, following 5 h of swelling study- 138%, 148%, 158%, and 168%, and following 8 h of swelling study 105%, 113%, 123%, and 127% respectively. Similarly, erosion percentage of the matrices F1, F2, F3, and F4 following 2 h in pH 1.2 dissolution solution was12%, 16%, 19%, and 23%, following 5 h- 25%, 29%, 33%, and 37%, and following 8 h of erosion study-39%, 43%, 46%, and 49% respectively. The elevation in erosion and swelling percentage of the semi-IPN matrices F1-F4 with the elevation in the TG weight percentage was due to accentuation in the water intrusion velocity through the hydrogel of the polymeric matrices (Table 9.4) ($p<0.05$). The elevation in the water intrusion velocity of matrices F1-F4 with the elevation in the TG weight percentage can be described in the following manner. TG is a highly hydrophilic polymer as it has abundant hydroxyl groups in its structure [18, 19].

These hydroxyl groups have high attraction with the dissolution media hydroxyl groups and forms hydrogen bonding with each other. Augmentation in the TG weight percentage provides increased number OH groups, which elevates the total hydrophilicity of the matrices. The water intrusion velocity in the semi-IPN matrices thus accentuates with the elevation in TG induced hydrophilicity of the matrices. The pure TG matrices swelling is itself very high due its high hydrophilicity. This was validated by swelling and erosion profiles of pure TG matrices (Fig. 9.5). Swelling percentage of pure TG matrices after 2 h, 5 h, and 8 h of the swelling study are 172%, 230%, and 135% respectively. Similarly, erosion percentage of pure TG matrices after 2 h, 5 h, and 8 h of erosion study are 33%, 45%, and 57% respectively. The increase in percentage swelling and erosion of matrices F15, pure TG matrices, and matrices F1-F4 were further ascertained by dynamic volume change of the matrices at various time periods and the results are demonstrated in Fig. 9.6. The volume of matrices F15 was 565 mm^3, 692mm^3, and 412mm^3 at 2 h, 5 h, and 8 h respectively. Incorporation of TG onto the matrices substantially augmented the matrices volume. Volume of the matrices F1-F4 at 2 h was 580 mm^3, 628mm^3, 670mm^3, and 701mm^3, at 5 h- 709mm^3, 745mm^3, 769mm^3, and 816mm^3, and 428mm^3, 447mm^3, 469mm^3, and 497mm^3 following 8 h of dynamic volume change study respectively. The pure TG matrices volume at 2 h, 5 h, and 8 h was 887mm^3, 1038mm^3, and 637mm^3 respectively. A hydrophilic polymer in an aqueous media starts to absorb water and begins to swell and subsequently enlarge in volume. The F15 matrices volume was low at all-time points, and the volume augmented with the increase in the percentage weight of TG in the matrices (F1-F4). The dynamic volume changes of the matrices F15 and F1-F4 perfectly correlates with the dynamic swelling and erosion pattern of matrices F15 and F1-F4. The pure TG matrices dynamic volume change also accorded with the swelling and erosion pattern of the pure TG matrices. Progressive substitution of TG in the matrices accounted for elevation in the swelling and erosion of the matrices, which expedited TH dissolution from the semi-IPN hydrogel matrices F1-F4. Similar results from Fe^{3+} cross-linked methyl cellulose-sodium alginate semi-IPN hydrogel beads were documented [20]. The author claimed that elevation in the proportion of methyl cellulose in semi-IPN hydrogel beads composition led to an increase in drug dissolution from the hydrogel beads. According to the author, the increased hydrophilic and swelling nature of methyl cellulose was the reason for faster drug dissolution from the sodium alginate-methyl cellulose semi-IPN hydrogel. Nochos et. al. also documented similar results regarding bovine serum albumin dissolution from alginate/hydroxyl propyl methyl cellulose hydrogel beads [6].

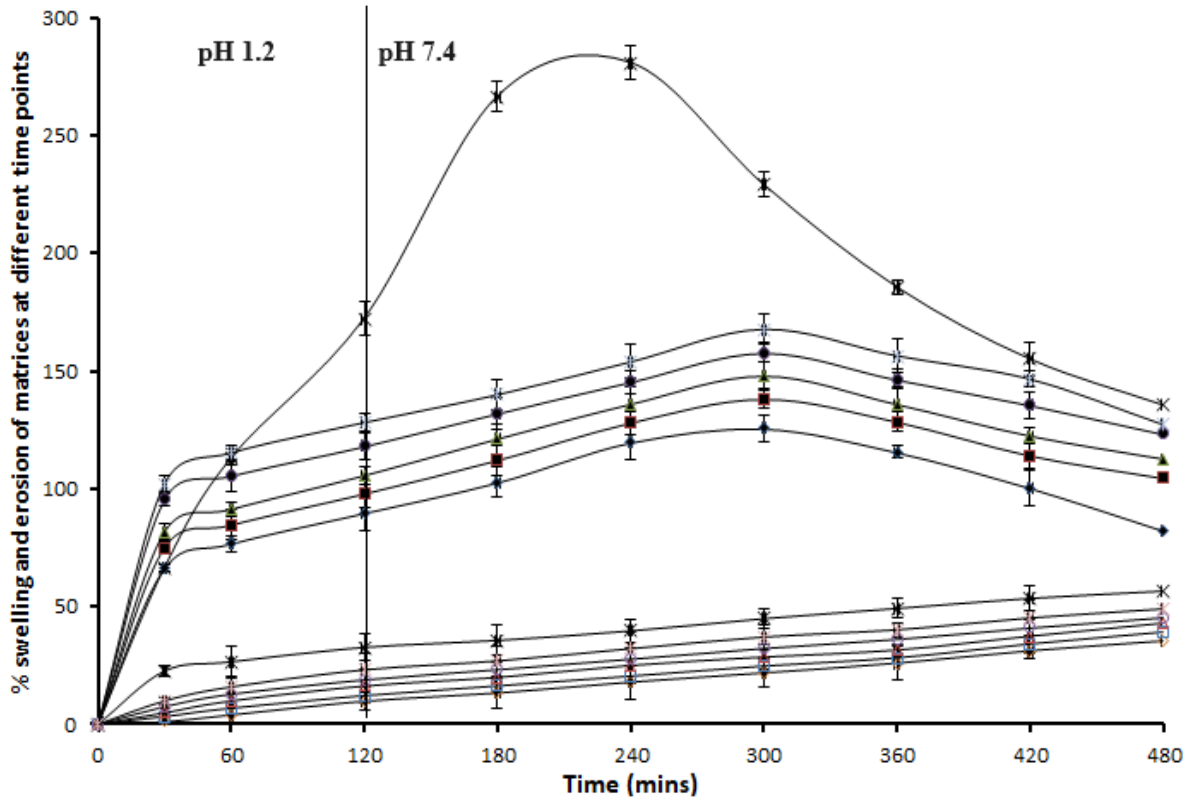

Fig. 9.5. Percentage swelling (filled markers) and erosion (hollow markers) of semi-IPN hydrogel matrices. Pure TG matrices (×), F15 (♦), F1 (■), F2 (▲), F3 (●), F4 (✳).

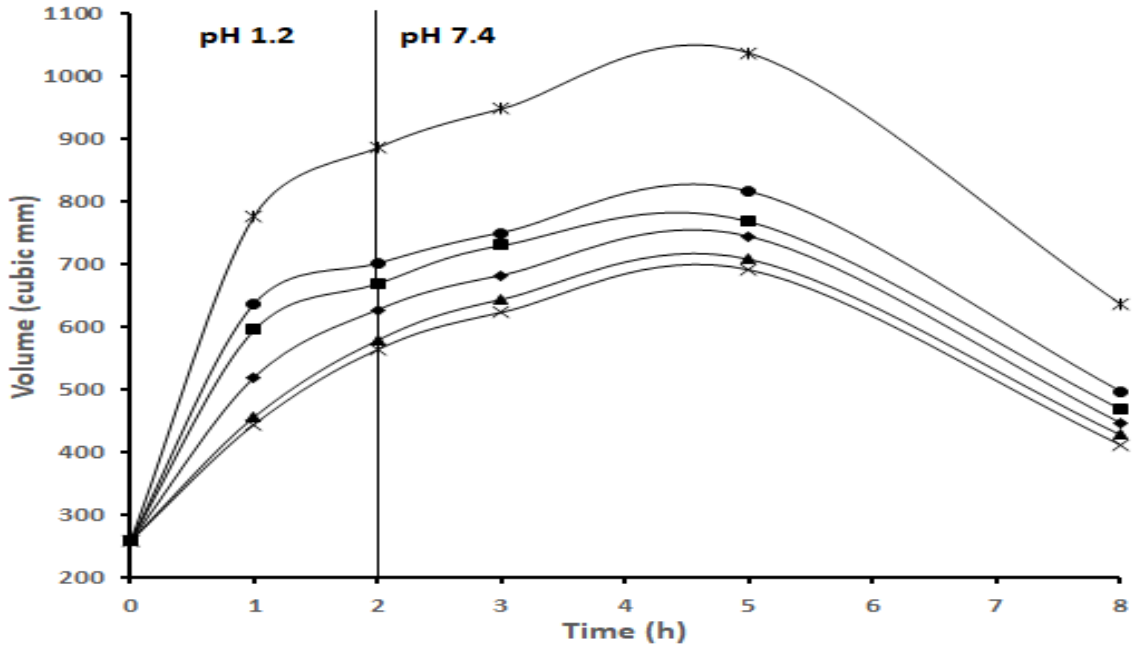

Fig. 9.6. Dynamic volume changes of the semi-IPN hydrogel matrices. Pure TG matrices (✳), F15 (×), F1 (▲), F2 (♦), F3 (■), F4 (●).

Table 9.4 Dynamic volume changes of the hydrogel matrices with time and water penetration velocity through the hydrogel matrices (mean±SD, n=3)

Formulation code	Dynamic volume of the matrices (mm^3)			Water Penetration Velocity (cm/s)
	2h	5h	8h	
F15	565±4.8	692±1.8	412±6.3	0.000325
F1	580±5.1	709±2.7	428±8.4	0.000875
F2	628±3.6	745±4.8	447±8.1	0.000920
F3	670±2.4	769±2.7	469±7.5	0.000989
F4	701±1.8	816±5.4	497±3.6	0.001025
Pure TG matrices	887±5.4	1038±6.3	637±1.5	--

Semi-IPN hydrogel matrices F1-F4 was unable to meet our objective by sustaining TH dissolution. Contrarily, it accelerated TH dissolution. In case of hydrogel matrices F1-F4, TG was mixed with TH and CMTG and then triturated with the cross-linking solutions to get the granules. We can say, TG and CMTG co-exists inside the granules i.e. TG is intragranular. By slightly fabricating the matrix development method, TG will not be there inside the granules, but will be inside the matrix. In other words, TH and CMTG will be triturated with the cross-linking solutions as usual and upon completion of the granulation, TG will be added and homogenously blended with the granules and then compressed. In such case, TG will be extragranular (outside the granules) such that TG will form a fine thin coating on the dual cross-linked CMTG granules. Extragranular semi-IPN hydrogel matrices F5-F8 have been developed with the same formulae as that of intragranular semi-IPN matrices F1-F4, with the only difference that TG was not present inside the granules (intragranular) but present inside the matrix (extragranular). The extragranular TG matrix development technique makes the process a hybrid (combination) of wet granulation and direct compression technique of matrix development.

The *in vitro* TH dissolution from semi-IPN extragranular hydrogel matrices F5-F8 are depicted in Fig. 9.7. Substantial changes in TH dissolution pattern were perceived from semi-IPN extragranular hydrogel matrices F5-F8. Burst TH dissolution observed with matrices F1-F4, is significantly reduced (12%-26%) from semi-IPN extragranular hydrogel matrices F5-F8 ($p<0.05$). Elevation in the extragranular TG quantity in hydrogel matrices F5 (5% w/w), F6 (10% w/w), and F7 (15% w/w) significantly declined TH dissolution ($p<0.05$). However,

further increment in the extragranular TG quantity to 20%w/w (matrices F8), significantly expedited TH dissolution. TH dissolution from semi-IPN extragranular matrices F5-F8 changed in the following fashion: following 2 h in pH 1.2 acidic dissolution solution – F5 (24%)>F6 (21%)>F7 (18%)< F8 (39%) and after 10h of dissolution F5 (68%)>F6 (60%)>F7 (53%)< F8 (85%). The AUCs declined for the matrices F5-F7 and then significantly increased for F8 (Table 9.3) ($p<0.05$). Similarly, MDT values augmented the matrices F5-F7 and then significantly declined for F8 (Table 9.3) ($p<0.05$). The above dissolution pattern is elucidated as follows. In an aqueous media, a hydrophilic polymer absorbs water and begins to swell. The swollen polymeric layer is essentially a thick and viscous layer of the polymer formed by simple intermingling of the polymeric chains. As time elapses, the polymer absorbs more water, relaxation of the polymeric chains occurs and erosion of the polymeric chains at the surface initiates, facilitating further infiltration of dissolution media into the inner layers of the viscous network structure. This viscous network structure has sufficient mechanical strength to obstruct the ingress and egress of the water (dissolution medium). The polymeric layer viscosity is directly proportional to the polymer concentration. Increase in polymer solution concentration will raise its viscosity, thereby enhancing its barrier effect. In case of semi-IPN extragranular matrices F5-F8, TG is present as a thin uniform coating over the dual cross-linked TH-laden granules. This TG layer acts as a barrier which impedes the ingress and egress of the dissolution fluid to and fro from the TH-rich granules. With the elevation in TG concentration around the TH-rich granules, the TG polymeric layer viscosity augments, which amplifies its barrier effect. Analysis of viscosity of TG dispersions simulating the compositions of semi-IPN extragranular matrices F5-F8 indicated an augmentation in TG dispersion viscosity with the elevation in TG concentration (Fig. 9.8). Increase in viscosity of the coating layer declines the rate of inflow of the dissolution solution to the TH-rich granules and outflow of the dissolved TH from the granules to the bulk of dissolution solution. This is the reason behind decrease in TH dissolution with the elevation in TG concentration in matrices F5-F7. However, at an elevated TG concentration (20% w/w, F8), TH dissolution augments. Increase in TH dissolution from semi-IPN extragranular matrices F8 may be due to two reasons. Firstly, TG is progressively substituted with CMTG (where the overall ratio between cross-linking ions/total polymer are constant). Elevation in TG amount proportionally decreases the quantity of CMTG available to cross-link with the Ca^{2+} and Al^{3+} ions. In such situations, the cross-linking ions will be surplus of what is necessary for optimum cross-link. The surplus cross-linking ions would create channels inside the matrix, promoting rapid TH dissolution. Secondly, TG is very hydrophilic with a high water absorption capacity. The elevated TG

concentration changes the hydrodynamic condition of the matrix such that it favors the dissolution of the highly water soluble TH. Decline in burst TH dissolution from the semi-IPN extragranular matrices F5-F8 was because the matrices surface was almost devoid of TH and primarily composed of TG.

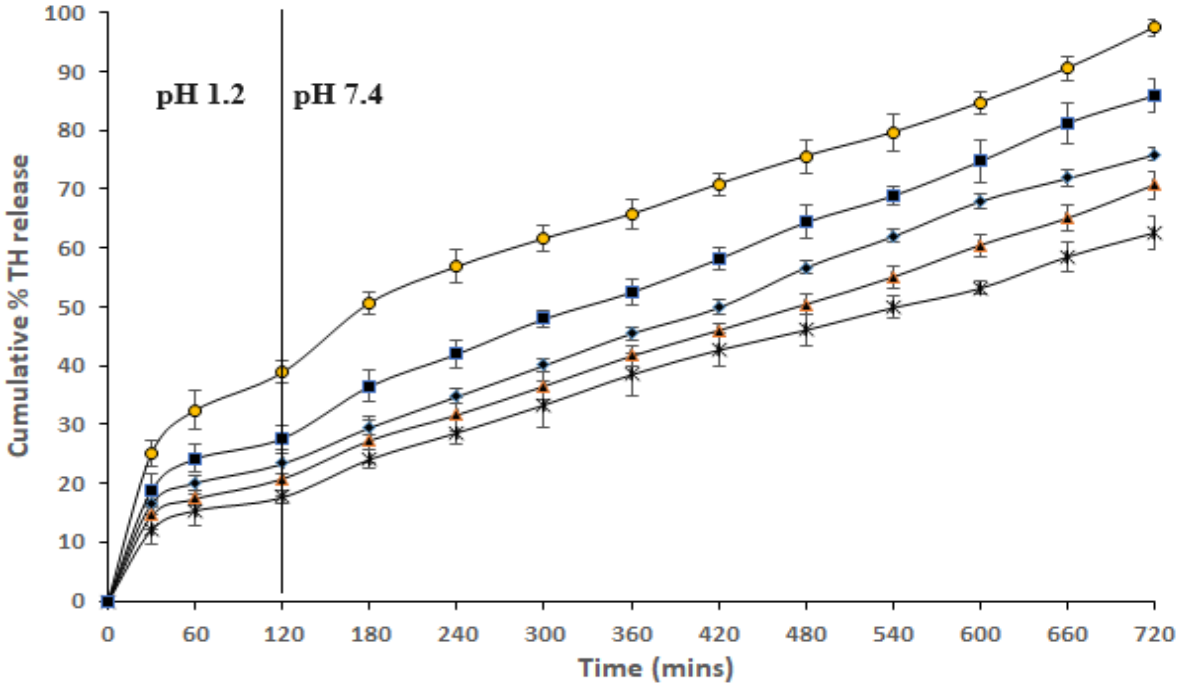

Fig. 9.7. TH dissolution from semi-IPN extragranular hydrogel matrices. F15 (■), F5 (♦), F6 (▲), F7 (✳), F8 (●).

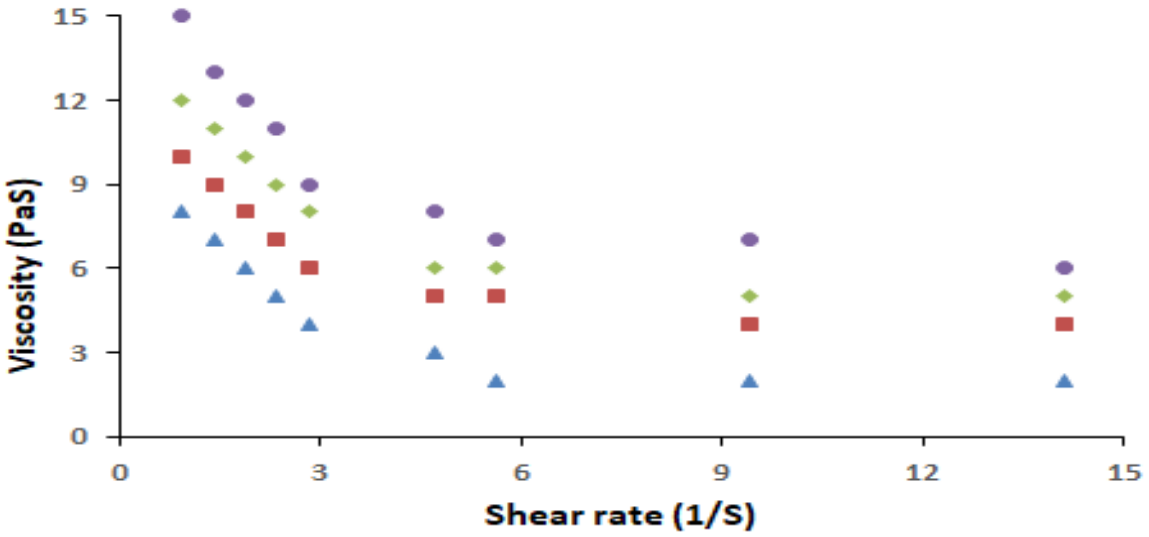

Fig. 9.8. TG dispersions viscosity mimicking matrices: F5 (▲), F6 (■), F7 (♦), F8 (●).

3.3 TH dissolution mechanism specifications

The drug dissolution data from a matrix (up to 60 %) is usually plotted to power law equation. Since our matrices gave burst TH dissolution within 30 min of dissolution, the dissolution data from 1 h to 60% TH dissolution was plotted in power law expression to get the TH dissolution mechanism. Prior research also testified plotting of dissolution data from 1 h to 60% drug dissolution associated with burst dissolution [2]. The TH dissolution from matrices F1-F8 obeyed Fickian diffusion (r^2 values 0.922-0.985) with release exponent (n) values less than 0.5 (Table 9.5). For water soluble drugs, the drug dissolution mechanism is controlled by diffusion [21]. The solvent penetration rate and solute diffusion through such systems is much greater than the polymer chain disentanglement/relaxation [21].

Table 9.5 Release mechanism specifications

Formulation code	Release exponent (n)	Kinetic constant (k)	Correlation coefficient (r^2)
F1	0.373	1.442	0.937
F2	0.341	1.482	0.922
F3	0.307	1.512	0.937
F4	0.392	1.519	0.991
F5	0.443	1.311	0.934
F6	0.490	1.241	0.961
F7	0.438	1.172	0.967
F8	0.392	1.508	0.985

3.4 *In vivo* pharmacokinetics study in rabbits

The pharmacokinetic specifications and plasma drug concentration-time curve following administration of oral TH solution and optimized hydrogel matrices (F7) administration are shown in Table 9.6 and Fig. 9.9. Differences in the pharmacokinetic parameters of the optimized hydrogel matrices and reference were significant statistically ($p<0.05$). The C_{max} in the reference group which were administered with TH oral solution was 141.17±7.76 ng/ml and that in test group administered with optimized hydrogel matrices F7 was 128.67±6.74 ng/ml. T_{max} of the reference was 2 h and the same in test group was 4.67±1.03h. The pharmacokinetic results (delayed T_{max} and lower C_{max}) of optimized hydrogel matrices indicate that it is able to prolong plasma TH concentration up to 24 h, compared to that of the oral TH

solution. The frequency of TH administration can be reduced by administering optimized hydrogel matrices.

The T_{max} and C_{max} also showed that the optimized hydrogel matrices had sustained-release characteristics than the oral TH solution. The $AUC_{0-\infty}$ and AUC_{0-24h} for the reference group was 967.95±124.79 ng.hr/ml and 766.99±100.90 ng.hr/ml respectively. The AUC_{0-24h} and $AUC_{0-\infty}$ for the test group was 3051.57±428.24 ng.hr/ml and 1424.04±89.53 ng.hr/ml respectively. The higher $AUC_{0-\infty}$ and AUC_{0-24h} of the optimized F7 hydrogel matrices was due to the sustained and slow TH dissolution and absorption. The higher $AUC_{0-\infty}$ and AUC_{0-24h} values also indicated the enhancement in bioavailability from the optimized F7 hydrogel matrices. The $t_{1/2}$ from the test and reference group was 15.98±2.32h and 5.67±0.78h respectively. The above pharmacokinetic data indicate that the reference group was devoid of any sustained TH dissolution effect while the test group exhibited sustained TH dissolution in the rabbit model. The values of C_{max}, $t_{1/2}$, and T_{max} from the test group abided the classical notion of SR dosage forms. The in vivo pharmacokinetic study demonstrated that the optimized hydrogel matrices produced sustained TH delivery and could decrease the TH dosage frequency.

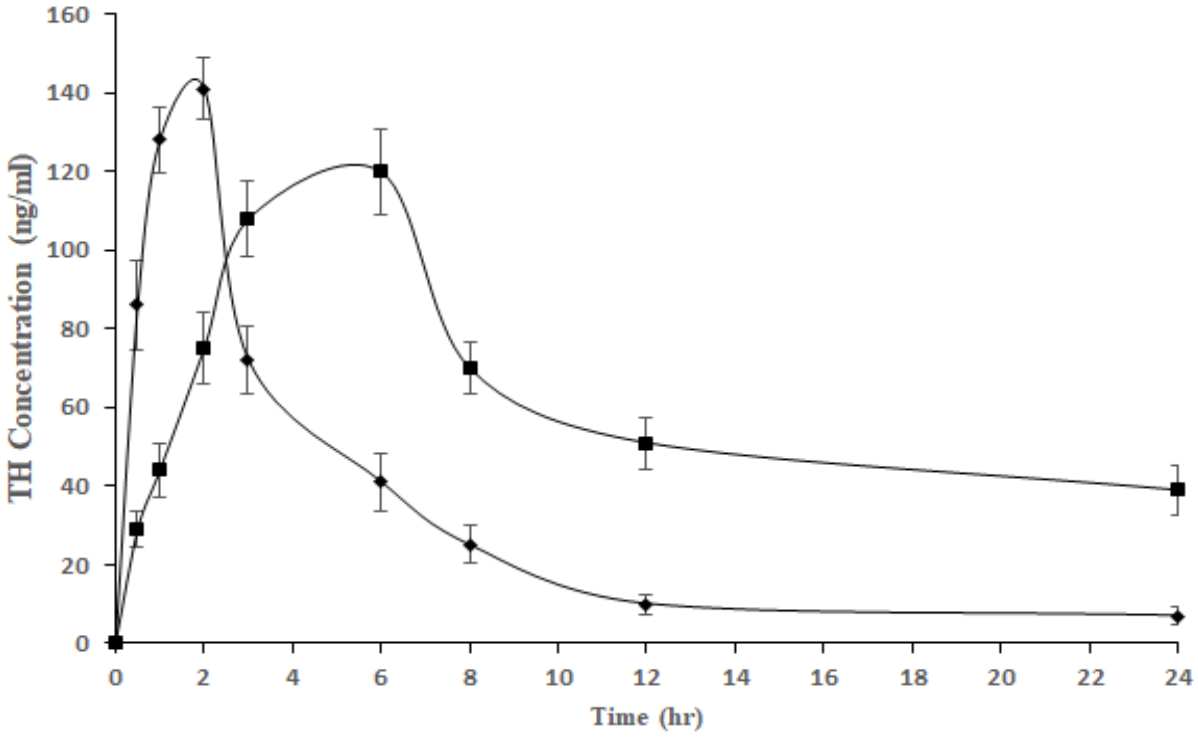

Fig. 9.9. TH Plasma concentration-time curve following oral administration of optimized final hydrogel matrices F7 (■) and oral TH solution (♦) to rabbit.

Table 9.6 Pharmacokinetic specifications

Pharmacokinetic parameters	Oral TH Solution	Optimized hydrogel matrix (F7)
tmax(hr.)	2.00±0.00	4.67±1.03
Cmax (ng/ml.)	141.17±7.76	128.67±6.74
AUC $_{0-\infty}$(ng.hr./ml.)	967.95±124.79	3051.57±428.24
AUC $_{0-24}$(ng. hr./ml.)	766.96±100.90	1424.04±89.53
$t_{1/2}$(hr.)	5.67±0.78	15.98±2.32
kel(hr.$^{-1}$)	0.124±0.016	0.044±0.006
Relative bioavailability	100%	185.67%

3.5 Accelerated stability study of the optimized semi-IPN hydrogel matrices

The accelerated stability study was conducted on the optimized semi-IPN hydrogel matrices F7. The matrices were kept at 40±2°C at RH 75±5% for 3 months. Following the accelerated stability studies, the matrices were checked for its hardness, friability, TH content and *in vitro* dissolution. Hardness of the tablets following the stability studies didn't deviate from the hardness of the original matrices and were found to be 4 kg/cm^2. Friability and TH content were the same as that of the original matrices (Table 9.7). The *in vitro* TH dissolution profiles of the matrices before and after the stability studies were almost same and the dissolution curves almost overlapped and merged (Fig. 9.10). The differences in the dissolution profiles were not reckoned significant ($p>0.05$). The accelerated stability studies indicted the stability of the developed hydrogel matrices under adverse storage conditions.

Table 9.7 Characterisation of hydrogel matrices before and after accelerated stability studies

Parameter		Before accelerated stability study	After accelerated stability study
Hardness		4 kg/cm^2	4 kg/cm^2
Friability		0.72 %	0.75 %
TH content		96.3 %	96.9 %
TH dissolution	2 h	18.71 %	17.29 %
	5 h	34.20 %	32.48%
	8 h	47.38 %	45.58 %

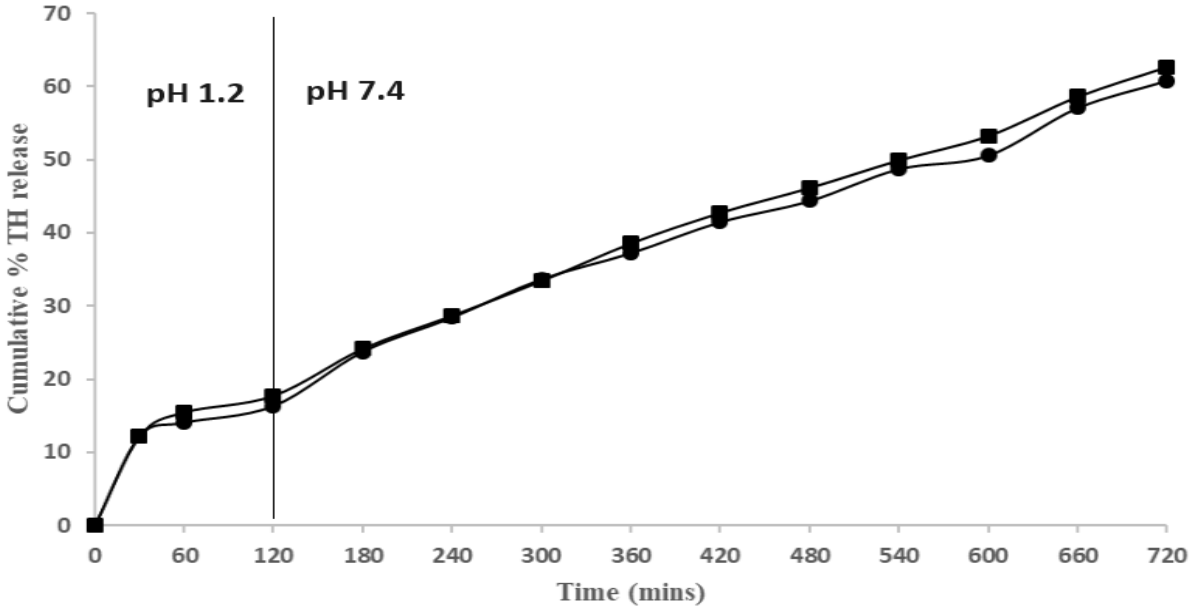

Fig. 9.10. TH dissolution comparison from optimized F7 matrices before and after accelerated stability study. Before stability study (■), after stability study (●).

3.6 Conclusion

Dual cross-linked semi-IPN hydrogel matrices of CMTG and TG were prepared for sustained gastrointestinal delivery of highly water soluble TH. FTIR, XRD, and DSC examination confirmed TH compatibility in the hydrogel matrices. TG was added to the dual cross-linked matrices with an objective to prolong TH dissolution from the matrices. TG was incorporated either within the granules (intragranular TG) or incorporated outside the granules but within the matrix (extragranular TG). Intragranular TG augments both swelling and erosion of the matrices and produces fast TH dissolution. Extragranular TG forms a thick viscous coating over the TH-rich granules to retard TH dissolution from the matrices. The in vivo pharmacokinetics of the optimized extragranular TG matrices revealed that the relative bioavailability from optimized matrices F7 was significantly more as compared to oral TH solution. The in vivo pharmacokinetic study also indicated that the optimized matrices produced sustained gastrointestinal TH dissolution.

References

1. Singh M, Shirazian S, Ranade V, Walker GM, Kumar A. Challenges and opportunities in modelling wet granulation in pharmaceutical industry – a critical review. Powder Technol. 2022;403:117380.

2. Singh R, Maity S, Sa B. Effect of ionic crosslink on the release of metronidazole from partially carboxymethylated guar gum tablet. Carbohydr. Polym. 2014;106:414–421.

3. Maity S, Sa B. Ca-carboxymethyl xanthan gum mini-matrices: swelling, erosion and their impact on drug release mechanism. Int. J. Biol. Macromol. 2014;68:78–85.
4. Giri TK, Thakur D, Alexander A, Badwaik H, Ajazuddin, Tripathy M, Tripathi DK. Biodegradable IPN hydrogel beads of pectin and grafted alginate for controlled delivery of diclofenac sodium. J. Mater. Sci. Mater. Med. 2013;24:1179–1190.
5. Ray R, Maity S, Mandal S, Chatterjee TK, Sa B. Development and evaluation of a new interpenetrating network bead of sodium carboxymethyl xanthan and sodium alginate for ibuprofen release. Pharmacol. Pharm. 2010;1:9–17.
6. Nochos A, Douroumis D, Bouropoulos N. In vitro release of bovine serum albumin from alginate/HPMC hydrogel beads. Carbohydr. Polym. 2008;74:451–457.
7. Reddy OS, Subha MCS, Jithendra T, Madhavi C, Rao KC. Fabrication and characterization of smart karaya gum/sodium alginate semi-IPN microbeads for controlled release of D-penicillamine drug. Polym. Polym. Compos. 2021;29(3):163–175.
8. Agnihotri SA, Aminabhavi TM. Novel interpenetrating network chitosan- poly (ethylene oxide-g-acrylamide) hydrogel microspheres for the controlled release of capecitabine. Int. J. Pharm. 2006;324:103–115.
9. Korsmeyer RW, Gurney R, Doelker E, Buri P, Peppas NA. Mechanisms of solute release from porous hydrophilic polymers. Int. J. Pharm. 1983;15:25–35.
10. M¨ockel JE, Lippold BC. Zero-order drug release from hydrocolloid matrices. Pharm. Res. 1993;10:1066–1070.
11. Kotta S, Bijumol C, Anith Y, Dileep KJ, Valsala K. Design, development and in vitro-in vivo study of tramadol-paracetamol inlay tablets. Pharm. Dev. Technol. 2012;19(1):1–9.
12. European Medicines Agency. ICH Topic Q1 A (R2). Stability Testing of new Drug Substances and Products. August 2003.
13. Deb P, Singha J, Chanda I, Chakraborty P. Formulation development and optimization of matrix tablet of tramadol hydrochloride. Recent Pat. Drug Deliv. Formul.2017;11:19–27.
14. Hartman M, Trnka O, Sÿolcova O. Thermal decomposition of aluminum chloride hexahydrate. Ind. Eng. Chem. Res. 2005;44:6591–6598.
15. Fernandes RA, Garcia-Rojas EE. Effect of cosolutes on the rheological and thermal properties of Tara gum aqueous solutions. J. Food Sci. Technol. 2021;58:2773–2782.
16. Maity S, Sa B. Development and evaluation of Ca^{+2} ion cross-linked carboxymethyl xanthan gum tablet prepared by wet granulation technique. AAPS Pharm. Sci. Tech. 2014;15(4):920–927.

17. Agnihotri SA, Aminabhavi TM. Novel interpenetrating network chitosan- poly (ethylene oxide-g-acrylamide) hydrogel microspheres for the controlled release of capecitabine. Int. J. Pharm. 2006;324:103–115.
18. Mukherjee K, Dutta P, Badwaik HR, Saha A, Das A, Giri TK. Food industry applications of Tara gum and its modified forms. Food Hydrocoll. Health. 2023;3:100107.
19. Ma Q, Wang L. Preparation of a visual pH-sensing film based on tara gum incorporating cellulose and extracts from grape skins. Sensors Actuators B Chem. 2016;235:401–407.
20. Bulut E. Development and optimization of Fe^{3+}-crosslinked sodium alginate-methylcellulose semi-interpenetrating polymer network beads for controlled release of ibuprofen. Int. J. Biol. Macromol. 2021;168:823–833.
21. Bruschi ML. Strategies to Modify the Drug Release From Pharmaceutical Systems. ed. Elsevier Ltd. Amsterdam. Netherlands. 2015.

Chapter 10: Summary and conclusion

1. **Summary**

Oral delivery is probably the most acceptable and favourable mode of drug delivery. The reason for such popularity is its non-invasiveness, self-administration, and low cost. This leads to high patient acceptability. Approximately 90% of all medications provided for a systemic effect are taken orally. The dosage forms for oral delivery of drugs primarily includes tablets, capsules and various liquid formulations. The tablets dosage form is one of the most preferred dosage form both by physicians and patients. Tablets are unit dosage forms where one unit of the dose is accurately loaded, which minimizes any error of administering the right dose of the drug. The tablet dosage form thus offers the minimum content variability and highest dose accuracy. Additionally, the cost of tablets is the lowest of all solid dosage form, and they are the compact and lightest of all oral dosage forms. Lastly, tablets are the most suited for large scale production with minimum tableting infrastructure among all unit oral forms.

The tablet dosage form when taken orally, first disintegrates to release the granules. The drug from the granules then solubilizes in the gastrointestinal medium, which is then absorbed and the drug reaches in the blood circulation. Since the total amount of drug is exposed in the gastrointestinal medium and is available for absorption, the rate and amount of drug absorption increases exponentially and the blood drug concentration steadily increases with time. As the blood drug concentration attains a certain concentration, the therapeutic onset of drug action takes place. Gradually with time the plasma drug concentration increases to attain the maximum drug plasma concentration. After the maximum plasma concentration, the blood drug concentration starts to decline. So far the drug concentration is above the minimum effective concentration, the therapeutic effect of the drug persists, after which the drug therapeutic effect terminates.

If it is necessary to keep a sustained therapeutic plasma level of drug between the medication intervals, then a greater drug dose has to be dispensed. This higher drug dose may produce inordinately high and often toxic drug levels for significant periods. For attenuating toxic manifestations due to high drug levels, the dose of the drug has to be reduced. This may, on the other hand, produce plasma levels of the drug which for much of the period of treatment will remain below the threshold efficacy. In either case, the fraction of administered dose utilized by the patient is depressingly small amount. Maximum availability of the drug from drug delivery systems utilizing minimum amounts of the drugs can be achieved by repeated administration of small increments of the total dose. However, uninterrupted dispensing of the drugs by conventional delivery systems is both impractical and impossible. Repeated administration of the drug may also be associated with chronic side effects of the drug. The

cost of therapy also escalates and all these factors contribute towards poor patient compliance and acceptability.

Thus, the conventional tablet dosage form has the following limitations. The blood drug concentration (i.e. the site of drug action) varies over subsequent dosing intervals even at the "steady state" situation. It is difficult to sustain a fixed therapeutic drug concentration at plasma for the duration of treatment. The variations in the plasma drug concentrations may result in an under or over medicated patient for periods of time. Frequent dosing for the drugs having shorter biological half-lives are necessary to maintain steady state plasma concentration within the therapeutic limits. For such drugs, maintaining therapeutic plasma concentration is dependent to the consequences of the overnight no dose period and missed doses. The regimens requiring frequent administration of conventional dosage form leads to patient non-compliance. This is an important reason behind therapeutic failure or inefficiency.

The problems associated with the conventional tablet dosage form can be overcome with modified release drug delivery systems. The sustained release form achieves the slow release of the medication over a prolonged duration after administration a single drug dose. The sustained release forms immediately release a drug dose to achieve the minimum plasma therapeutic concentration and then maintain the same for a long duration. The sustained release forms reduce variations of plasma drug levels, frequency of drug administration, adverse effects, and overall therapy cost. All these factors contribute towards enhanced patient conformity and convenience.

Matrix tablets are prominent oral sustained release drug delivery systems because of their high level of reproducibility, simplicity, stability of the dosage forms and easy to scale-up, manufacturing, and process validation. Scientific progress in the field of matrix tablet formulations have made sustained release product formulation easier, simpler, and improved. Matrix technologies are able to deliver a wide range of drugs with divergent biopharmaceutical and physicochemical properties. The basic components of a sustained release matrix tablet include the drug, matrix former (release controlling agent), release modifiers (wicking agents, channelling agents etc), and lubricants and flow aiding agents. The matrix materials or the release controlling agents may be lipid matrices, insoluble polymer matrices, and hydrophilic colloidal matrices.

Polysaccharides are the most widely available polymers and can be obtained from algal, plant and animal sources. Polysaccharides consists of monosaccharide units linked together by glycosidic bonds. They are carbohydrates having great number of sugar molecules covalently interconnected by glycosidic bonds. They can be non-ionic (like tara gum, xanthan gum),

cationic (like chitosan) and can also be anionic (like sodium alginate, pectin). The polysaccharide can also be of plant origin (tara gum), animal origin (chitosan), and algal origin (alginate). Natural polysaccharides have been extensively used to develop sustained release matrix tablets owing to their biocompatibility, easy availability, non-toxicity and wide regulatory acceptance. Different hydrophilic polysaccharides like xanthan gum, guar gum, sodium alginate, gellan gum have been successfully used as matrix materials for sustained delivery of drugs.

Drug dissolution from a natural hydrophilic polysaccharide matrix is generally dictated by the erosion, swelling, and viscous nature of the concerned polysaccharide. Drug solubilization from such matrixes can be tailored by controlling the viscosity, erosion and swelling of the polysaccharide. Crosslinking of the polysaccharide polymeric chains is a simple procedure to control the viscosity, erosion and swelling of the polysaccharide and thus to monitor the drug release from the hydrophilic polysaccharide matrix. Cross-linking can ionic or chemical. Chemical cross-linking of the polysaccharide polymer chains involves the use of harmful chemical reagents like glutaraldehyde, tripolyphosphate, and is thus not recommended. Ionic crosslink can be done under mild aqueous conditions by use of metal cations like Ca^{2+}, Ba^{2+}, Al^{3+}, Fe^{3+}. Ionic crosslink of natural polysaccharide chains is thus advocated.

Natural polysaccharides as matrix materials for sustained delivery of drugs have been extensively exploited. But they suffer from some drawbacks. Natural polysaccharides are prone to microbial contaminations, varying physicochemical properties, batch-to-batch variations and possibility of heavy metal contaminations. More importantly, the aqueous solubility, uncontrolled rate of hydration and swelling, and rapid matrix erosion and degradations inhibit the natural polymers from becoming an effective matrix material.

The polysaccharide polymeric chains have diverse chemical compositions and functional groups which lend themselves for various chemical derivatization. The derivatization of the polysaccharide polymeric chains can bypass the inherent problems of the polysaccharide and opens up for newer avenues of applications. Chemical derivatization of polysaccharides includes phosphorylation, sulfation, thiolation, carboxymethylation etc. Tailor made derivatives of the natural polysaccharides can be synthesised under simple and mild conditions. These tailored derivatives have been utilized in drug delivery and allied fields.

The derivatization of the natural polysaccharides are done to modify the physicochemical, rheological, and biological properties of the polysaccharides, to make them potential candidates as drug delivery carriers. The solubility and viscosity profiles, swelling and erosion

characteristics of the polysaccharides are fine-tuned according to the requirements of the drug delivery carriers by the chemical derivatization process.

Carboxymethylation is one of the most versatile and popular derivatization process. Carboxymethylation is done under mild alkaline aqueous environments and involves the incorporation of o-carboxymethyl groups in the polysaccharide polymeric chains. The hydroxyl groups of the polymers are substituted by the o-carboxymethyl groups during the reaction. Carboxymethylation imparts an anionic nature to the polysaccharide making it amenable to crosslink with divalent and trivalent metal ions and form water insoluble hydrogels, by a process known as ionotropic gelation. Ionotropic cross-linking of the polysaccharide polymeric chains is a suitable procedure for controlling the erosion, swelling, and drug delivery from the polysaccharide hydrogel matrix.

Tara gum (TG) is a seed endosperm galactomannan non-ionic polysaccharide obtained from caesalpinia spinose tree. TG backbone is primarily comprised of a linear main chain of (1–4)-β- d -mannopyranose units joined by (1–6) linkage with α- d -galactopyranose units. TG is a popular stabilizer and thickener in the food industry and is also used as edible films in food packaging industry. Grafted TG based superabsorbent hydrogels have also been synthesized. However, TG is highly hydrophilic and its rheological properties are not suited for the development of sustained release matrices. Carboxymethylation modifies the rheological, physicochemical, hydrophilic and swelling attributes of the natural polysaccharide. With this context, TG was derivatized to carboxymethyl TG (CMTG) by incorporating O-carboxymethyl groups in TG polymeric chains, with an anticipation to introduce ionic nature to TG making it amenable to cross-link with metal ions and also alter its swelling and hydrophilic characteristics.

Tramadol hydrochloride (TH), is a synthesized analgesic having both opioid and non-opioid characteristics. TH mainly works on the CNS. TH was sanctioned by the United States Food and Drug Administration (USFDA) for controlling, treating and mitigating modest to extreme pain in 1955. TH has structural similarities to morphine and codeine, but 10-times and 6000-times less potent than codeine and morphine respectively. It has a half-life of about 5.5 h and oral administration of 50 mg to 100 mg is required every 4-6 h. The daily maximum oral dose of tramadol is 400 mg. To reduce frequency of dosing, dose related side effects, and enhance patient compliance, sustained/controlled release of TH is necessary. Tramadol sustained/controlled release forms are documented in literature. Oral administration of tramadol sustained release tablets attains a bioavailability of 87% - 95%, compared with capsules. Long term treatment with tramadol produces satisfactory osteoarthritic, low back,

and post-operative pain management with minimum side effects and enhanced patient acceptability. Considering all the above factors, formulation of tramadol sustained release hydrogel tablets was undertaken.

Modification of TG to CMTG was performed in an alkaline milieu by reacting TG with MCA. The degree of substitution (DS) of the carboxymethylation reaction was determined. The carboxymethylation reaction was confirmed by ^{13}C solid state NMR and FTIR studies. XRD, DSC analysis of CMTG was performed. The DS of optimized CMTG was 0.84. The ^{13}C spectra of TG displayed three specific absorption signals at δ = 62.10 ppm for C6 carbon of the mannose unit, δ = 72 ppm for merging of signals of mannan carbon atoms at 2, 3, 4, and 5 position, and δ = 101.70 ppm for C1 mannan carbon atom. The solid state ^{13}C spectra of the CMTG revealed three extra signals at δ = 179.1, 169.2, and 167ppm, representing the carbonyl atom of the carboxymethyl groups at 6-O, 3-O, and 2-O positions respectively. The appearance of the three additional signals in the spectra of CMTG confirms the carboxymethyl reaction at all three locations. The IR spectrum of TG showed a wide peak at 3303 cm^{-1} representing the stretching of the OH moieties of the gum. The peak intensity at 3303 cm^{-1} in the IR spectrum of CMTG appears to be of diminished intensity indicating that the OH groups are substituted with the carboxymethyl groups, ascertaining the insertion of the carboxymethyl groups onto TG structure. Moreover, CMTG displayed characteristics absorption peaks at 1591 cm^{-1} signifying the COO^- asymmetric stretching. Spectrums at 1414 cm^{-1} and 1321 cm^{-1} stands for symmetric stretching of COO^-. These peaks were not present in the IR spectrum of TG. The occurrence of the extra new peaks in the spectrum of CMTG indicated that the OH groups of TG are substituted by the carboxymethyl moieties. The XRD trace of TG indicates its amorphous nature. The XRD pattern of CMTG also seems like an amorphous hallow, except the appearance of twin intense peaks of intensities 877cps and 484cps at diffraction 2θ 31.68º and 45.40º respectively. The presence of the two intense peaks in the XRD pattern of CMTG highlighted the slight improvement in crystallinity of TG after the carboxymethylation reaction. The thermogram of TG is characterised by the presence of an expanded endotherm at 69ºC assignable to the loss of water from the polymer sample. An exotherm at 306ºC indicates the thermal decomposition or degradation of the gum. The DSC curve of CMTG displayed an expanded endothermic event between temperature 70ºC and 120ºC. This event represents water loss from CMTG sample. A second exothermic event for CMTG appeared at 259ºC signifying the thermal decomposition or degradation of CMTG. Comparison of the thermal events of the TG and CMTG highlights that the decomposition temperature of CMTG is lower compared to TG.

The synthesised gum was evaluated for sub chronic oral toxicity to gather some knowledge about the health risks that may happen following oral intake of the gum. As per the outcomes of the sub chronic oral toxicity study, it can be concluded that the synthesized CMTG was bereft of any suggestive feature of haematological toxicity, behavioural toxicity, hepatotoxicity and nepherotoxicity in any dose group. Nil lethality in all the dose groups pointed out that the LD_{50} of CMTG is above 2000mg/kg. According to the GHS, if the LD_{50} value is higher than 2000 mg/kg dose, then the sample under investigation will fall under "category 5" and the toxicity will be rated "zero". Therefore, CMTG falls under "category 5" with "zero" toxicity rating.

Following synthesis, optimization and characterisation of CMTG, aluminium and/or calcium cross-linked CMTG hydrogel matrices were developed by wet granulation method. The weight percentage of the aluminium and calcium ions were varied from 0-12% and 0-15% w/w of the matrices respectively. The impact of the cross-linking ions on the erosion, swelling and *in vitro* TH release from the matrices have been explored. Aluminium and calcium cross-linked CMTG matrices swelled immediately to various extents in pH 1.2 acid solution, and subsequently the swelling progressively reduced demonstrating mass loss (erosion) of the matrices. Uncross-linked CMTG matrices swelled 381% after 2 h in pH 1.2 acid solution, thereafter the swelling gradually declined (194% after 8 h). The erosion of uncross-linked CMTG matrices showed an early burst erosion (34% at 2 h), following which the erosion gradually increased with time (69% at 8 h). $AlCl_3$ incorporation in the hydrogel matrices changed the erosion and swelling characteristics of the matrices substantially. Accentuating $AlCl_3$ concentration in the hydrogel matrices from 3-9% w/w declined the erosion and swelling characteristics. But, further elevation in $AlCl_3$ concentration to 12% w/w stimulated the matrix erosion, although the swelling declined. Reduced water intrusion velocity through the thick polymeric or gel-like matrices was the cause of fall in swelling rate of the hydrogel matrices with the rise in $AlCl_3$ concentration. Elevation in the $AlCl_3$ amount in the matrices effected the decline of water intrusion velocity. The stiff hydrogel layer slowed down matrix dissolution and decrease in the percentage erosion of the hydrogel matrices with the rise in the $AlCl_3$ concentration. Like aluminuim ions, calcium ions also changed the erosion, swelling characteristics of the matrices substantially. Elevation in the Ca^{2+} ions concentration in the hydrogel matrices from 3-12% w/w declined the erosion and swelling. But additional rise in the Ca^{2+} ions concentration to 15% w/w escalated the matrix erosion, however the swelling declined. Like Al-CMTG matrices, the water intrusion velocity declined through the calcium cross-linked dense and viscous hydrogel layer, resulting in decline in swelling of the matrices. The fall in erosion was

attributable to the development of firm hydrogel layer with lesser matrix dissolution rate. Calcium and aluminium cross-linked CMTG matrices swelling kinetics followed Fickian diffusional kinetics.

The *in vitro* TH dissolutions from uncross-linked, and aluminium or calcium cross-linked CMTG matrices revealed the significant impact that the cross-linking ions had on the TH release behaviour. Matrices formulated with CMTG only liberated 46% and 96% of TH at 2 h and 8 h respectively. Aluminium ion cross-linking of the CMTG matrices significantly changed the TH dissolution pattern. Increase in $AlCl_3$ concentration in the matrices from 3% w/w to 9% w/w decreased the TH dissolution rate. However, elevation in the $AlCl_3$ amount to 12% w/w increased the TH dissolution rate significantly. The AUCs dropped with the increase in $AlCl_3$ concentration 3%-9% w/w of the matrices, and then again augmented at 12% w/w $AlCl_3$ concentration considerably. The MDT increased with the increase in $AlCl_3$ concentration 3%-9% w/w of the matrices, and then again declined at 12% w/w $AlCl_3$ concentration considerably. The TH dissolution characteristics was simultaneous with erosion, swelling characteristics of the hydrogel matrices. Similar results were observed for calcium cross-linked CMTG matrices. Increase in $CaCl_2$ concentration in the matrices from 3% w/w to 12% w/w decreased the TH dissolution rate. However, elevation in the $CaCl_2$ amount to 15% w/w increased the TH dissolution rate significantly. The AUCs dropped with the increase in $CaCl_2$ concentration 3%-12% w/w of the matrices, and then again augmented at 15% w/w $CaCl_2$ concentration considerably. The MDT increased with the increase in $CaCl_2$ concentration 3%-12% w/w of the matrices, and then again declined at 15% w/w $CaCl_2$ concentration considerably. The TH dissolution characteristics was simultaneous with erosion, swelling characteristics of the hydrogel matrices. Viscosity of solutions mimicking the compositions of different hydrogel matrices was also in accordance with the TH dissolution behaviour. Photographs of hydrogel matrices at different time intervals and SEM microimages of the hydrogel matrices also bolstered the TH dissolution behaviour.

The TH dissolution from optimised single cross-linked hydrogel matrices containing 9% w/w $AlCl_3$ was compared with a marketed commercial tablet TRD-CONTIN® (TH 100 mg). TH dissolution from optimised single cross-linked hydrogel matrices and commercial tablet in pH 1.2 acid media almost overlapped and merged with each other and difference was not significant. However, TH dissolution from optimised single cross-linked hydrogel matrices and marketed commercial tablet in pH 7.4 buffer media was reckoned significant. TH dissolution from optimized optimised single cross-linked hydrogel matrices was more sustained and

slower as compared to marketed tablet in pH 7.4 buffer media. Thus, the developed matrices had a better sustained dissolution pattern as compared to the marketed commercial tablet.

Al-CMTG matrices containing 9% w/w $AlCl_3$ and Ca-CMTG matrices containing 12% w/w $CaCl_2$ gave the most sustained TH dissolution form the matrices. Development of dual cross-linked (containing both Al^{3+} and Ca^{2+}) hydrogel matrices was done at the already optimized concentrations of the cross-linking ions. TH dissolution from CMTG hydrogel matrices cross-linked with different weight ratios of Ca^{2+} and Al^{3+} ions (where the overall cross-linking ion concentrations was maintained at 9% w/w of the matrices) demonstrated that increase in the weight percentage of Ca^{2+} ions in the matrices expedited TH dissolution from the matrices. TH dissolution from CMTG hydrogel matrices cross-linked with different weight ratios of Ca^{2+} and Al^{3+} ions (where the overall cross-linking ion concentrations was maintained at 12% w/w of the matrices) demonstrated that increase in the weight percentage of Al^{3+} ions in the matrices slowed down TH dissolution from the matrices. The dual cross-linked hydrogel matrices where the overall cross-linking ion concentrations was 12% w/w of the matrices, and weight ratio between Al^{3+} and Ca^{2+} ions was 1:1 gave the most sustained TH dissolution releasing 75% TH after 10 h of dissolution.

With the purpose to further prolong TH dissolution from the matrices, TG was incorporated to the optimized dual cross-linked hydrogel matrices. Accordingly, semi-IPN hydrogel matrices of CMTG and TG have been prepared. The erosion, swelling, and TH dissolution from the semi-IPN matrices have been investigated. Keeping all the variables (ratio between Al^{3+}/Ca^{2+} ions and polymer: cross-linker) of the dual cross-linked hydrogel matrices constant, CMTG was progressively substituted with TG in the matrices. Weight percentage of TG was 5% w/w, 10% w/w, 15% w/w, and 20% w/w of the total polymer. Incorporation of TG onto the dual cross-linked matrices produced substantial changes in the in vitro TH dissolution profile. TH dissolution progressively augmented with the elevation in the TG weight percentage in the matrices. MDT and AUCs progressively increased with the elevation in the TG weight percentage in the matrices. This was due to the elevation in the swelling and erosion characteristics of the semi-IPN matrices.

Semi-IPN hydrogel matrices was unable to meet the objective of sustaining TH dissolution. Contrarily, it accelerated TH dissolution. By slightly fabricating the matrix development method, TG was not incorporated inside the granules, but incorporated inside the matrix. In other words, TH and CMTG was triturated with the cross-linking solutions as usual and upon completion of the granulation, TG was added and homogenously blended with the granules and then compressed. In such case, TG was extragranular (outside the granules) such that TG

will form a fine thin coating on the dual cross-linked CMTG granules. Substantial changes in TH dissolution pattern were perceived from semi-IPN extragranular hydrogel matrices. Burst TH dissolution observed with all previously developed hydrogel matrices, is significantly reduced from semi-IPN extragranular hydrogel matrices. Elevation in the extragranular TG quantity in hydrogel matrices 5% w/w, 10% w/w, and 15% w/w significantly declined TH dissolution. However, further increment in the extragranular TG quantity to 20%w/w, significantly expedited TH dissolution. This was due to the formation of thick and highly viscous coating over the TH-rich granules, which hindered TH dissolution from the matrices. However, at an elevated TG concentration (20% w/w), TH dissolution augments. This was due to the imbalance created between the ratio of CMTG and the cross-linking ions and also due to change in the hydrodynamic condition of the matrix. Decline in burst TH dissolution from the semi-IPN extragranular matrices was because the matrices surface was almost devoid of TH and primarily composed of TG. The TH dissolution from matrices obeyed Fickian diffusion (R^2 values 0.922-0.985) with release exponent (n) values less than 0.5.

The pharmacokinetic specifications and plasma drug concentration-time curve following administration of oral TH solution and optimized hydrogel matrices have been investigated. The in vivo pharmacokinetic study demonstrated that the optimized hydrogel matrices produced sustained TH delivery and could decrease the TH dosage frequency.

The accelerated stability study was conducted on the optimized extragranular semi-IPN hydrogel matrices containing 15% w/w of TG in the matrices. The matrices were kept at 40±2°C at RH 75±5% for 3 months. Following the accelerated stability studies, the matrices were checked for its hardness, friability, TH content and in vitro dissolution. Hardness, friability and TH content of the tablets following the stability studies didn't deviate from the hardness, friability and TH content of the original matrices. The in vitro TH dissolution profiles of the matrices before and after the stability studies were almost same and the dissolution curves almost overlapped and merged. The accelerated stability studies indicted the stability of the developed hydrogel matrices under adverse storage conditions.

2. Conclusion

In this research work, we synthesised and characterised CMTG. The synthesised CMTG had a DS of 0.84 and the synthesis was ascertained by FTIR, ^{13}C solid state NMR, XRD and DSC studies. The synthesised CMTG was cross-linked with either Al^{3+} and Ca^{2+} ions or with both Al^{3+} and Ca^{2+} ions to develop hydrogel matrices. It was observed that the cross-linking ions had a significant impact of the swelling, erosion and TH dissolution from the hydrogel matrices. Elevation in the concentration of the cross-linking ions significantly retarded TH

dissolution, swelling and erosion of the matrices. It was also observed that Al^{3+} ions had a greater impact on the hydrogel matrices compared to Ca^{2+} ions. At the same concentration of the cross-linking ions, retardation of swelling, erosion, and TH dissolution for the hydrogel matrices was more pronounced in case of Al^{3+} ions. When the overall concentration of the cross-linking ions was held constant and the amount of Al^{3+} and Ca^{2+} ions was varied, it was observed that elevation in the concentration of the Al^{3+} ions sustained TH dissolution, and the reverse pattern was observed with the Ca^{2+} ions. In this research work we also reported the development of a novel, one of its kind hydrogel matrix development process, which is a combination of both direct compression and wet granulation method of tablet preparation. TG was added to the hydrogel matrices in two ways. It was incorporated within the granules (intragranlar TG) or within the matrices (extragranular TG). The development of the extragranular TG hydrogel matrices made the process a combination of both direct compression and wet granulation method of tablet preparation. Intragranular TG accelerated TH dissolution, while extragranular TG retarded TH dissolution. In vivo pharmacokinetic studies confirmed the sustained release properties of the extragranular TG hydrogel matrices. Finally, accelerated stability studies indicted the stability of the hydrogel matrices under adverse storage conditions.

Annexures

TAAB BIOSTUDY SERVICES
69, IBRAHIMPUR ROAD, 1ST FLOOR, FLAT NO. 1A, JADAVPUR, KOLKATA-700032
Telefax : (033) 2499-0628, Mobile : 098300 36297 / 098304 66363
E-mail : taab_bio@yahoo.com, Website : www.taabbiostudy.com

Institutional Animal Ethics Committee

TAAB BIOSTUDY SERVICES

69, IBRAHIMPUR ROAD, FLAT 1A,

JADAVPUR, KOLKATA – 700032

INSTITUTIONAL ANIMAL ETHICS COMMITTEE

TAAB Biostudy Services, 69 Ibrahimpur Road, Jadavpur, Kolkata – 700 032

Study No: PKS (Rbt) CMTG 0117

Date: 01.02.2023

The members of the **Institutional Animal Ethics Committee (IAEC)** have scrutinized the various aspects of the protocols for carrying out following study on **Rabbits** and have approved the same to be performed at the Animal House of TAAB Biostudy Services, Kolkata – 700 032.

Study Title:

"**Comparative Randomized Cross Over Oral Bioavailability Study of Tramadol Test Drug of 9 mg by Using Reference Raw Drug of Tramadol 9 mg in 12 Rabbits**"

Anirbandeep Bose

Dr. Anirbandeep Bose
Chairperson, Institutional Animal Ethics Committee
Registration No. 1938/PO/Rc/S/17/CPCSEA

TAAB BIOSTUDY SERVICES
69, IBRAHIMPUR ROAD, 1ST FLOOR, FLAT NO. 1A, JADAVPUR, KOLKATA-700032
Telefax : (033) 2499-0628, Mobile : 098300 36297 / 098304 66363
E-mail : taab_bio@yahoo.com, Website : www.taabbiostudy.com

Institutional Animal Ethics Committee

TAAB BIOSTUDY SERVICES

69, IBRAHIMPUR ROAD, FLAT 1A,

JADAVPUR, KOLKATA – 700032

INSTITUTIONAL ANIMAL ETHICS COMMITTEE

TAAB Biostudy Services, 69 Ibrahimpur Road, Jadavpur, Kolkata – 700 032

Study No: TOXSC (R) CMTG 0117

Date: 013.01.2023

The members of the **Institutional Animal Ethics Committee (IAEC)** have scrutinized the various aspects of the protocols for carrying out following study on **Rats** and have approved the same to be performed at the Animal House of TAAB Biostudy Services, Kolkata – 700 032.

Study Title:

"SUB CHRONIC (28 DAYS) ORAL TOXICITY STUDY OF CARBOXYMETHYL TARA GUM (CMTG) IN RATS"

Anirbandeep Bose

Dr. Anirbandeep Bose
Chairperson, Institutional Animal Ethics Committee
Registration No. 1938/PO/Rc/S/17/CPCSEA

International Journal of Biological Macromolecules 232 (2023) 123448

Contents lists available at ScienceDirect

International Journal of Biological Macromolecules

journal homepage: www.elsevier.com/locate/ijbiomac

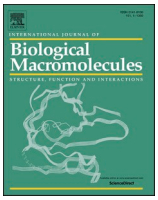

Al^{3+}/Ca^{2+} cross-linked hydrogel matrix tablet of etherified tara gum for sustained delivery of tramadol hydrochloride in gastrointestinal milieu

Kaushik Mukherjee, Pallobi Dutta, Tapan Kumar Giri *

Department of Pharmaceutical Technology, Jadavpur University, Kolkata 700032, West Bengal, India

ARTICLE INFO

Keywords:
Carboxymethyl tara gum
Sustained delivery
Hydrogel
Matrix tablets
Tramadol hydrochloride

ABSTRACT

Tara gum (TG) was derivatized to carboxymethyl TG (CMTG) and then cross-linked with Al^{3+}/Ca^{2+} ions to prepare Al/Ca cross-linked CMTG matrices for sustained delivery of Tramadol Hydrochloride (TH), a highly water-soluble drug. The effect of Al^{3+}/Ca^{2+} ions concentration on swelling, erosion, and drug release behavior from Al/Ca-CMTG matrices was investigated. Al-CMTG matrices had greater cross-linking density, produced a more rigid and denser hydrogel layer than Ca-CMTG matrices. The rate of swelling, erosion, and in vitro drug release from Al-CMTG matrices was slower than from Ca-CMTG matrices. The most important finding of our study indicated that at the same concentration of cross-linking ions, the release of TH from Al-CMTG matrices was slower compared to Ca-CMTG matrices. The optimized formulation containing 9 % *w*/w $AlCl_3$ in CMTG matrices released TH in a sustained manner up to 12 h in the gastrointestinal milieu. Moreover, it was observed that the prepared optimized formulation exhibited a more sustained release of TH compared to the marketed product.

1. Introduction

Matrix materials based on natural polysaccharides have been widely utilized for the development of modified release tablets because of their non-toxicity, biodegradability, biocompatibility, and broad regulatory acceptance [1–3]. In this context, various hydrophilic polysaccharides like sodium alginate, xanthan gum, grewia gum, chitosan, tragacanth gum, etc. were effectively utilized as matrix materials for drug delivery [4–15]. These hydrophilic polysaccharides have the unique ability to hydrate and swell upon contact with water forming a thick viscous gel layer around the surface of matrix tablets. Drug release from such swollen and viscous gel layer is mainly by diffusion of drug particles and sometimes through erosion of the polymeric matrix. Drug release from water-insoluble polymers is generally due to the erosion of the polymeric matrix, while diffusion is the main process of drug release for hydrophilic polymers [16–20]. The overall process of drug release may be either erosion or diffusion or a fusion of both, although one process may prevail over the other [21]. The relationship between viscosity, diffusion, erosion, and drug release has been well documented in the literature [22]. Thus viscosity, swelling, and erosion of the polymeric gel layer plays a pivotal role in the drug release mechanism, and controlling such factors will be crucial to get the desired drug release pattern from the matrices.

Cross-linking is a simple procedure for controlling the swelling and erosion of hydrophilic polymeric matrices and controlling the rate of drug release from the matrices [22]. Polysaccharides with a net negative charge have been used to cross-link with metal cations and control the swelling, erosion, and drug release characteristics from the matrices. Literature reports similar investigations on drug release behavior from calcium cross-linked pectinate and alginate matrices and also aluminium cross-linked carboxymethyl cellulose matrices [23–25]. The non-ionic polysaccharides have been derivatized by simple modification of their functional groups to make them anionic. Carboxymethylation is one of such modification technique through which anionic *O*-carboxymethyl groups can be introduced to the polysaccharide chains to make them amenable to cross-link with metal ions [26]. In this context, xanthan gum and guar gum have been carboxymethylated and cross-linked with calcium ions [21,22]. Drug release, swelling, and erosion behavior from such calcium cross-linked carboxymethyl guar and xanthan gum matrices have been investigated.

Tara gum (TG) is a non-ionic galactomannan polysaccharide derived from the seed endosperm of the *Caesalpinia spinosa* tree [27]. The primary backbone of galactomannan TG is made up of a linear β-D-mannose and β-D-galactose units which are connected by glycosidic

* Corresponding author.
E-mail address: tapan_ju01@rediffmail.com (T.K. Giri).

https://doi.org/10.1016/j.ijbiomac.2023.123448
Received 2 December 2022; Received in revised form 16 January 2023; Accepted 24 January 2023
Available online 26 January 2023
0141-8130/© 2023 Elsevier B.V. All rights reserved.

International Journal of Biological Macromolecules 253 (2023) 127176

Contents lists available at ScienceDirect

International Journal of Biological Macromolecules

journal homepage: www.elsevier.com/locate/ijbiomac

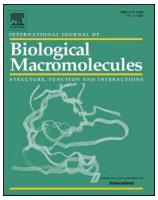

Effect of intragranular/extragranular tara gum on sustained gastrointestinal drug delivery from semi-IPN hydrogel matrices

Kaushik Mukherjee [a], Sukanta Roy [b], Tapan Kumar Giri [a,*]

[a] Department of Pharmaceutical Technology, Jadavpur University, Kolkata 700032, West Bengal, India
[b] Bioequivalence Study Center, TAAB Biostudy Services, Ibrahimpore Road, Kolkata 700032, India

ARTICLE INFO

Keywords:
Hydrogel matrix
Semi-IPN
Sustained release
tara gum

ABSTRACT

The present research was undertaken to develop semi-IPN hydrogel matrix tablets of tara gum (TG) and carboxymethyl TG (CMTG) for sustained gastrointestinal delivery of highly water soluble tramadol hydrochloride (TH). The matrix tablets were developed by a hybrid process of wet granulation and direct compression technique. Carboxymethyl TG was crosslinked with dual cross-linking ions (Al^{3+}/Ca^{2+}). The uncross-linked component of the semi-IPN matrix was either incorporated within the granules (intragranular TG) or incorporated outside the granules (extragranular TG), prior to compression. The effect of intragranular/extragranular TG on the swelling, erosion and TH release characteristics from the semi-IPN hydrogel matrix tablets was investigated. The key finding of the investigation indicated that intragranular TG expedited TH release, while extragranular TG sustained TH release. Moreover, the effect of cross-linking ions on viscosity, rigidity, cross-link density and TH release behavior from hydrogel matrices was investigated. In-vivo pharmacokinetic performance of the optimized extragranular TG semi-IPN hydrogel matrix (F15) indicated sustained TH release in gastrointestinal milieu.

1. Introduction

Hydrophilic natural polysaccharides have been widely used for delivery of drugs and pharmaceuticals because of their non-toxic, biodegradable and bio-safe characteristics [1]. The delivery agents may be matrix tablets, hydrogel beads, microparticles, bilayer tablets, and compression coated tablets [2–6]. Recently, formulation of hydrophilic matrix tablets has been illustrious with the publication of numerous research articles and patents and their application in new products [7]. The success of the hydrophilic matrix tablets may be attributed to its ease of processibility using the economical, simple and reproducible tablet manufacturing infrastructure [8]. Moreover, the versatility and robustness of the tablet manufacturing process gives an option to the formulation development scientist to fabricate the matrix development process for getting the desired drug dissolution characteristics from the matrix tablets. Additionally, the dissolution of drug from the matrices can also be modulated by adjusting the swelling, erosion, viscous nature, and hydrophilicity of the polysaccharide concerned [9,10].

Fabrication of the matrix development process for achieving the desired drug release characteristics has been studied [7]. Cross-linking of the polysaccharide polymeric chains as a tool for modulating the swelling, erosion and viscosity profiles of the polysaccharide has been widely used by researchers across the world [9,10]. Ionic (physical) crosslink of anionic polysaccharide polymeric chains by metal cations like aluminium, calcium, and barium ions for controlling the swelling, erosion, viscous nature, and hydrophilicity of the polysaccharide has been extensively investigated [2,9,10].

Again, when a single polymeric matrix is unable to meet the specific requirements of a drug delivery agent, the polymer blend technology has been effectively used to meet the specific requirements of a formulation [3]. Combination of two or more polymers have been used to achieve the tailor-made functional properties of the delivery agent like swelling, erosion, viscosity profiles and hydrophilicity of the polymeric matrix, and are thus beneficial to achieve the desired drug dissolution characteristics. In the presence of one another, when both polymers independently cross-link (interlink), they form an interpenetrating polymeric network (IPN) structure [11,12]. On the other hand, when one of the polymer is linear and the other is cross-linked, they form a semi-IPN network structure [13,14].

TG is a galactomannan seed endosperm polysaccharide extracted from *Caesalpinia spinosa* tree [15]. The rheological characterization, molecular and structural features of TG are available in literature

* Corresponding author.
E-mail address: tapan_ju01@rediffmail.com (T.K. Giri).

https://doi.org/10.1016/j.ijbiomac.2023.127176
Received 1 August 2023; Received in revised form 20 September 2023; Accepted 29 September 2023
Available online 30 September 2023
0141-8130/© 2023 Elsevier B.V. All rights reserved.

Food Hydrocolloids for Health 3 (2023) 100107

Contents lists available at ScienceDirect

Food Hydrocolloids for Health

journal homepage: www.elsevier.com/locate/fhfh

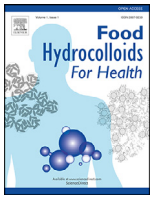

Food industry applications of Tara gum and its modified forms

Kaushik Mukherjee[a], Pallobi Dutta[a], Hemant Ramachandra Badwaik[b], Arpita Saha[a], Ankita Das[a], Tapan Kumar Giri[a,*]

[a] Department of Pharmaceutical Technology, Jadavpur University, Kolkata, West Bengal 700032, India
[b] Rungta college of Pharmaceutical Sciences and Research, Kurud Road, Kohka, Bhilai, Chhattisgarh 490023, India

ARTICLE INFO

Keywords:
Tara gum
Polysaccharide
Modification

ABSTRACT

Over the last few decades, a lot of investigations have been directed towards naturally occurring polymers because of their useful physicochemical properties. Among the naturally occurring polymers, the polysaccharides have received much attention in drug delivery and biomedical fields. Tara gum is one of such polysaccharides being widely explored in nutraceutical, pharmaceutical, and biomedical fields like protection of bioactives from environmental degradation, packaging of food materials, controlled release drug delivery systems, etc. The gum has also been suitably derivatized. Its modified forms have been explored in biomedical applications like superabsorbent polymers which find application in diapers, gardening, and agriculture in arid regions. However, summarizations of this progress are not available in the literature. This article thus aims to give a summary of the source, structural interpretation, and rheological analysis of the gum. The article also aims to furnish the depth of information available in the literature emphasizing the applications of the gum and its modified form in pharmaceutical and biomedical areas.

1. Introduction

The uses of natural polymers in pharmaceutical and allied industries have increased over the years (Badwaik et al., 2020). Natural polymers offer significant advantages over synthetic ones due to their nontoxicity, economical, easy availability, biosafety, biodegradability, and broad regulatory acceptance (Maity & Sa, 2014a). Among the natural polymers, polysaccharides are on focus by researchers across the world for their potential use in drug delivery, food packaging, agricultural and biomedical applications. Polysaccharides are widely prevalent in nature and can be of microbial (pullulan and curdlan gum), animal (hyaluronic acid and heparin), and plant (cellulose and locust bean gum) origin. These polysaccharides have various functional groups attached to their molecular chains and can be suitably utilized for various chemical and biochemical derivatizations (Mukherjee, Kundu & Sa, 2012). The different derivatization methods are insertion of functional groups (sulfation, thiolation, and etherification), covalent cross-linking with glutaraldehyde and epichlorhydrin, and ionic cross-linking with divalent and trivalent metal ions (Prajapati, Jani, Moradiya & Randeria, 2013). These derivatizations improve the functional properties of polysaccharides. Thus, the polysaccharides offer the researcher an advantage to tailor the polymer to meet the requirements of specific applications.

Several polysaccharides including xanthan gum, alginate, tamarind gum, pectin, guar gum (GG), gum acacia, tragacanth gum, and gum arabic have been derivatized and used in drug delivery systems and allied fields (Mandal, Basu & Sa, 2010; Singh, Maity & Sa, 2014; Maity & Sa, 2014b; Jana, Sharma, Maiti & Sen, 2016; Wei, Sun, Wu, Yin & Wu, 2006; Hassanzadeh-Afruzi, Heidari, & Maleki, 2022; Hassanzadeh-Afruzi, Maleki & Zare, 2022; Janani, Zare, Salimi & Makvandi, 2020). Additionally, these polysaccharides being hydrophilic in nature absorb and swell in water. The swelling and water absorption characteristics of these hydrophilic polysaccharides are dependent on the modification methods used. This enables the scientists to formulate various sustained and controlled release formulations wherein the release of the drug from the delivery devices can be controlled or triggered as per the need. With the advent of these obvious advantages, the naturally occurring polysaccharides find extensive applications as pharmaceutical adjuvants like emulsifying agents, thickening agents, suspending agents, binders, and film-forming agents (Femi-Oyewo, Adedokun & Olusoga, 2004; Ibrahim, Abo-Shosha, Allam & El-Zairy, 2010; Roman-Guerrero et al., 2009; Rutz et al., 2013; Sarojini, Kunam, Manavalan & Jayanthi, 2010; Yadav, Igartuburu, Yan & Nothnagel, 2007). Natural polysaccharides can also be safely used as drug delivery vehicles/carriers (Rajamma, Yogesha & Sateesha, 2012). Biomedical applications of different polysaccharide gums are represented in Table 1.

Among the various polysaccharides, tara gum (TG), a galactomannan polysaccharide of high molecular weight, is one of the emerging potential candidates which find wide applications in the pharmaceutical

* Corresponding author.
E-mail address: tapan_ju01@rediffmail.com (T.K. Giri).

https://doi.org/10.1016/j.fhfh.2022.100107
Received 5 July 2022; Received in revised form 4 November 2022; Accepted 29 November 2022
2667-0259/© 2022 The Author(s). Published by Elsevier B.V. This is an open access article under the CC BY-NC-ND license (http://creativecommons.org/licenses/by-nc-nd/4.0/)

26TH ANNUAL NATIONAL CONVENTION

PSIT Kanpur

APTICON 2023

Fiesta of Innovation, Research and Collaboration: Thriving towards excellence in Pharmacy Teaching

ASSOCIATION OF PHARMACEUTICAL TEACHERS OF INDIA (APTI)
AND
PSIT-PRANVEER SINGH INSTITUTE OF TECHNOLOGY (PHARMACY), KANPUR

CERTIFICATE
OF APPRECIATION

This is to certify that

Prof./Dr./Mr./Ms. KAUSHIK MUKHERJEE

From Department of Pharmaceutical Technology, Jadavpur University

has presented an **ORAL PRESENTATION** on the topic entitled Effect of Compressional force and drug load on tramadol Hydrochloride release from Al^{3+}/Ca^{2+} Crosslinked carboxymethyl Jaya gum hydrogel matrix Tablets.

in the **26th Annual National Convention** of the **Association of Pharmaceutical Teachers of India -2023** held at **PSIT- Pranveer Singh Institute of Technology (Pharmacy), Kanpur (India)** from 2nd to 3rd September 2023.

Dr. Pranay Wal	Dr. A K Rai	Dr. Deependra Singh	Dr. Milind J. Umekar
Organising secretary	Head of the Institute	LOC Chairman	APTI president

Our Esteemed Sponsors

ALKEM · SES · SIGNA · IDEAL CURES · SBS College of Pharmacy